12-2021

Exploring the Role of AMPK in Nutrient Sensing and Signaling in the Human Parasite Trypanosoma brucei

Jessica Jones
jjone29@g.clemson.edu

12-2021

Exploring the Role of AMPK in Nutrient Sensing and Signaling in the Human Parasite *Trypanosoma brucei*

Jessica Jones

EXPLORING THE ROLE OF AMPK IN NUTRIENT SENSING AND SIGNALING IN THE HUMAN PARASITE *TRYPANOSOMA BRUCEI*

A Dissertation
Presented to
the Graduate School of
Clemson University

In Partial Fulfillment
of the Requirements for the Degree
Doctor of Philosophy
Biochemistry and Molecular Biology

---

by
Jessica Jones
December 2021

Accepted by:
James Morris, Committee Chair
Kimberly Paul
Cheryl Ingram-Smith
Jennifer Mason

ABSTRACT

African trypanosomes are protozoan parasites that cause the diseases African sleeping sickness and nagana, in humans and cattle respectively. These parasites have complex life cycles with infection of a mammalian host, ~5mM glucose, following transmission by an insect vector, essentially zero glucose. With these pathogens being exposed to rapidly changing glucose abundance in a host-dependent manner, the ability to sense and rapidly respond to changes in the availability of the hexose are critical. First, I provide a review of glucose metabolism in *Trypanosoma brucei*. Then, we explore the role of the catalytic α subunit of AMPK, a eukaryotic master regulator of energy, in procyclic form *T. brucei*. We found that the larger species of AMPKα1, coined AMPKα1+, was more abundant in the presence of glucose, and other metabolizable sugars. Subcellular location of AMPKα1 was similar regardless of glucose abundance. Phosphorylated AMPKα1 had an association with membranes, hypothesized to connect nutrient sensing and signaling pathways. Lastly, we describe how pleomorphic parasites respond to glucose depletion with a focus on parasite changes in energy metabolism and growth. Long slender bloodstream form parasites were rapidly killed as glucose concentrations fell, while short stumpy bloodstream form parasites persisted to differentiate into the insect stage procyclic form parasite. Both differentiation and growth of resulting procyclic form parasites were inhibited by glucose and non-metabolizable glucose analogs and these parasites were found to have upregulated amino acid metabolic pathway component gene expression. In summary, glucose transitions from the primary metabolite of the blood stage infection to a

negative regulator of cell development and growth in the insect vector. These data suggest that glucose is not only a key metabolic agent but is also an important signaling molecule and may be signaling through TbAMPK.

DEDICATION

I dedicate this to my parents, Becky and Douglas Jones, and my spouse, Nicholas Briggs. Your love and support has given me the strength to achieve my goals.

ACKNOWLEGMENTS

I would like to sincerely thank my mentor, Dr. James Morris, for his guidance and support as a mentor have shaped me into the scientist that I am today. I also want to thank Dr. Meredith Morris, as she has always been there to provide encouragement and assistance throughout my graduate career. The Drs. Morris have created a wonderful working environment with a focus on collaboration and challenged our thinking. I would like to thank all of my lab members past and present. Dr. Jimmy Suryadi and Dr. Evan Qiu for their patience and mentorship, Jillian Milanes for her support and friendship, and Matthew Morgan for taking up my mantle. I would also like to thank members of Dr. Meredith Morris' lab, Dr. Logan Crowe, Dr. Christina Wilkinson, Emily Knight, and Sabrina Pizarro, for their encouragement and continuing roles in my graduate career. I have been blessed to be in an environment that began as work and turned into a family. I greatly appreciate the overwhelming support from my lab, the labs within EPIC, and the labs within the department.

I would also like to thank my committee members, Dr. Cheryl Ingram-Smith, Dr. Kimberly Paul, and Dr. Jennifer Mason, for their unwavering support, in not only my science, but my growth as a person. I would like to deeply thank the NIH for funding of my graduate career and the Department of Defense SMART scholarship for the funding and future career. Lastly, I want to especially thank Dr. Jordan Wesel and Dr. Christina Wilkinson for their steadfast friendship, love, and support of my science and in my life.

TABLE OF CONTENTS

Page

TABLES OF CONTENTS (continued)

Page

TABLE OF CONTENTS (continued)

Page

LIST OF TABLES

Table Page

LIST OF FIGURES

LIST OF FIGURES (continued)

Figure Page

LIST OF FIGURES (continued)

Figure Page

CHAPTER ONE

LITERATURE REVIEW

GLUCOSE METABOLISM AND REGULATION IN AFRICAN TRYPANOSOMES

Introduction

Trypanosoma brucei

Kinetoplastids are a group of flagellated protozoa which include the species *Trypanosoma* and *Leishmania*. Kinetoplastids can cause disease in humans and economically important animal species, causing a substantial economic burden in impacted areas. The parasites in this group that cause human disease include *Trypanosoma cruzi, T. brucei,* and *Leishmania spp* and cause Chagas disease, African sleeping sickness, and leishmaniasis, respectively. These parasites have complex life cycles with infection of a mammalian host following transmission by an insect vector (**Figure 1.1**) (1).

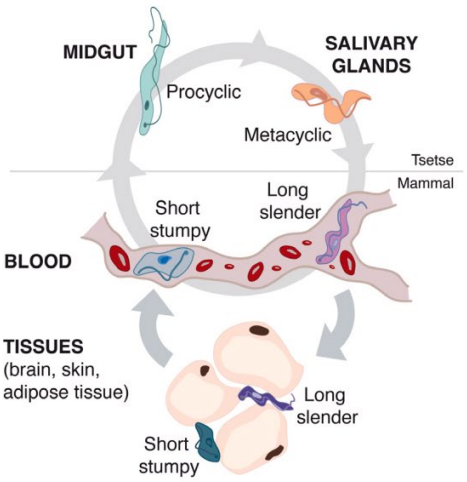

Tsetse - midgut	Procyclic form (PF)
Preferred nutrient	Proline (and glucose, if available)
Main secreted products	Alanine, (acetate and succinate)
Main pathways for ATP production	Oxidative phosphorylation (and glycolysis)
Respiratory chain	Active
Proliferation (Doubling Time)	~12 hr

Mammal - blood	Long slender (B-LS)	Short stumpy (B-SS)
Preferred nutrient	Glucose	Glucose
Main secreted products	Pyruvate	Pyruvate (Acetate and Succinate)
Main pathways for ATP production	Glycolysis	Glycolysis (and Oxidative Phosphoryation?)
Respiratory chain	Inactive (TAO maintains redox)	Probably Active
Proliferation (Doubling Time)	~7 hr	Quiescent

T. brucei is a unicellular protozoan parasite that is transmitted by the tsetse fly. Non-proliferative metacyclic trypomastigotes are injected from the salivary gland of the fly into the mammalian host during a blood meal (2). These parasites receive a variety of environmental cues, including temperature, nutrient availability, and host immune response, which induce differentiation into the long slender form (LS). LS parasites are proliferative and establish an infection in the bloodstream. Interestingly, the *T. brucei* life cycle is completely extracellular, compared to *T. cruzi* and *Leishmania spp*. Eventually, LS parasites overcome the blood-brain barrier and establish infection in the brain. LS parasites differentiate into short stumpy forms (SS) in a density dependent fashion in the mammalian bloodstream (3). Upon receiving molecular cues from neighboring parasites, LS alter their surface membrane proteins (4,5), remodel metabolism (6,7), and become non-dividing SS. This differentiation is cued by a small molecule termed the stumpy-inducing factor, SIF (8). Rojas et al have shown that oligopeptides are partially responsible for the composition of SIF (9). Parasite secreted proteases to degrade host proteins, which are then perceived by the parasites by an orphan G-protein-coupled receptor, TbGPR89, and trigger SS formation (10).

When a tsetse fly takes a bloodmeal from an infected mammal LS and SS parasites are ingested. Evidence suggests that SS are preadapted to the fly midgut environment, having a unique surface molecule composition and altered metabolism that seems to be appropriate for life in the fly (11). Our understanding of SS differentiation into procyclic forms (PF) is more extensive, due to the historical belief that SS were key intermediates in the process (12). SS parasites are cued to become PF by changes in nutrient availability, temperature

change, and low pH and protease activity and differentiate into PF (13,14). Coincident with differentiation, amino acids become important metabolites for the PF parasites. In the fly hemolymph parasites consume primarily proline, through oxidative phosphorylation, to generate ATP. Parasites migrate from the midgut into the salivary glands of the fly where they differentiate into epimastigotes and establish infection. Proliferative epimastigotes differentiate into quiescent metacyclic trypomastigotes in the salivary gland, a mechanism that is not well understood. When this infected fly takes a bloodmeal it injects metacyclic parasites into the mammalian bloodstream, completing the parasites life cycle (2).

Nutrient availability in the various host environments is different. Glucose, for example, can have marked availability differences between host and vector. Additionally, the abundance of glucose can vary in the different tissues of the mammal and insect. For example, glucose is abundant in the mammalian bloodstream and in organs like the brain, being maintained at millimolar levels by the host (15). Concentrations in other tissues is likely considerably lower, with adipose glucose half as abundant as blood glucose (16). Additionally, glucose levels in the insect vectors can differ from those in the mammal. Trypanosomes taken up in a bloodmeal by the tsetse fly experience a precipitous loss of glucose in the environment, with the blood sugar falling from ~5mM to nearly undetectable within 15 minutes of the fly feeding (17).

With these pathogens being exposed to rapidly changing glucose abundance in a host-dependent manner, the ability to sense and rapidly respond to changes in the availability of glucose are critical. Responses to changes in glucose availability include alteration of metabolic strategies, requiring the regulation of different pathways to meet the

needs of the cell. In this review, mechanisms used by yeast and mammalian cells to perceive and respond to changes in glucose availability, and their connection to AMPK signaling, will be considered and then similarities and differences in *T. brucei* will be discussed.

Glucose metabolism

Glucose serves as a critical nutrient for most organisms. Glucose enters cells through either active or passive mechanisms. Once glucose enters the cell it is catalyzed to glucose-6-phosphate (G6P) by an enzyme of the hexokinase, or glucokinase, family. The fate of G6P is varied and depends on the metabolic needs of the cell- which is dependent on the environment in which the cell resides. Eukaryotic glucose metabolism is summarized in **Figure 1.2**. Under conditions of metabolic demand (low ATP) G6P enters glycolysis. The metabolism of this sugar through glycolysis yields two NADH reducing equivalents, two ATP, and two pyruvate molecules per molecule of glucose. The pyruvate may be further metabolized by oxidation in the citric acid (TCA) cycle, and subsequently the electron transport chain (ETC), to generate additional ATP. The combination of these two metabolic pathways, TCA cycle and ETC, is known as oxidative phosphorylation. Glucose uptake may be upregulated under conditions of nutrient depletion to increase the influx of glucose to meet cellular demands. Conversely, other metabolites can be used to generate ATP.

Glucose is also metabolized for use in the pentose-phosphate pathway, which generates reducing equivalents and nucleotide biosynthetic intermediates. G6P enters the pentose phosphate pathway to generate NADPH and pentose sugars. This process happens in

parallel with glycolysis and is primarily regulated through the abundance of reducing equivalents in the cell.

Glucose abundance may be low in some environments, so eukaryotes employ other mechanisms to generate glucose for essential cellular processes. In some organisms glycogen, a polymer of glucose, is stored in some cells and can be broken down during periods of glucose starvation in a process called glycogenolysis. Gluconeogenesis is the process which eukaryotes reverse much of glycolysis to shuttle G6P into other essential pathways when glucose abundance is low in the environment.

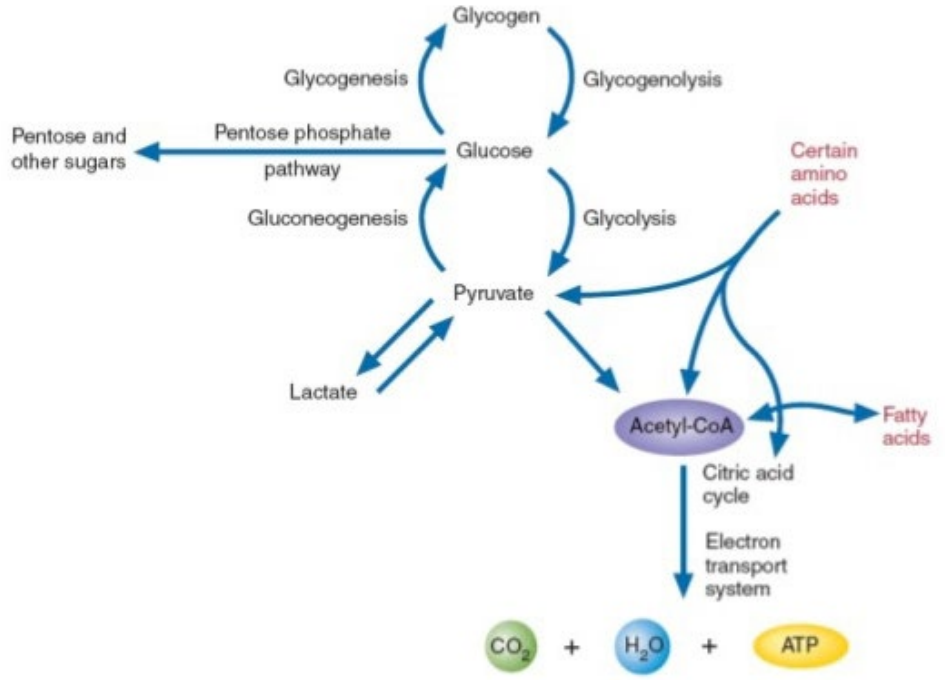

Figure 1.2: Schematic of eukaryotic carbohydrate metabolism (Taken from BioVision website). Glucose is central in several metabolic pathways. Glucose is broken down into pyruvate through glycolysis to generate ATP. Pyruvate is converted into acetyl-CoA and is metabolized through the citric acid (TCA) cycle , and subsequently the electron transport chain (ETC) to generate ATP. Pyruvate can also be converted into lactate for excretion. Glucose can also be utilized in the pentose-phosphate pathway to generate other molecules. Some amino acids can be shuttled into various metabolic pathways to generate ATP. Fatty acids can be degraded into acetyl-CoA to go through the TCA cycle and ETC to generate ATP. Pyruvate can be metabolized into glucose through gluconeogenesis. Glucose can be polymerized into glycogen molecules for cellular storage through glycogenesis. Glycogen can be degraded into glucose monomers through glycogenolysis.

Yeast

Glucose metabolism

Yeast use concentration-dependent facilitated diffusion to acquire stereospecific hexoses (18). This uptake occurs through a broad family of transporters that includes both high and low affinity hexoses transports with members of the Hxt family (19,20) (**Figure 1.3**, Hxt). These hexose transporters vary in binding affinity for glucose, fructose, and mannose, and are differentially expressed based on the extracellular environment of the yeast. Low affinity hexose transport occurs through facilitated diffusion. These transporters are constitutively expressed throughout the yeast life cycle (21). Cells begin to express the high affinity hexose transporters as hexoses become depleted from the environment. High affinity hexose transport is inhibited by the presence of hexose in the environment, through general repression control. This transport is reliant on the activity of glucokinase, which phosphorylates free glucose to yield G6P, functionally reducing the intracellular pool of free glucose (19).

High affinity glucose transporters include SNF3, HXT1, and HXT2. SNF3 has been shown to play a role in glucose repression, although it is not required for regulation (22). Intracellular glucose levels are sensed by some hexose transporters as glucose crosses the plasma membrane (23) (**Figure 1.3**, Hxt, Rgt2/Snf3, Gpr1). These hexose transporters serve as signaling proteins which increases metabolic efficiency and are common among eukaryotes. The variation of hexose transporters allows the cells to express the appropriate transporter for the environmental sugar concentration. The regulation of hexose transporter abundance on the plasma membrane is regulated at the both the transcriptional and

translational levels through Rgt1, central to all three glucose signaling pathways in yeast (24) (**Figure 1.3**, Rgt1).

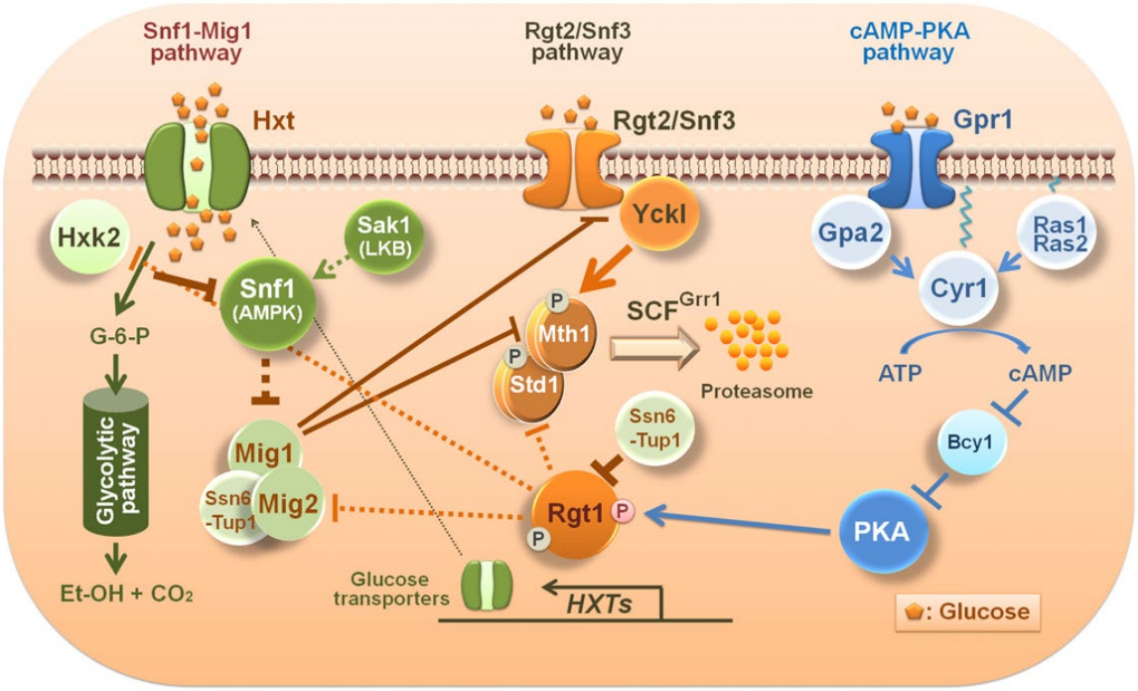

Figure 1.3: Glucose signaling pathways in yeast. The hexose transporters, Hxt, transport glucose into the cytoplasm and signal through Snf1, which is influenced by hexokinase activity, Hxk2 (Snf1-Mig1 pathway -left). Depending on extracellular glucose concentration either Rgt2 or Snf3 transduces the signal to the cytoplasm and signals for glucose-based gene repression (Rgt2/Snf3 pathway - middle). The cAMP-PKA pathway (right) responds to extracellular glucose concentrations and transduces the intracellular signal through the increase in cytoplasmic cyclic AMP (cAMP) and activates the glucose

repressed gene expression. Reprinted with permission from Elsevier Science & Technology Journals, General Subjects. Copyright: Elsevier Science & Technology Journals, 2013 (25).

Snf3 and Rgt2 proteins are transmembrane proteins that bind glucose, but do not transport it (**Figure 1.3**, middle pathway). Snf3 and Rgt2 have cytoplasmic C-terminal tails that are responsible for intracellular signal transduction from extracellular glucose concentrations (26). These C-terminal tails recruit a signaling complex which is responsible for transducing the signal of glucose abundance and controlling the gene expression of HXTs (23).

Yeast regulates gene expression based on available carbon source (27). Transcription initiation and activation can be regulated in response to glucose abundance through multi-protein complexes that interact with DNA promoter regions. Nuclear localization of Hxk2 (**Figure 1.3**, left pathway) has been shown to repress gene expression in the presence of glucose. This occurs when Hxk2 binds the promoter, not allowing the transcription initiation complex to form (23). Transcriptional regulation may also involve small molecules or cofactors, whose concentration may affect the protein complexes associated with gene promoters, altering the activity of those complexes. This commonly occurs through allosteric regulation by intermediate metabolites. For example, fructose-2,6-bisphosphate has an inhibitory effect on FBPase through a substrate negative feedback mechanism (28).

Yeast control translation based on nutrients and environmental stresses by means of protein degradation, modification, and translocation (29). In response to high glucose abundance yeast utilize glycolysis to generate ATP. As ATP is metabolized and ADP accumulate this signals to protein kinase A (PKA) (**Figure 1.3**, PKA), target of rapamycin complex 1 (TORC1), and Snf1 which initiates the alteration of transcription (30). PKA and TORC1 have been found to play a role in regulating ribosome biogenesis and protein synthesis, as well as gene expression of the hexose transporters, which is important because these pathways are regulated by cellular cAMP levels (31) (**Figure 1.3**, right pathway).

SNF1 - AMPK homologue

The signaling molecule Snf1 also transduces signals, through its kinase activity, based on glucose concentrations, by means of gene regulation (26) (**Figure 1.3**, Snf1- left pathway). When environmental glucose is low, SNF1 acts to derepress glucose-repressible genes. SNF1 is not transcriptionally regulated, but rather modified at the protein level (32). SNF1 is a heterotrimeric serine/threonine protein kinase containing the catalytic α subunit (Snf1), the scaffold β subunit (Gal83/Sip1/Sip2), and the regulatory γ subunit (Snf4). SNF1 is a master regulator of yeast environmental response, including nutrient abundance (33). Activation of SNF1 involves phosphorylation of Threonine 210 of the catalytic α subunit, this phosphorylation is a hallmark of SNF1 activation (34). The largest contributor to SNF1 activity is AMP:ATP ratios. When the intracellular AMP:ATP ratio is high, then SNF1 transduces signals to induce catabolic activities while suppressing anabolic activities (35). Regulation of SNF1 occurs through post-translational modifications (PTM) by upstream

phosphatases and kinases, and various allosteric mechanisms (36). SNF1 directly plays a role in glucose uptake and metabolism (25).

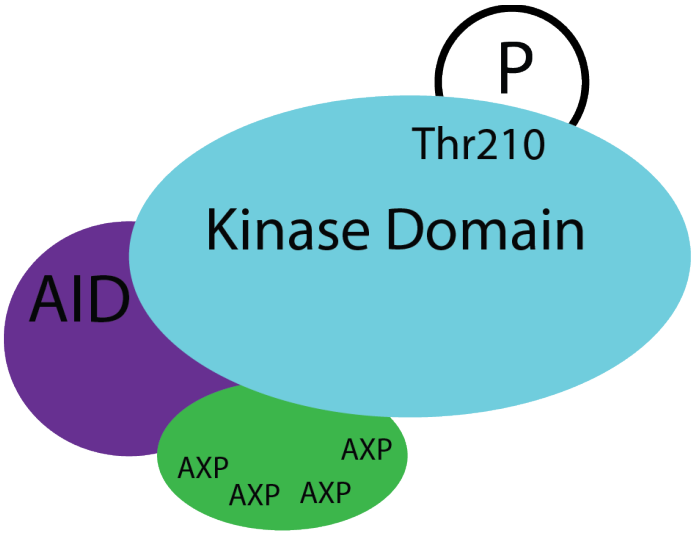

Figure 1.4: AMPK complex in Yeast. Schematic of the heterotrimeric AMP-Kinase complex. Snf1 (blue) - the catalytic subunit, contains the active site for kinase activity and complex activation occurs through phosphorylation on Threonine 210. Snf4 (purple) - the scaffold subunit, contains autoinhibitory domain (AID) of Snf1. Gal83 (green) - the regulatory subunit contains the binding domains for adenosine nucleotides (AXP) for intracellular energy sensing.

Mammals

Glucose metabolism

Mammalian cells use two mechanisms for glucose uptake, facilitated diffusion and sodium-glucose co-transport (37). Na+-glucose symport is found in a limited number of mammalian cell types whereas facilitated diffusion occurs in a plethora of cell types and tissues. Facilitated diffusion of glucose is carried out through the GLUT family of proteins (**Figure 1.5**, GLUT). Like the yeast Hxts, the GLUT proteins vary in their affinity for glucose and are differentially expressed in response to environmental stimuli, being most abundant in particular tissue types. For example, GLUT2 is the primary transporter of the liver, where GLUT4 is found in adipose and muscle tissues. GLUT1 is common to many tissues, and is the low affinity glucose transporter, where GLUT4 has high affinity for glucose transport. (38).

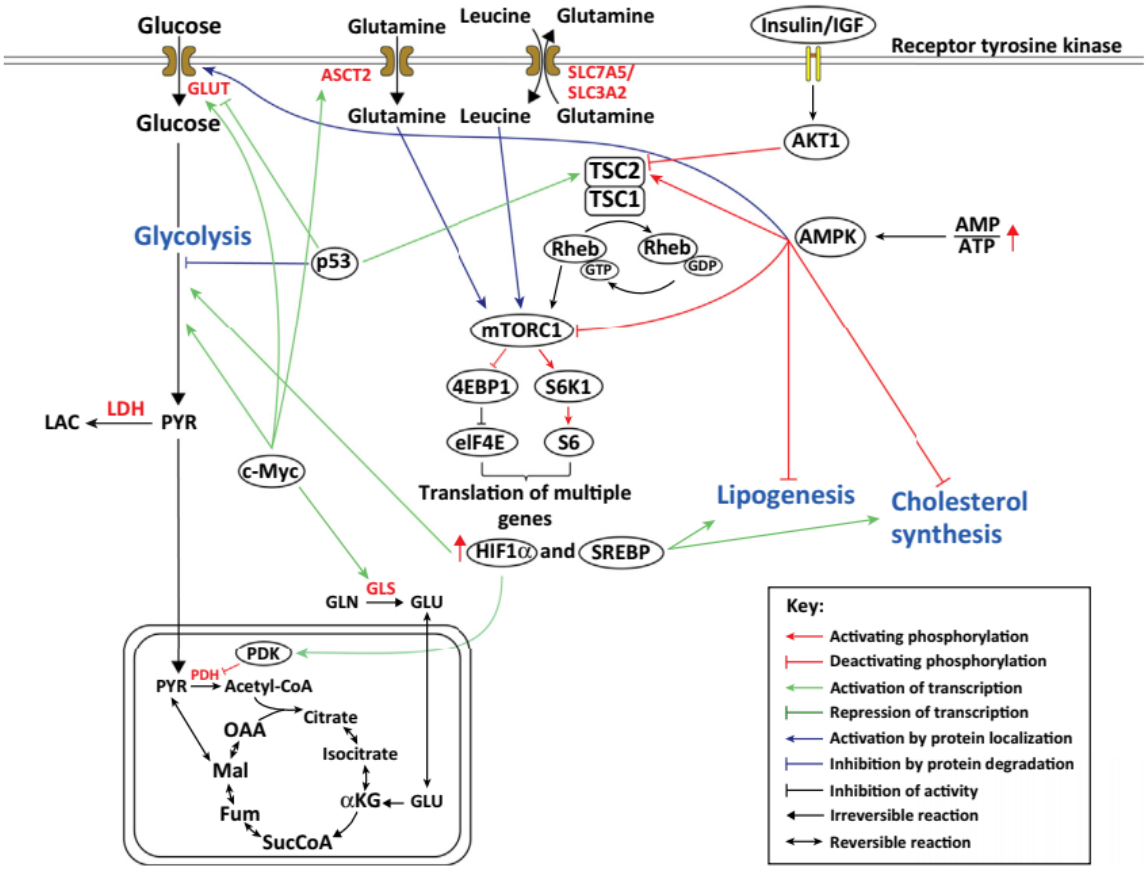

Figure 1.5: Overview of regulation of glucose metabolism through signaling pathways. Schematic of glucose metabolism and nutrient metabolism in mammals. Regulation occurs through nutrient abundance (glucose, glutamine, or leucine), or cellular energy abundance ($\frac{\text{AMP}}{\text{ATP}}$). Lipogenesis and cholesterol synthesis are inhibited when cellular energy is low, but activated in the presence of SREBP. Reprinted with permission from Elsevier, Trends in Biotechnology. Copyright: Elsevier, 2016 (39).

Mammalian multi-cellularity increases the complexity of glucose perception and response pathways. The most studied example of glucose gene regulation in mammals is the insulin-based pathway (**Figure 1.5**, through a receptor tyrosine kinase). Complex carbohydrates from the diet are digested to yield glucose monomers that are used for cellular metabolism. In response to increasing glucose levels from the meal, the pancreas secretes the hormone insulin into the bloodstream, while simultaneously inhibiting glucagon secretion. Insulin, promotes glucose uptake in other tissues (40). Generally, by triggering an increase in GLUT gene expression and protein translocation to the plasma membrane. Insulin induces expression of both GLUT1 & 4 to increase overall glucose transport. Steroids decrease overall GLUT family expression, and in turn decrease intracellular glucose, and lead to cellular degradation of glycogen (38).

The first reaction of glycolysis (**Figure 1.5**, glycolysis), glucose into glucose-6-phosphate (G6P), is catalyzed by a hexokinase, which is distinct from the yeast glucokinase. Mammalian cells have four types of hexokinases, with type IV being glucokinase. Glucokinase differs from the three other types of hexokinases by having a lower affinity (~ 6mM) and higher specificity for glucose, as well as lacking the traditional negative allosteric feedback of G6P (41,42). Glucokinase plays a role in glucose response through tissue specific expression, through a mechanism distinct from GLUT expression (43). Glucokinase is repressed in hepatocytes during glucose depletion, whereas in the pancreatic β-islet cells glucokinase expression remains unchanged (44). β-islet cells respond to the metabolism of glucose into glucose-6-phosphate through glucokinase, utilizing glucokinase activity as a metabolic sensor (45–47). The glucose concentration for

optimal glucokinase activity mirrors blood glucose levels under normal conditions. Hypoglycemia leads to inactivation of glucokinase, which is perceived by the β-islet cells and leads to glucagon secretion. The downstream metabolic intermediates, from either glycolysis or the pentose phosphate pathway, trigger differential gene expression through transcription factors (48,49) (**Figure 1.5**).

AMPK

Nutrients, hormones, and other stimulants can influence proteins through post-translational modifications or allosteric mechanisms. These include proteins within signaling pathways and transcription factors (50). The master regulator AMP kinase (AMPK), a homolog of yeast SNF1, is a heterotrimeric complex (**Figure 1.6**) and is activated in response to high AMP/ADP:ATP levels, sensing low intracellular energy, and signaling catabolic pathways. Inversely, mTORC1 is activated in the presence of insulin, and signals anabolic pathways (39) (**Figure 1.5**, mTORC1).

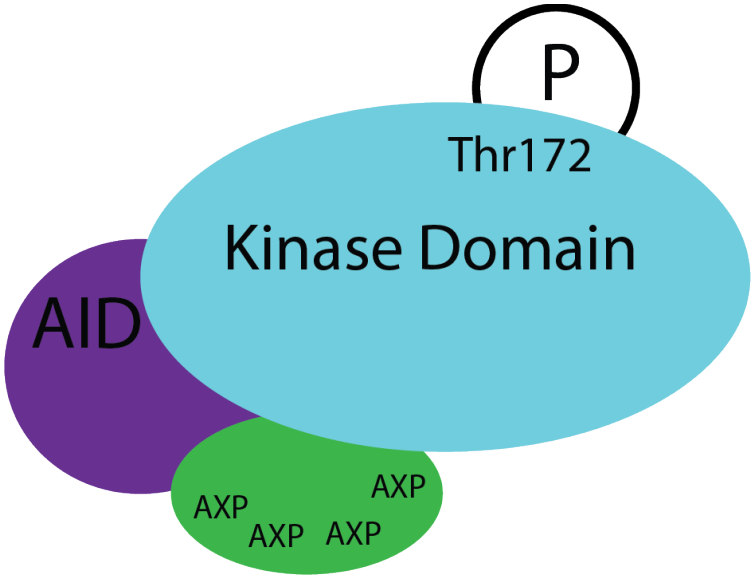

Figure 1.6: AMPK complex in Mammals. Schematic of the heterotrimeric AMP-Kinase complex. AMPKα (blue) - the catalytic subunit, contains the active site for kinase activity and complex activation occurs through phosphorylation on Threonine 172. AMPKβ (purple) - the scaffold subunit, contains autoinhibitory domain (AID) of AMPKα. AMPKγ (green) - the regulatory subunit contains the binding domains for adenosine nucleotides (AXP) for intracellular energy sensing.

The enzymatically active AMPK is comprised of three unique subunits. The catalytic α subunit, the scaffold β subunit, and the regulatory γ subunit (**Figure 1.6**). The mammalian genome encodes two α isoforms, three β subunit isoforms, and two γ subunit isoforms, for a possible combination of 12 distinct AMPK complexes (51). Regulation of AMPK can occur through any one of the three subunits (51). Phosphorylation of the

catalytic α subunit on threonine 172 leads to kinase activation. The scaffold β subunit can be myristoylated, altering the subcellular location of the AMPK complex through interactions with membranes (52). The regulatory γ subunit is responsible for sensing the adenine nucleotides, and in turn allowing the activation of the catalytic α subunit (51). These modifications of AMPK that alter activity occur in the cell by an increase in AMP:ATP ratios, presence of cAMP or its analogs, or change of subunit isoforms (53,54). Canonical activation of AMPK occurs through the increase in AMP:ATP ratio, triggering the phosphorylation of Thr172 on the α subunit, which can occur through depletion of environmental glucose. The resulting active complex phosphorylates a multitude of proteins, activating some while simultaneously repressing others. AMPK activation has been shown to act as a sensor for glucose, as well as association with some organellar membranes (55).

African Trypanosomes

Glucose metabolism

Trypanosoma brucei infects the bloodstream of mammals and the digestive tract of the tsetse fly, living as an extracellular parasite during its entire life cycle. The glucose concentration of mammalian blood is ~5 mM and is relatively constant (56). In the blood, the parasite utilizes low affinity glucose transporters (trypanosome hexose transporter type 1s, THT1s) to acquire glucose through facilitated diffusion from the host environment (57–59). Glucose moves from the cytoplasm to the glycosome through an unknown mechanism, where a hexokinase phosphorylates it into glucose-6-phosphate (G6P), reducing the concentration of glucose in the cell and enabling continued sugar uptake. Glycosomes are parasite-specific specialized peroxisomes that compartmentalize most of glycolysis, along with components of other metabolic pathways. These organelles have an unknown glucose transport mechanism (60,61).

The differentiation from proliferative LS parasites into quiescent SS parasites occurs in a density dependent fashion in the mammalian bloodstream (3) (**Figure 1.7**, slender to stumpy in the bloodstream). As parasitemia increases in the mammalian bloodstream, so does the concentration of the 'stumpy inducing factor' (SIF). LS parasites sense environmental SIF, arrest their growth, and differentiate into SS forms (62). SS parasites are characterized by quiescence, having a shortened morphology, with molecular markers that include the upregulation of mitochondrial transcripts coincident with mitochondrial expansion (**Figure 1.7**, Stumpy associated hallmarks). Additionally, the SS

cells are resistant to mild acids and have proteins associated with differentiation (PAD) on the cell surface (63,64). This quorum-sensing mechanism of parasite development has been recently reviewed (in 3). It has been hypothesized that this stepwise transition in the parasite lifecycle is necessary for colonization in the tsetse fly midgut and successful transition into PF parasites (12). However, recent studies have shown that LS parasites can differentiate directly into PF forms without the need for the SS lifecycle stage (66) and LS have been shown to establish viable infections in tsetse flies without the SS intermediates (67).

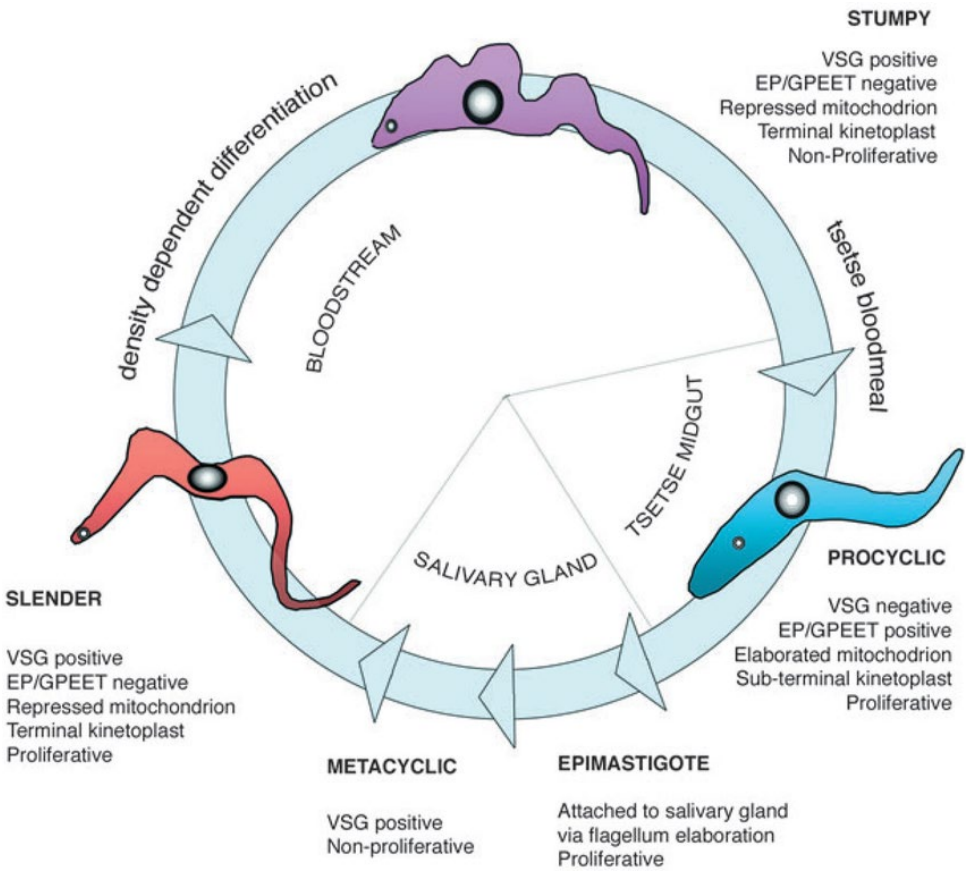

Figure 1.7: Differentiation between Slender to Stumpy to Procyclic form *T. brucei*. Slender form parasites reside in the mammalian bloodstream and have the associated hallmarks. Stumpy forms are also present in the bloodstream but are morphologically and metabolically distinct. Procyclic form parasites are generated in the tsetse fly midgut after a bloodmeal and have the associated hallmarks. While progressing through the tsetse fly parasites differentiation into epimastigotes forms then subsequently metacyclic forms to be injected into a mammalian bloodstream during a tsetse bloodmeal and become slender forms, completing their lifecycle. Reprinted with permission from The Company of Biologists, Journal of cell science. Copyright: The Company of Biologists, 2005 (68).

When a tsetse fly takes a bloodmeal from an infected mammal, both LS and SS *T. brucei* parasites are ingested by the fly. Within 15 minutes the bloodmeal is digested in the midgut and glucose levels become undetectable, an event that can trigger differentiation of the short stumpy parasites into the insect stage procyclic form (PF) *in vitro* (17). The PF parasites remodel their metabolism to overcome the absence of glucose and, in turn, upregulate amino acid metabolism to consume primarily proline from the tsetse fly hemolymph to generate ATP. Even though amino acids serve as the predominant carbon source for the PFs, they express a high affinity glucose transporter, THT2, for uptake of glucose that may be introduced into the fly midgut. THT2 transcripts are present in both PF and BSF parasites, albeit at a significantly lower abundance in BSF parasites, whereas THT1 transcripts are only present in BSF parasites (69,70). The mechanism of THT2 glucose uptake, facilitated diffusion, is similar to THT1 although the transporter has a much higher affinity for glucose (71).

One of the canonical pathways for triggering SS to PF differentiation is citrate/cis-aconitate treatment of SS forms (72). The TCA intermediate is taken up by the cells through the PAD surface proteins and this triggers metabolic reprogramming and surface protein alterations required for the PF stage (73). Other hallmarks of PF parasites include fully functional mitochondria, kinetoplast repositing, and proliferation (63) (**Figure 1.7**, procyclic associated hallmarks). During the transition from SS, parasites begin remodeling their metabolism, to perform oxidative phosphorylation of amino acids while altering cell surface proteins to successfully become PF (**Figure 1.7**, procyclic form in the tsetse midgut with associated hall marks). The differentiation from SS parasites into PF parasites can

occur in response to a number of stimuli, in addition to treatment with citrate/cis-aconitate (74) (**Figure 1.7**, tsetse bloodmeal). One is the depletion of extracellular glucose, discussed in Chapter Two (73).

Glycosomes are involved in *T. brucei* differentiation signaling. The development from SS to PF is driven by protein phosphorylation-based signaling. Two proteins are key to this response, TbPTP1 and TbPIP39 (14,75). TbPTP1 (protein tyrosine phosphatase 1) is a negative regulator of PF development that inactivates TbPIP39 (TbPTP1-interacting protein, 39kDa) to prevent the SS to PF transition. TbPIP39 transcript is abundant in SS parasites, while protein levels increase in PF parasites. SS parasites receive signals in the fly midgut and inactivate TbPTP1, which allows the phosphorylation, or activation, of TbPIP39 and differentiation into PF parasites (63,75). Once phosphorylated, TbPIP39 relocates to glycosomes where it remains activated and unable to interact with TbPTP1 (75). This mechanism suggests a role for protein phosphorylation cascades coordinating lifecycle-dependent changes in parasite metabolism.

Glucose enters the parasites through the THTs and it has been hypothesized that these transports may be playing a secondary role in glucose sensing and signaling (71). PF parasites utilize proline as their main metabolite, but preferentially metabolize glucose if available. Under these conditions, when glucose becomes available, PF parasites rapidly down-regulate proline transport and metabolism (76). Conversely, when PF parasites are starved for glucose and have amino acids available to metabolize they up-regulate tricarboxylic acid cycle transcripts (77).

Previous work on trypanosomes discovered that glucose metabolism affects surface molecule glycoprotein expression in PF parasites (78). Environmental glucose depletion, or silencing of glycolytic enzymes, led to changes in expression of surface procyclins that mirrored developmental responses in the fly that are coordinated with glucose reduction in the bloodmeal fly midgut (78). Early PF parasites express GPEET procyclins but through time they are replaced by EP procyclins (4). These data suggest a mechanism for modulating PF surface molecule composition that is tied to glucose metabolism.

AMPK

All three AMP kinase subunits have been recently annotated in the trypanosome genome. The catalytic AMPKα subunit has two annotated isoforms, 1 and 2 (Tb927.10.5310 and Tb927.3.4560, respectively) (79). The scaffold AMPKβ subunit has one annotated gene (Tb927.8.2450), as well as the regulatory AMPKγ subunit (Tb927.10.3700) (80). TbAMPKα isoform 1 and 2 are highly similar (**Figure 1.8**). Upon further sequence analysis within the activation loop of the catalytic AMPKα subunit the threonine associated with enzyme activation was conserved. The threonine is found at position human AMPK (Thr183), yeast SNF1 (Thr210), TbAMPKα (Thr165) and TbAMPKα2 (Thr167) (**Figure 1.8**).

By immunoprecipitation of the TbAMPK complexes, Saldivia et al characterized two unique AMPK complexes with distinct protein components (79). Combining the immunoprecipitation data with proteins previously published to be associated with of

TbAMPK (80), they concluded that *T. brucei* form two distinct AMPK complexes (**Figure 1.9**). TbAMPKα1 is associated with AMPKβ and AMPKγ subunits, as well as translation factors and RNA binding proteins (**Figure 1.9**, top). Interestingly, when AMPKβ was used for immunoprecipitation both isoforms of AMPKα were detected, along with hexokinase 1 (TbHK1) and other metabolic enzymes (**Figure 1.9**, bottom).

A comparison of AMPK homolog sequences, using human PRKAA1, human PRKAA2, yeast SNF1, TbAMPKα1 and TbAMPKα2 (**Table 1.1**) revealed that yeast SNF1 had approximately 41% protein identity to each human AMPKα isoform, compared to approximately 51% identity to either trypanosome AMPKα isoform. This modest level of identity may reflect the unique mechanisms of activation and regulation between the three different eukaryotes. The identity between the two human isoforms, PRKAA1 and PRKAA2, was approximately 76%. Human AMPKα isoforms were approximately 47% identical to each trypanosome AMPKα isoform. This discrepancy between human and trypanosome sequences may be worth exploiting to discover novel therapeutics. The identity between the two trypanosome isoforms was approximately 50%, which may reflect different roles for the two distinct AMPK complexes discovered during immunoprecipitation (**Figure 1.9**) (79).

Protein	SNF1	PRKAA1	PRKAA2	TbAMPKα1	TbAMPKα2
SNF1		41%	42%	51%	53%
PRKAA1	41%		76%	46%	48%
PRKAA2	42%	76%		47%	48%
TbAMPKα1	51%	46%	47%		50%
TbAMPKα2	53%	48%	48%	50%	

Table 1.1: Percent identity of protein sequences between AMPKα homolgues. SNF1 uniprot P06782, PRKAA1 uniprot Q13131 (human AMPKα1), PRKAA2 uniprot P54646 (Human AMPKα2), TbAMPKα1 TriTryp Tb927.10.5310, TbAMPKα2 TriTryp Tb927.3.4560. Protein sequence of subject (top row) was aligned to the protein sequence of query (left column) using NCBI blastp suite-2sequences program.

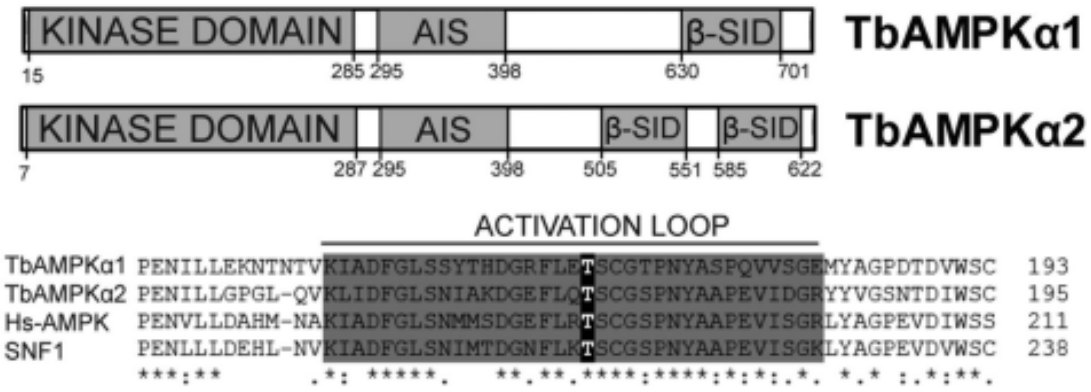

Figure 1.8: TbAMPKα isoform sequence analysis. Protein domain schematic of the two trypanosome AMPKα isoforms (AIS: autoinhibitory site, β-SID: β-scaffold interacting domain). Sequence alignment of the activation loop, highlighted in grey, within the kinase domain of both trypanosome AMPKα isoforms against human AMPK and yeast SNF1. Conserved threonine residue is highlighted in black. TbAMPKα1 Thr165, TbAMPKα2 Thr167, Hs-AMPK Thr183, SNF1 Thr210. Reprinted with permission from Elsevier Science & Technology Journals, Cell reports. Copyright: Elsevier Science & Technology Journals, **(**79)**.**

GENE ID	PROTEIN	
Tb927.10.5310	TbAMPKα1	21
Tb927.10.3700	TbAMPKγ	10
Tb927.8.2450	TbAMPKβ	8
Tb927.10.1890	Calpain	31
Tb927.4.2500	Eukaryotic translation initiation factor 2	25
Tb927.6.4670	TbMORN1	20
Tb927.11.7150	NGG1 interacting factor 3-like	12
Tb927.10.13570	RNA-binding protein, putative (RBP27)	8
Tb927.5.4460	Major vault protein	2

GENE ID	PROTEIN	
Tb927.10.3700	TbAMPKγ	25
Tb927.3.4560	TbAMPKα2	22
Tb927.10.5310	TbAMPKα1	21
Tb927.8.2450	TbAMPKβ	18
Tb927.6.2360	Adenosine kinase	12
Tb927.11.1430	TbCMF2	10
Tb927.10.2010	Hexokinase (HK1)	6
Tb927.9.5750	Tryparedoxin peroxidase (TRYP1)	6
Tb927.3.3780	Tryparedoxin 1a, TXNa1	6
Tb927.8.1990	Tryparedoxin peroxidase (TRYP2)	3
Tb927.10.13780	Glycogen synthase kinase 3 (GSK3)	2

Figure 1.9: Two individual AMPK complexes interacting partners. Proteins found by mass spectrometry analysis to be associated with either TbAMPKα1 (top) or TbAMPKβ (bottom) through immunoprecipitation or previously published biochemical analysis. Reprinted with permission from Elsevier Science & Technology Journals, Cell reports. Copyright: Elsevier Science & Technology Journals, **(**79**).**

Clemmens et al have shown that AMPK plays a role in regulating surface molecule expression in *T. brucei* (80). One experiment performed was mass-spectrometry analysis on procyclin isolates from PF parasites cultured in the presence of glucose, or PF parasites with a knock-down of the AMPKβ subunit, or a knockdown of the AMPKγ subunit (**Figure 1.10**). PF parasites had several species of EP procyclin molecules detected after procyclin isolation (**Figure 1.10A**). However, after the knockdown of either the AMPKβ or AMPKγ subunit PF parasites were found to express GPEET procyclin much like the parasites cultured in the absence of glucose (78) (**Figure 1.10B**). These experiments concluded that the knockdown of two of the AMPK subunits (β or γ) caused an alteration in PF surface molecule composition. The mass-spectrometry data from the AMPK subunit knockdowns mirrored the profiles of PF parasites starved of glucose (78). Taken together, these data suggest that AMPK may be playing a role regulating in surface molecule composition in response to glucose metabolism.

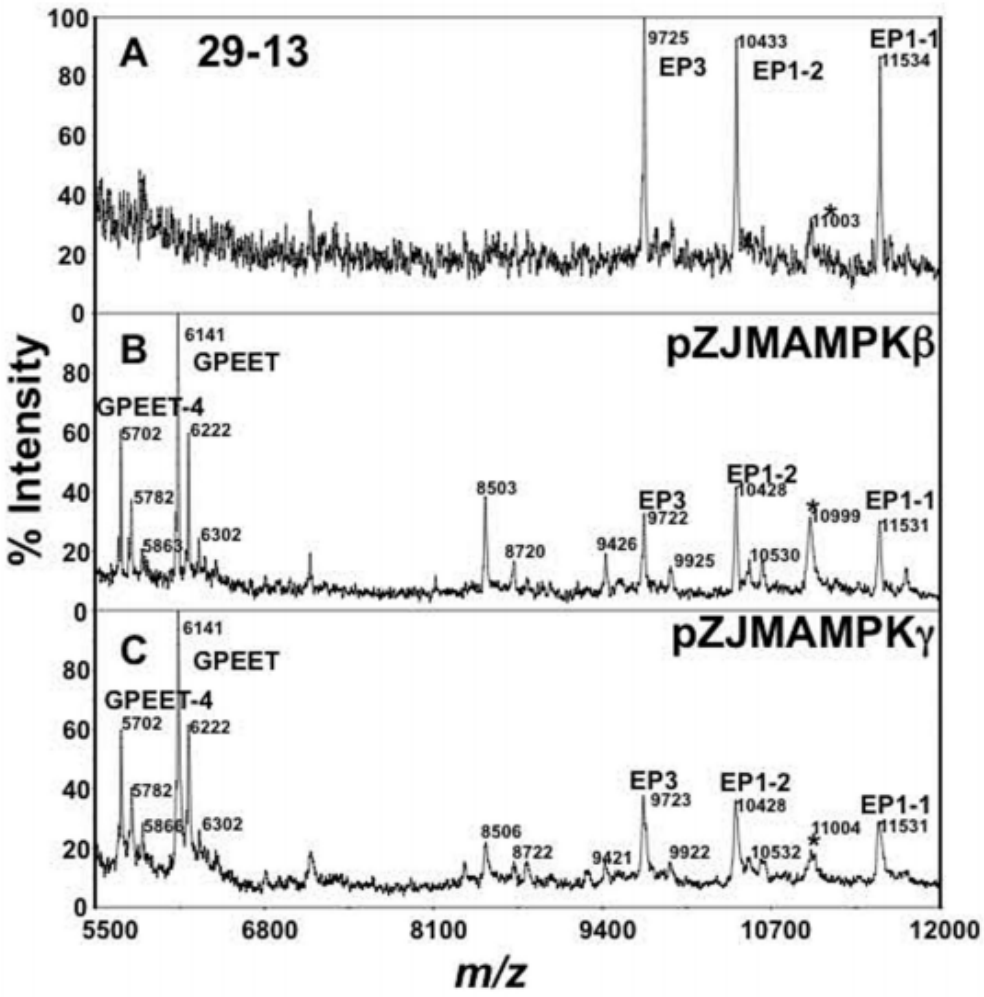

Figure 1.10: PF surface molecule mass-spectrometry profile changes with the knockdown of individual AMPK subunits A- Mass-spectrometry profile of procyclin isolates of parental PF parasites (29-13) B- Mass-spectrometry profile of procyclin isolates of PF parasites with AMPKβ knocked down (pZJMAMPKβ) C- Mass-spectrometry profile of procyclin isolates of PF parasites with AMPKγ knocked down (pZJMAMPKγ). Reprinted with permission from Elsevier Science & Technology Journals, Experimental Parasitology. Copyright: Elsevier Science & Technology Journals, 2009 (80).

AMPK responds to high AMP:ATP ratios, which may occur inside the parasites during glucose starvation required for differentiation from SS into PF. How other environmental signals play a role in *T. brucei* differentiation have been reviewed (11,62,81). Low cellular ATP seems to be the common thread among several eukaryotic differentiation signaling pathways (82). The AMP analog (8-pCT-2'-O-Me-5'-AMP) can activate TbAMPK in LS parasites (79). Parasites treated with the analog upregulated stumpy hallmark transcripts (**Figure 1.11**, PAD1 and PAD2) and PF specific transcript (**Figure 1.11**, EP) while down-regulating LS associated transcripts (**Figure 1.11**, THT-1, HpHbR, MYO (myosin), and VSG221). Treatment of TbAMPKα1 with the AMPK analog led to an increase in phosphorylation of TbAMPKα1, suggesting activation of the subunit (**Figure 1.12**) (79). This increase in TbAMPKα1 phosphorylation (presumably activation) was proposed to result in a signaling cascade that contributed to the remodeling of LS into a SS transcript profile. Taken together, these data suggest a central role of TbAMPKα1 in *T. brucei* differentiation. The role of TbAMPKα1 phosphorylation and glucose metabolism will be explored in Chapter Three.

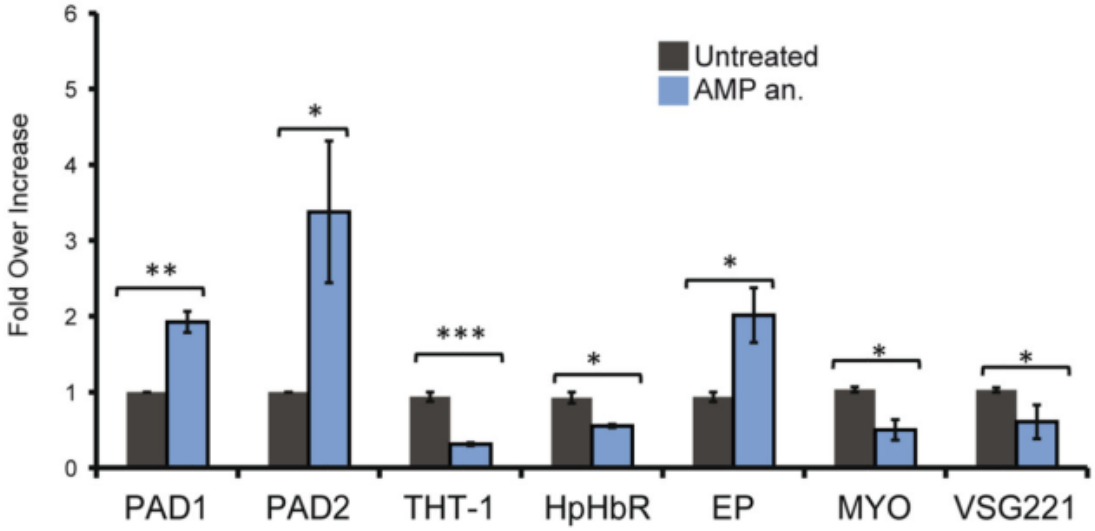

Figure 1.11: Activation of TbAMPKα1 in LS parasites induces a stumpy-like transcript profile. qRT-PCR analysis of transcripts from untreated LS parasites (grey) compared to LS parasites treated with the AMP analog, 8-pCT-2'-O-Me-5'-AMP (blue). MYO- myosin. * = $p < 0.05$, ** = $p < 0.01$, *** = $p < 0.005$. Reprinted with permission from Elsevier Science & Technology Journals, Cell reports. Copyright: Elsevier Science & Technology Journals, **(**79**).**

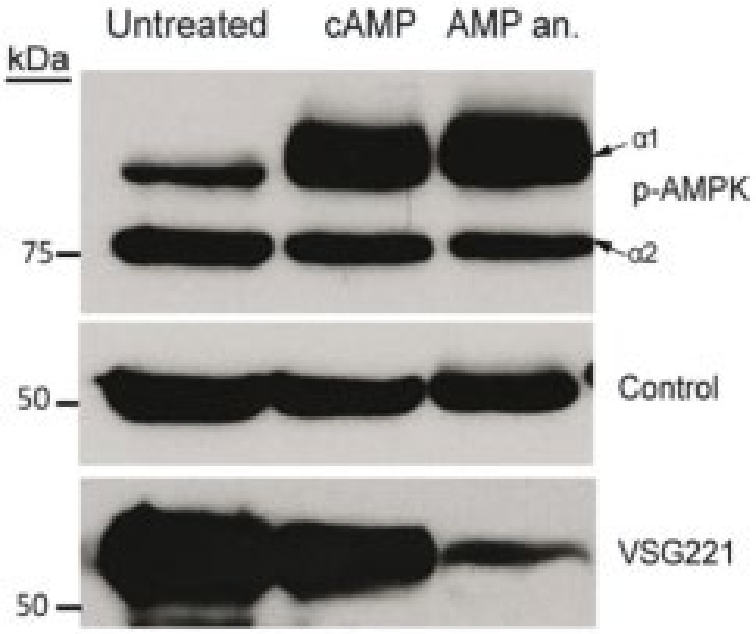

Figure 1.12: Activation of TbAMPKα1 in LS parasites with an AMP analog. Western blot detecting both isoforms of phosphorylated TbAMPKα (TbAMPKα1 is 80.6 kDa and TbAMPKα2 is 70.6kDa). Treatment with either cAMP or the AMP analog (8-pCT-2'-O-Me-5'-AMP) only increases phosphorylation of TbAMPKα1, not TbAMPKα2. p-AMPK detects both activated TbAMPKα isoforms. Control- loading control of cell equivalents. VSG221- LS parasite specific surface molecule VSG protein abundance. Reprinted with permission from Elsevier Science & Technology Journals, Cell reports. Copyright: Elsevier Science & Technology Journals, **(**79**).**

AMPK signaling is hypothesized to be at the center of coordination of parasite differentiation, influencing metabolic changes in the mitochondria and glycosomes (83), a notion supported by the finding that AMPK is central to nutrient stress responses in the related parasite *T. cruzi* (84). This connection of positive and negative regulators of parasite development is currently under further study, with an interest in separating individual pathways and establishing interacting partners. **Figure 1.13** is a cartoon rendition of the proposed model that activation of TbAMPKα1 plays in LS to SS differentiation (79). The presence of 5'-AMP analogs stimulates activation of TbAMPKα1 while inhibiting TbTOR4 signaling, which is a negative regulator of LS into SS development (85). This cascade allows mitochondrial activation and drives parasites to SS differentiation. If however, TbAMPKα1 is inhibited by TbGSK3 or Compound C, TbTOR4 remains active, leaving the mitochondria silent and causing the parasites to retain their LS characteristics.

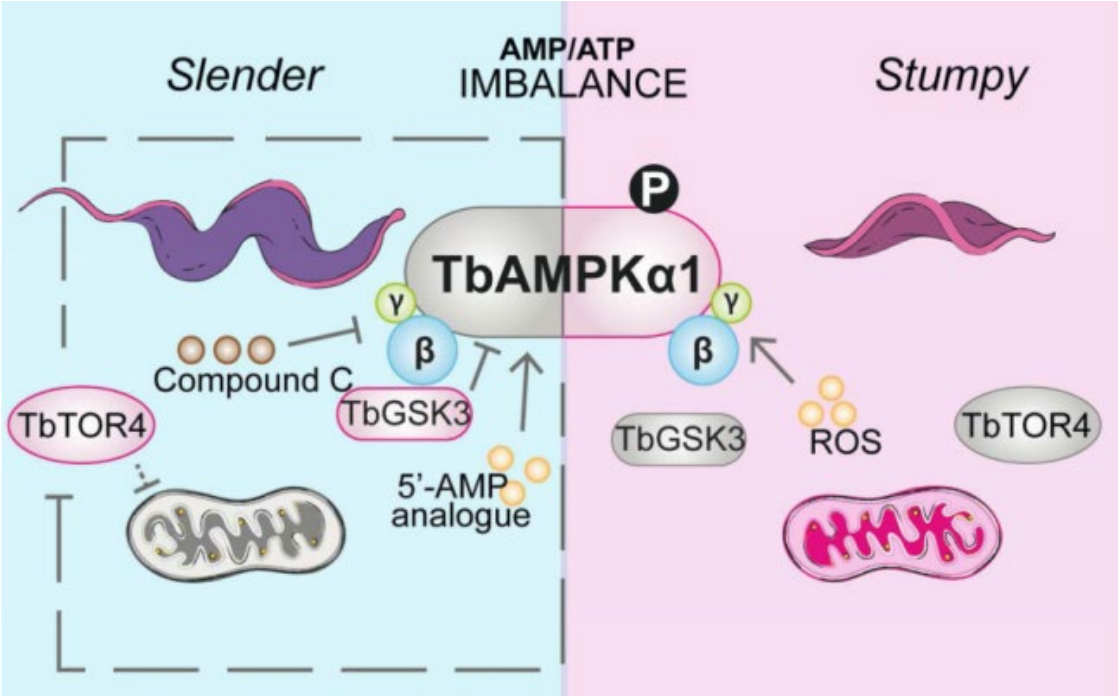

Figure 1.13: Model of TbAMPKα1 regulation of parasite differentiation. TbAMPKα1 activation is essential to drive LS to SS parasite differentiation. Inhibition of TbAMPKα1, through TbGSK3 or Compound C, keeps parasites in the LS life cycle stage. Activation of TbAMPKα1, through 5'-AMP analogs, drives parasites to differentiate into the SS life cycle stage. Reprinted with permission from Elsevier Science & Technology Journals, Cell reports. Copyright: Elsevier Science & Technology Journals, **(**79**).**

References

1. Smith TK, Bringaud F, Nolan DP, Figueiredo LM. Metabolic reprogramming during the Trypanosoma brucei life cycle. F1000Research. 2017;6(May):683.

2. Barry JD, Graham S V., Fotheringham M, Graham VS, Kobryn K, Wymer B. VSG gene control and infectivity strategy of metacyclic stage Trypanosoma brucei. Mol Biochem Parasitol. 1998;91(1):93–105.

3. Tyler KM, Higgs PG, Matthews KR, Gull K. Limitation of Trypanosoma brucei parasitaemia results from density-dependent parasite differentiation and parasite killing by the host immune response. Proc R Soc B Biol Sci. 2001;268(1482):2235–43.

4. Roditi I, Schwarz H, Pearson TW, Beecroft RP, Liu MK, Richardson JP, et al. Procyclin gene expression and loss of the variant surface glycoprotein during differentiation of Trypanosoma brucei. J Cell Biol. 1989;108(2):737–46.

5. Bülow R, Nonnengässer C, Overath P. Release of the variant surface glycoprotein during differentiation of bloodstream to procyclic forms of Trypanosoma brucei. Mol Biochem Parasitol. 1989;32(1):85–92.

6. Bienen EJ, Saric M, Pollakis G, Grady RW, Clarkson AB. Mitochondrial development in Trypanosoma brucei brucei transitional bloodstream forms. Mol Biochem Parasitol. 1991;45(2):185–92.

7. Cronín CN, Nolan DP, Paul Voorheis H. The enzymes of the classical pentose

phosphate pathway display differential activities in procyclic and bloodstream forms of Trypanosoma brucei. FEBS Lett. 1989;244(1):26–30.

8. Sollelis L, Marti M. A Major Step towards Defining the Elusive Stumpy Inducing Factor in Trypanosoma brucei. Trends Parasitol [Internet]. 2019;35(1):6–8. Available from: http://dx.doi.org/10.1016/j.pt.2018.11.009

9. Toh JY, Nkouawa A, Sánchez SR, Shi H, Kolev NG, Tschudi C. Identification of positive and negative regulators in the stepwise developmental progression towards infectivity in Trypanosoma brucei. Sci Rep [Internet]. 2021;11(1):1–14. Available from: https://doi.org/10.1038/s41598-021-85225-2

10. Rojas F, Silvester E, Young J, Milne R, Tettey M, Houston DR, et al. Oligopeptide Signaling through TbGPR89 Drives Trypanosome Quorum Sensing. Cell. 2019;176(1–2):306-317.e16.

11. Szöőr B, Silvester E, Matthews KR. A Leap Into the Unknown – Early Events in African Trypanosome Transmission. Trends Parasitol. 2020;36(3):266–78.

12. Tasker M, Wilson J, Sarkar M, Hendriks E, Matthews K. <Tasker et al_A novel selection regime for differentiation.pdf>. 2000;11(May):1905–17.

13. Sbicego S, Vassella E, Kurath U, Blum B, Roditi I. The use of transgenic Trypanosoma brucei to identify compounds inducing the differentiation of bloodstream forms to procyclic forms. Mol Biochem Parasitol. 1999;104(2):311–22.

14. Szöor B, Dyer NA, Ruberto I, Acosta-Serrano A, Matthews KR. Independent Pathways Can Transduce the Life-Cycle Differentiation Signal in Trypanosoma brucei. PLoS Pathog. 2013;9(10).

15. Liu X, Shah SA, Eid TJ, Shek A. Differences in Glucose Levels Between Left and Right Arm. J Diabetes Sci Technol. 2019;13(4):794–5.

16. Tiessen RG, Rhemrev-Boom MM, Korf J. Glucose gradient differences in subcutaneous tissue of healthy volunteers assessed with ultraslow microdialysis and a nanolitre glucose sensor. Life Sci. 2002;70(21):2457–66.

17. Vickerman K. DEVELOPMENTAL CYCLES AND BIOLOGY OF PATHOGENIC TRYPANOSOMES. Br Med Bull. 1985;41(2):105–14.

18. Cirillo VP. Yeast Cell Membrane. 1962;485–91.

19. Bisson LF. High-affinity glucose transport in Saccharomyces cerevisiae is under general glucose repression control. J Bacteriol. 1988;170(10):4838–45.

20. Özcan S, Dover J, Johnston M. Glucose sensing and signaling by two glucose \nreceptors in the yeast Saccharomyces cerevisiae. EMBO J [Internet]. 1998;17(9):2566–73. Available from: http://www.nature.com/emboj/journal/v17/n9/pdf/7590965a.pdf

21. McClellan CJ, Bisson LF. Glucose uptake in Saccharomyces cerevisiae grown under anaerobic conditions: effect of null mutations in the hexokinase and glucokinase structural genes. J Bacteriol. 1988;170(11):5396–400.

22. Celenza JL, Marshall-Carlson L, Carlson M. The yeast SNF3 gene encodes a glucose transporter homologous to the mammalian protein. Proc Natl Acad Sci U S A. 1988;85(7):2130–4.

23. Gancedo JM. The early steps of glucose signalling in yeast. FEMS Microbiol Rev. 2008;32(4):673–704.

24. Özcan S, Johnston M. Function and Regulation of Yeast Hexose Transporters. Microbiol Mol Biol Rev. 1999;63(3):554–69.

25. Kim JH, Roy A, Jouandot D, Cho KH. The glucose signaling network in yeast. Biochim Biophys Acta - Gen Subj [Internet]. 2013;1830(11):5204–10. Available from: http://dx.doi.org/10.1016/j.bbagen.2013.07.025

26. Kayikci Ö, Nielsen J. Glucose repression in Saccharomyces cerevisiae. FEMS Yeast Res. 2015;15(6):1–8.

27. Foy JJ, Bhattacharjee JK. Biosynthesis and regulation of fructose-1,6-bisphosphatase and phosphofructokinase in Saccharomyces cerevisiae grown in the presence of glucose and gluconeogenic carbon sources. J Bacteriol. 1978;136(2):647–56.

28. Mazón MJ, Gancedo JM, Gancedo C. Inactivation of yeast fructose-1,6-bisphosphatase. In vivo phosphorylation of the enzyme. J Biol Chem. 1982;257(3):1128–30.

29. Hahn S, Young ET. Transcriptional regulation in saccharomyces cerevisiae:

Transcription factor regulation and function, mechanisms of initiation, and roles of activators and coactivators. Genetics. 2011;189(3):705–36.

30. Galdieri L, Mehrotra S, Yu S, Vancura A. Transcriptional regulation in yeast during diauxic shift and stationary phase. Omi A J Integr Biol. 2010;14(6):629–38.

31. Kunkel J, Luo X, Capaldi AP. Integrated TORC1 and PKA signaling control the temporal activation of glucose-induced gene expression in yeast. Nat Commun [Internet]. 2019;10(1):1–11. Available from: http://dx.doi.org/10.1038/s41467-019-11540-y

32. Celenza JL, Carlson M. Structure and expression of the SNF1 gene of Saccharomyces cerevisiae. Mol Cell Biol. 1984;4(1):54–60.

33. Hedbacker K, Carlson M. SNF1/AMPK pathways in yeast. Front Biosci. 2008;13(7):2408–20.

34. Ruiz A, Liu Y, Xu X, Carlson M. Heterotrimer-independent regulation of activation-loop phosphorylation of Snf1 protein kinase involves two protein phosphatases. Proc Natl Acad Sci U S A. 2012;109(22):8652–7.

35. Hardie DG. AMP-activated/SNF1 protein kinases: Conserved guardians of cellular energy. Nat Rev Mol Cell Biol. 2007;8(10):774–85.

36. Crozet P, Margalha L, Confraria A, Rodrigues A, Martinho C, Adamo M, et al. Mechanisms of regulation of SNF1/AMPK/SnRK1 protein kinases. Front Plant Sci. 2014;5(MAY):1–17.

37. Bell GI, Kayano T, Buse JB, Burant CF, Takeda J, Lin D, et al. Molecular Biology of Mammalian Glucose Transporters. Diabetes Care. 1990;13(3):198–208.

38. Devaskar SU, Mueckler MM. The mammalian glucose transporters. Pediatr Res. 1992;31(1):1–13.

39. Mulukutla BC, Yongky A, Le T, Mashek DG, Hu WS. Regulation of Glucose Metabolism – A Perspective From Cell Bioprocessing. Trends Biotechnol [Internet]. 2016;34(8):638–51. Available from: http://dx.doi.org/10.1016/j.tibtech.2016.04.012

40. Daniel BYPM, Love ER, Pratt E. Insulin-stimulated entry. 1975;273–88.

41. Magnuson MA. Glucokinase gene structure. Functional implications of molecular genetic studies. Diabetes. 1990;39(5):523–7.

42. Irwin DM, Tan H. Evolution of glucose utilization: Glucokinase and glucokinase regulator protein. Mol Phylogenet Evol. 2014;70(1):195–203.

43. Rutter GA, Tavare JM, Palmer DG. Regulation of Mammalian Gene Expression by Glucose. News Physiol Sci. 2000;15.

44. Iynedjian PB. Mammalian glucokinase and its gene. Biochem J. 1993;293(1):1–13.

45. Kahn A. Transcriptional regulation by glucose in the liver. Biochimie. 1997;79(2–3):113–8.

46. Mithieux G. Role of glucokinase and glucose-6 phosphatase in the nutritional regulation of endogenous glucose production. Reprod Nutr Dev. 1996;36(4):357–

62.

47. Zelent D, Najafi H, Odili S, Buettger C, Weik-Collins H, Li C, et al. Glucokinase and glucose homeostasis: Proven concepts and new ideas. Biochem Soc Trans. 2005;33(1):306–10.

48. Da Silva Xavier G, Leclerc I, Salt IP, Doiron B, Hardie DG, Kahn A, et al. Role of AMP-activated protein kinase in the regulation by glucose of islet beta cell gene expression. Proc Natl Acad Sci U S A. 2000;97(8):4023–8.

49. Sternisha SM, Miller BG. Molecular and Cellular Regulation of Human Glucokinase. Arch Biochem Biophys. 2019;(663):199–213.

50. Towle HC. Glucose as a regulator of eukaryotic gene transcription. Trends Endocrinol Metab. 2005;16(10):489–94.

51. Ross FA, MacKintosh C, Hardie DG. AMP-activated protein kinase: a cellular energy sensor that comes in 12 flavours. FEBS J. 2016;283:2987–3001.

52. Oakhill JS, Chen ZP, Scott JW, Steel R, Castelli LA, Linga N, et al. β-Subunit myristoylation is the gatekeeper for initiating metabolic stress sensing by AMP-activated protein kinase (AMPK). Proc Natl Acad Sci U S A. 2010;107(45):19237–41.

53. Kim J, Yang G, Kim Y, Kim J, Ha J. AMPK activators: Mechanisms of action and physiological activities. Exp Mol Med [Internet]. 2016;48(4):e224-12. Available from: http://dx.doi.org/10.1038/emm.2016.16

54. Rourke JL, Hu Q, Screaton RA. AMPK and Friends : Central Regulators of b Cell Biology. Trends Endocrinol Metab [Internet]. 2018;29(2):111–22. Available from: http://dx.doi.org/10.1016/j.tem.2017.11.007

55. Hardie DG, Lin S-C. AMP-activated protein kinase – not just an energy sensor. F1000Research [Internet]. 2017 Sep 22;6(0):1724. Available from: https://f1000research.com/articles/6-1724/v1

56. Comp RI, Glucose T, Cell RB, Humans A, Society AP. Red blood cell as glucose carrier: significance for placental and cerebral glucose transfer. 2021;(68).

57. GRUENBERG J, SHARMA PR, DESHUSSES J. D-Glucose Transport in Trypanosoma brucei. Eur J Biochem. 1978;89:461–9.

58. SEYFANG A, DUSZENKO M. Specificity of glucose transport in Trypanosoma brucei Effective inhibition by phloretin and cytochalasin B. Eur J Biochem. 1991;202(1):191–6.

59. Ter Kuile BH, Opperdoes FR. Glucose uptake by Trypanosoma brucei. Rate-limiting steps in glycolysis and regulation of the glycolytic flux. J Biol Chem. 1991;266(2):857–62.

60. VISSER N, OPPERDOES FR. Glycolysis in Trypanosoma brucei. Eur J Biochem. 1980;103(3):623–32.

61. Kessler PS, Parsons M. Probing the role of compartmentation of glycolysis in procyclic form Trypanosoma brucei: RNA interference studies of PEX14,

hexokinase, and phosphofructokinase. J Biol Chem. 2005;280(10):9030–6.

62. Mony BM, Matthews KR. Assembling the components of the quorum sensing pathway in African trypanosomes. Mol Microbiol. 2015;96(2):220–32.

63. Silvester E, McWilliam K, Matthews K. The Cytological Events and Molecular Control of Life Cycle Development of Trypanosoma brucei in the Mammalian Bloodstream. Pathogens [Internet]. 2017;6(3):29. Available from: http://www.mdpi.com/2076-0817/6/3/29

64. Rolin S, Hanocq-Quertier J, Paturiaux-Hanocq F, Nolan DP, Pays E. Mild acid stress as a differentiation trigger in Trypanosoma brucei. Mol Biochem Parasitol. 1998;93(2):251–62.

65. Rojas F, Matthews KR. Quorum sensing in African trypanosomes. Curr Opin Microbiol [Internet]. 2019;52:124–9. Available from: https://doi.org/10.1016/j.mib.2019.07.001

66. Quintana JF, Zoltner M, Field MC. Evolving Differentiation in African Trypanosomes. Trends Parasitol [Internet]. 2021;37(4):296–303. Available from: https://doi.org/10.1016/j.pt.2020.11.003

67. Schuster S, Lisack J, Subota I, Zimmermann H, Reuter C, Müller T, et al. Unexpected plasticity in the life cycle of trypanosoma brucei. Elife. 2021;10.

68. Matthews KR. The developmental cell biology of Trypanosoma brucei. J Cell Sci [Internet]. 2005;118(2):283–90. Available from:

http://jcs.biologists.org/cgi/doi/10.1242/jcs.01649

69. Barrett MP, Tetaud E, Seyfang A, Bringaud F, Baltz T. Functional expression and characterization of the Trypanosoma brucei procyclic glucose transporter, THT2. Biochem J. 1995;312(3):687–91.

70. Bringaud F, Baltz T. Differential regulation of two distinct families of glucose transporter genes in Trypanosoma brucei. Mol Cell Biol. 1993;13(2):1146–54.

71. Wille U, Seyfang A, Duszenko M. Glucose uptake occurs by facilitated diffusion in procyclic forms of Trypanosoma brucei. Eur J Biochem. 1996;236(1):228–33.

72. OVERATH P, CZICHOS J, HAAS C. The effect of citrate/cis-aconitate on oxidative metabolism during transformation of Trypanosoma brucei. Eur J Biochem. 1986;160(1):175–82.

73. Qiu Y, Milanes JE, Jones JA, Noorai RE, Shankar V, Morris JC. Glucose signaling is important for nutrient adaptation during differentiation of pleomorphic African trypanosomes. bioRxiv. 2018;3(5):1–18.

74. MacDonald MJ, Stoker SW, Hasan NM. Anaplerosis from glucose, α-ketoisocaproate, and pyruvate in pancreatic islets, INS-1 cells and liver mitochondria. Mol Cell Biochem. 2008;313(1–2):195–202.

75. Szöor B, Ruberto I, Burchmore R, Matthews KR. A novel phosphatase cascade regulates differentiation in Trypanosoma brucei via a glycosomal signaling pathway. Genes Dev. 2010;24(12):1306–16.

76. Azema L, Claustre S, Alric I, Blonski C, Willson M, Perié J, et al. Interaction of substituted hexose analogues with the Trypanosoma brucei hexose transporter. Biochem Pharmacol. 2004;67(3):459–67.

77. Haindrich AC, Ernst V, Naguleswaran A, Oliveres QF, Roditi I, Rentsch D. Nutrient availability regulates proline/alanine transporters in Trypanosoma brucei. J Biol Chem [Internet]. 2021;296(17):100566. Available from: https://doi.org/10.1016/j.jbc.2021.100566

78. Morris JC, Wang Z, Drew ME, Englund PT. Glycolysis modulates trypanosome glycoprotein expression as revealed by an RNAi library. EMBO J. 2002;21(17):4429–38.

79. Saldivia M, Ceballos-Pérez G, Bart JM, Navarro M. The AMPKα1 Pathway Positively Regulates the Developmental Transition from Proliferation to Quiescence in Trypanosoma brucei. Cell Rep. 2016;17(3):660–70.

80. Clemmens CS, Morris MT, Lyda TA, Acosta-serrano A, Morris JC. Trypanosoma brucei AMP-Activated Kinase Subunit Homologs Influence Surface Molecule Expression. 2010;123(3):250–7.

81. Walsh B, Hill KL. Right place, right time: Environmental sensing and signal transduction directs cellular differentiation and motility in Trypanosoma brucei . Mol Microbiol. 2021;0–1.

82. Quintana JF, Zoltner M, Field MC. Evolving Differentiation in African

Trypanosomes. Trends Parasitol [Internet]. 2020;xx(xx):1–8. Available from: https://doi.org/10.1016/j.pt.2020.11.003

83. Tripathi A, Singha UK, Paromov V, Hill S, Pratap S, Rose K, et al. Erratum for Tripathi et al., "The Cross Talk between TbTim50 and PIP39, Two Aspartate-Based Protein Phosphatases, Maintains Cellular Homeostasis in Trypanosoma brucei " . mSphere. 2019;4(5):1–20.

84. Sternlieb T, Schoijet AC, Genta PD, Alonso GD. AMP-activated protein kinase: A key enzyme to manage nutritional stress responses in parasites with complex life cycles. Vol. 2490, bioRxiv. 2020.

85. Barquilla A, Saldivia M, Diaz R, Bart J-M, Vidal I, Calvo E, et al. Third target of rapamycin complex negatively regulates development of quiescence in Trypanosoma brucei. Proc Natl Acad Sci [Internet]. 2012;109(36):14399–404. Available from: http://www.pnas.org/cgi/doi/10.1073/pnas.1210465109

CHAPTER TWO

GLUCOSE SIGNALING IS IMPORTANT FOR NUTIRENT ADAPTATION DURING DIFFERENTATION OF PLEOMORPHIC AFRICAN TRYPANOSOMES

Yijian Qiu[1], Jillian E. Milanes[1], Jessica A. Jones[1], Rooksana E. Noorai[2], Vijay Shankar[2], and James C. Morris[1*]

[1]Department of Genetics and Biochemistry, Eukaryotic Pathogens Innovation Center, Clemson University, Clemson SC 29634

[2]Clemson University Genomics & Computational Biology Laboratory, Clemson University, Clemson SC 29634

[*]Corresponding Author

Email: jmorri2@clemson.edu (JCM)

Contributions

I contributed to this work parasite preparation from mouse blood. This included preparation of the buffy coats and purification of parasites through DEAE chromatography. I performed flow cytometry experiments on parasite surface molecule staining. This required fixing cells at determined time points and performing EP staining for analysis by flow cytometry. EP staining was performed on parasites from glucose/citrate/cold-shock experiments (**Figure 2.3**). Additionally, I prepared cells for epifluorescence microscopy. This involved fixing cells at determined time points for later immunofluorescence assays for EP or PAD1 proteins for visualization by microscopy (**Figure 2.2**). I prepared LS parasites in low glucose media supplemented with amino acids (**Figure 2.4**). I isolated RNA samples from parasites for use in qRT-PCR and RNA-seq analysis. I also performed qRT-PCR analysis of LS and PF parasites of several genes (THT1, THT2A, EP1, PAD, TbHK1, COX VI, RBP5, RBP6, GAPDH) (**Figure 2.7**). Additionally, I assisted with cell culture throughout all experiments.

Abstract

The African trypanosome has evolved mechanisms to adapt to changes in nutrient availability that occur during its lifecycle. During transition from mammalian blood to insect vector gut, parasites experience a rapid reduction in environmental glucose. Here we describe how pleomorphic parasites respond to glucose depletion with a focus on parasite changes in energy metabolism and growth. Long slender bloodstream form parasites were rapidly killed as glucose concentrations fell, while short stumpy bloodstream form parasites persisted to differentiate into the insect stage procyclic form parasite. The rate of differentiation was slower than that triggered by other cues but reached physiological rates when combined with cold shock. Both differentiation and growth of resulting procyclic form parasites were inhibited by glucose and non-metabolizable glucose analogs and these parasites were found to have upregulated amino acid metabolic pathway component gene expression. In summary, glucose transitions from the primary metabolite of the blood stage infection to a negative regulator of cell development and growth in the insect vector, suggesting that the hexose is not only a key metabolic agent but is also an important signaling molecule.

Introduction

Organisms that occupy multiple biological niches must adapt to different environments. Such is the case for the vector-borne African trypanosome, *Trypanosoma brucei*, a kinetoplastid parasite that is the causative agent of African sleeping sickness. This parasite, which is transmitted by tsetse flies, undergoes a series of developmental steps that yield lifecycle stages which are uniquely adapted for life in the distinct hosts. These adaptations include alterations to metabolic pathways that parallel differences in substrate availability and expression of distinct surface molecules that are required for successful colonization of the new environment.

In *T. brucei* development, differentiation events occur in both the mammalian host and insect vector. As their density increases in the vertebrate bloodstream, long slender (LS) blood form parasites perceive a quorum-dependent parasite-derived signal that triggers differentiation into short stumpy (SS) blood form parasites, a non-dividing form arrested in G0 of the cell cycle (1). When these SS parasites, which are pre-adapted for life in the tsetse fly vector (2), are engulfed by a tsetse fly during a blood meal, they quickly differentiate into dividing procyclic form (PF) parasites that are competent for completion of the lifecycle in the fly.

Development is carefully coordinated with environmental setting, ensuring that the appropriate lifecycle stage is initiated in the correct host and tissue. The ability to perceive and respond to the environment requires detection of cues that trigger signaling pathways to modulate gene expression. SS trypanosomes are exposed to an array of potential signals including fluctuating temperatures, exposure to digestive processes in the fly gut, and

interaction with other trypanosomes. Additionally, there are an assortment of small molecules generated while the blood meal vehicle in which the SS parasites reside is digested by the fly.

In resolving these sensing pathways, potential cues associated with development have been tested. Exposure of SS parasites to a cold shock, specifically a change in environmental temperature of more than 15°C, has been shown to trigger a nearly immediate and reversible expression of the procyclic form (PF) surface molecule EP procyclin (3). However, these cells failed to grow. As cell growth is a critical feature of the transition from SS to PF, this observation suggested that that cold shock alone was insufficient for complete initiation of the developmental program. Notably, cold shock also triggered the expression of a family of carboxylate transporter proteins called "proteins associated with differentiation (PAD)" that have been implicated in the differentiation response triggered by a distinct cue, citrate and cis-aconitate (CCA). Without exposure to cold shock, a high concentration of CCA (6 mM) is required to initiate differentiation. However, exposure of SS parasites to cold shock, which results in increased surface expression of PAD2, triggers EP procyclin expression at extremely low levels of cis-aconitate (0.6-6 μM) (3,4). The tsetse fly midgut contains similar levels of citrate (15.9 μM) and this carboxylic acid has been found to mirror the impact of CCA in SS to PF development, an observation that defines CCA as a potentially physiologically relevant cue (3,5).

Additional cues may be associated with cold shock and citrate that enhance differentiation from SS to PF parasites. These include exposure to mild acid or protease

treatment (5-9). Treatment of SS parasites with either of these cues rapidly initiated EP procyclin expression (~2 hours), but the response mechanisms were different. Mild acid treatment, much like exposure to high levels of CCA, led to phosphorylation of TbPIP39, a phosphatase component of the CCA differentiation cascade (10). This phosphorylation event indicates activation of this differentiation pathway, which was not observed after protease treatment. This suggested the response was due to a distinct signaling pathway (9).

One aspect of differentiation is the adaptation to nutrients available in a particular host. In mammalian blood, LS parasites are exposed to ~5 mM glucose and the hexose serves as a critical carbon source for this form of the parasite. When bloodstream form parasites are taken up by a feeding tsetse fly they experience a rapid drop in glucose concentration, with the sugar depleted from the blood meal in ~15 minutes (11). In this environment, SS parasites persist and differentiate into PF parasites. Reflecting the reduced glucose levels in the environment, PF parasites complete the activation of metabolic pathways that were initiated in the SS lifecycle stage required for metabolism of amino acids like proline and threonine (12-14).

Glucose is a critical carbon source for African trypanosomes but its role in development is unresolved. Manipulation of glucose levels *in vitro* has been shown to alter developmental patterns and gene expression, suggesting a role for the sensing of the sugar in parasite development. Cultured monomorphic bloodstream form (BF) parasites that do not differentiate into SS could be prompted to differentiate into PF parasites by removal of glucose and addition of glycerol to the growth medium (15). The low survival and

differentiation rates, along with the phenomena being noted in a developmentally defective strain, however, call into question the biological relevance of glucose as a single cue to initiate this process. Additional evidence that glucose sensing may play a potential role in development includes the observation that partial inhibition of glycolysis in monomorphic BF with phloretin, a plant-derived dihydrochalcone, or 2-deoxy-glucose (2-DOG), triggered genome-wide transcriptome changes that resembled expression patterns found in SS to PF parasite differentiation. These transcriptome changes included the upregulation of EP procyclin and many genes involved in energy metabolism (16,17). Lastly, PF parasites were found to alter surface molecule expression in a glucose-dependent manner (18,19) in a process that is regulated by mitochondrial enzymes (19). These studies suggest that while glucose manipulation is not sufficient for initiation of a rapid differentiation program in BF parasites, it may play a role in development across several lifecycle stages.

Here, we present evidence that culturing SS parasite in medium with minimal glucose (~5 μM) triggers differentiation to PF parasites. The rate of this glucose-responsive differentiation as measured by EP procyclin expression and initiation of growth was slower than rates observed with other known cues of differentiation. However, the rate was enhanced to physiologically relevant levels when cells were also exposed to a brief cold shock, which is a known potentiator of other differentiation cues. The resulting PF parasites upregulated genes involved in amino acid metabolism to a greater extent than those differentiated through CCA treatment, indicating a potential role for glucose in nutrient adaptation.

Results

Bloodstream form parasite rapidly deplete glucose from the environment

Responses to new environments are particularly important to parasitic microbes that inhabit different hosts during their lifecycles. As African trypanosomes transition from the glucose-rich blood of the mammalian host to the tsetse fly gut, they undergo a marked change in environment. One major change is the rapid (~15 min) depletion of environmental glucose, the primary carbon source used to generate ATP during bloodstream infection (11). This reduction in available glucose is at least in part due to the metabolic activity of the parasites in the blood meal. Both pleomorphic LS and SS parasites isolated from infected rodents rapidly consume glucose *in vitro* with 0.5 mM glucose being nearly depleted from culture medium after a single day by both lifecycle stages (**Fig 2.1A**). After one day, glucose levels were reduced to 37 ± 0.70 and 62 ± 0.60 μM for LS and SS, respectively and the hexose concentration continued to fall on day two, reaching 1.7 ± 0.70 and 15 ± 0.90 μM. The precipitous decline in glucose availability had an impact on LS parasite viability even though the potential carbon sources proline and threonine were included in the medium. While more than 80% of the LS parasites were dead after two days of culture under the very low glucose conditions, SS parasites were less sensitive with >80% of the population viable after the same period (**Fig 2.1B**).

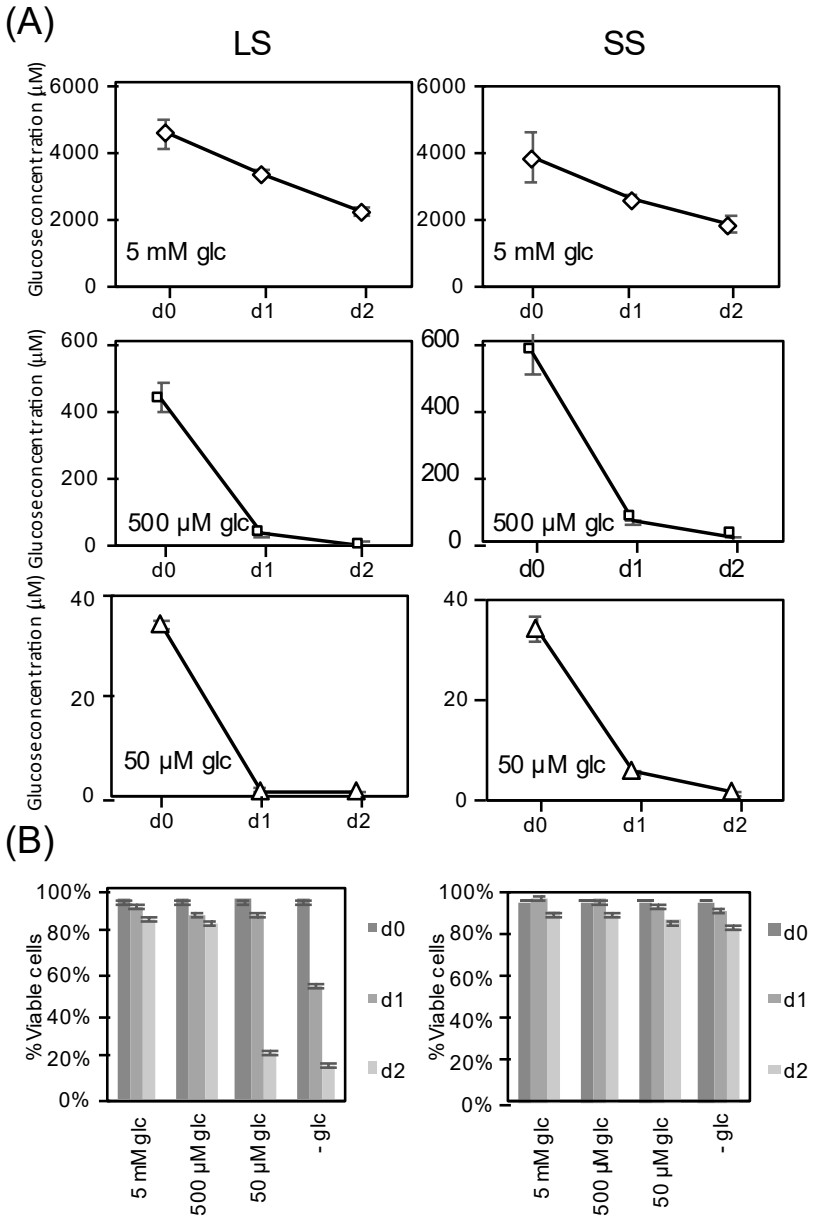

Fig 2.1: Slender form (LS) and short stumpy form (SS) *T. brucei* rapidly deplete glucose. Parasites isolated from rodent buffy coats by chromatography were washed extensively in PBS and then resuspended (4 x 10^5/cells/mL for LS and 5 x 10^5 cells/mL for SS) in RPMIθ supplemented with proline and threonine and different concentrations of glucose.

Fig 2.1: Slender form (LS) and short stumpy form (SS) *T. brucei* rapidly deplete glucose. LS parasites (left column) were isolated after four days of infection and made up nearly 100% of the parasite population as determined by microscopy, while the SS samples (right columns) contained a mixture of SS (~90%) and LS (~10%) parasites as scored by cytometry of PAD1-labeled parasites (not shown). (A) Glucose concentrations in the medium were measured through time as described in the Materials and Methods and standard deviation from experiments performed in triplicate indicated. (B) Parasite viability was scored by propidium iodide staining.

Impact of glucose depletion on the differentiation and proliferation of pleomorphic SS and LS and monomorphic BF parasites

Monomorphic BF parasites cultured in very low glucose medium supplemented with glycerol undergo an inefficient differentiation to PF parasites (15). This process is likely to be a response of monomorphic BF parasites to metabolic stress instead of an orchestrated program in response to a developmental cue. To determine if glucose depletion had a similar impact on cell development in different mammalian lifecycle stages, pleomorphic LS and SS form parasites were incubated in SDM79θ, a very low glucose (~5 μM) PF culture medium that contains amino acids but that lacks glycerol. Culture of SS parasites in SDM79θ under conditions that would normally support PF *in vitro* growth (27°C, 5% CO_2) led to detectable parasite outgrowth by day 3 (**Fig 2.2A**, open

circles). This rate of outgrowth was considerably slower than that generated by known differentiation cues, which we have termed glucose-responsive slow differentiation (GRS differentiation). SS parasites maintained in SDM79θ supplemented with 5 mM glucose (filled circles) did not appreciably grow. While the highly motile and proliferative LS pleomorphic parasites are superficially most similar to the BF monomorphic cells, the LS parasites were different in that they did not tolerate culture in glucose depleted conditions even when glycerol was added to the medium (S1 Fig A).

SS forms in the mammalian bloodstream are arrested in the cell cycle and do not divide, suggesting that the cell proliferation observed after incubation in SDM79θ was a consequence of these SS differentiating to PF. To confirm this, parasites were probed with antiserum specific to the PF marker protein, EP procyclin, and analyzed by immunofluorescence (IF) (**Fig 2.2B**). IF analysis of growing cells revealed that the parasites were morphologically similar to PF cells, expressing a surface coat of EP procyclin not observed in SS or in SS cultured in the presence of glucose (**Fig 2.2B**).

As an additional marker for development, parasites were probed with antiserum specific for PAD1, a marker for SS parasites, and the highest signal was observed on the surfaces of SS parasites freshly isolated from rodent blood, as has been described (**Fig 2.2C**) (4). Growing parasites generated by culture without glucose led to reduced PAD1 labeling, while the majority of those cultured in the presence of glucose for the same period died. However, the few that persisted frequently harbored multiple nuclei, accumulated PAD1 signal in the flagellum, and became elongated (**Fig 2.2C**). The inability of these cells to progress further along the lifecycle suggests that glucose is a negative regulator of

cellular development in the SS parasite. The outgrowth of the normally quiescent SS parasites together with EP procyclin expression and reduction of PAD1 labeling was only observed in the absence of glucose. The majority of the cells remained viable throughout the treatment and the resulting parasites proliferated rapidly as long as they were maintained in very low glucose medium. Together, the expression of PF parasite markers and resumption of growth was indicative of differentiation to the insect form lifecycle stage (S1 Fig B).

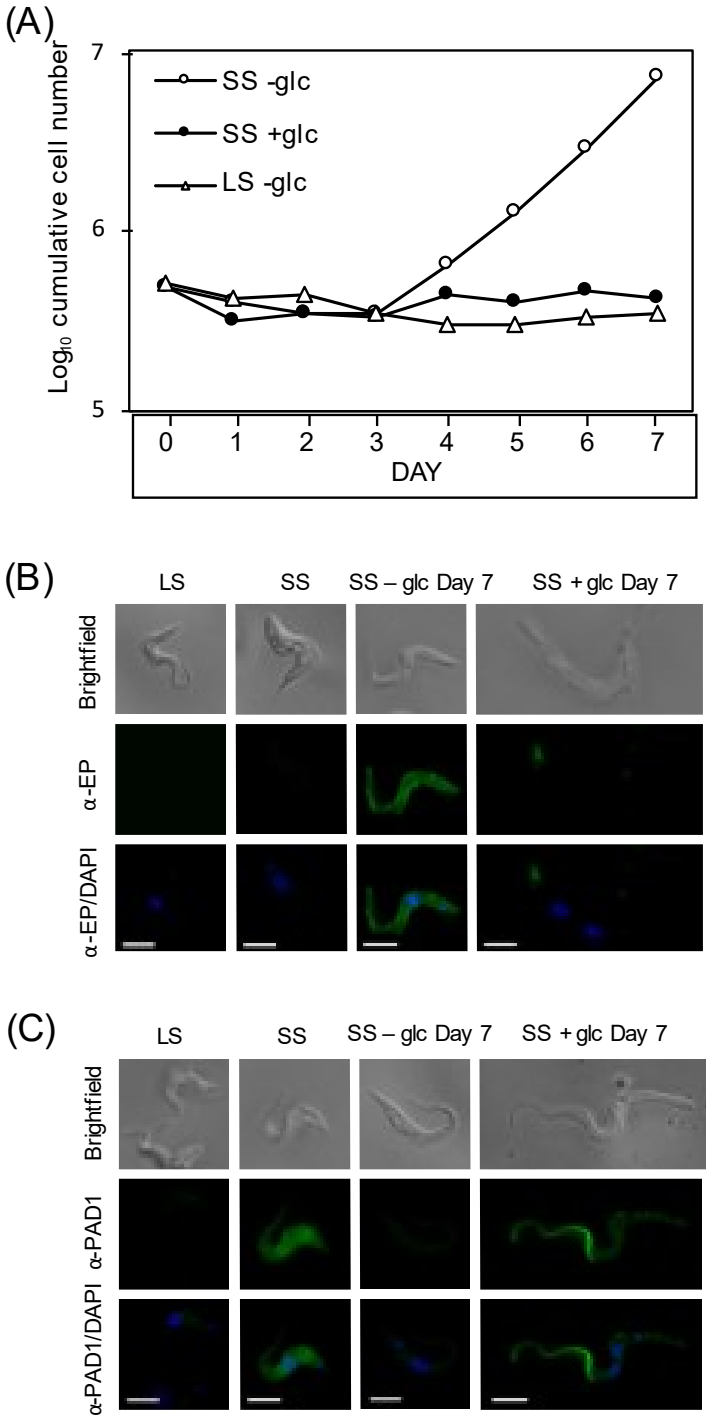

Fig 2.2: *T. brucei* SS growth and surface molecule expression are influenced by environmental glucose availability.

Fig 2.2: *T. brucei* SS growth and surface molecule expression are influenced by environmental glucose availability. (A) LS and SS parasites isolated from rodents were washed extensively and resuspended in very low glucose PF medium, SDM79θ (-glc, ~5 μM), supplemented with (5 mM) or without additional glucose at 27ºC and growth monitored. Growth curves are representative of at least two assays. (B and C) IF analysis of parasites after incubation for seven days with or without glucose. Fixed parasites were visualized by epifluorescence microscopy using antiserum against EP procyclin (B) or PAD1 (C). DAPI was added with anti-fade reagent to stain the nucleus and kinetoplast DNA in all samples. Scale bar = 5 μm.

GRS differentiation rates reach physiologically relevant rates when combined with cold shock

Triggers that initiate SS to PF lifecycle stage differentiation have been widely studied (3-9). While differentiation of SS parasites as a result of glucose depletion alone was delayed when compared to other described triggers, the parasite is likely exposed to multiple environmental conditions in the tsetse fly that could influence this rate. To investigate the effect of additional cues on GRS differentiation, rates of surface molecule expression and growth were monitored (**Fig 2.3**). Exposure of SS parasites to cold shock in combination with citrate levels found in the tsetse fly midgut (15.9 μM, (5)) triggered EP procyclin expression after three hours and cell growth after four days (**Fig 2.3B and**

C). The doubling time of these cells between days 4 and 7 was ~64.5 hours (**Fig 2.3C**, asterisks). Similarly, the combination of cold shock and the near-absence of glucose yielded EP procyclin expression after three hours and cell proliferation was noted within one day. In addition to proliferation, these cells also grew more rapidly compared to those where citrate was added, with a doubling time of ~21.5 hours (open triangles) between days 4 and 7.

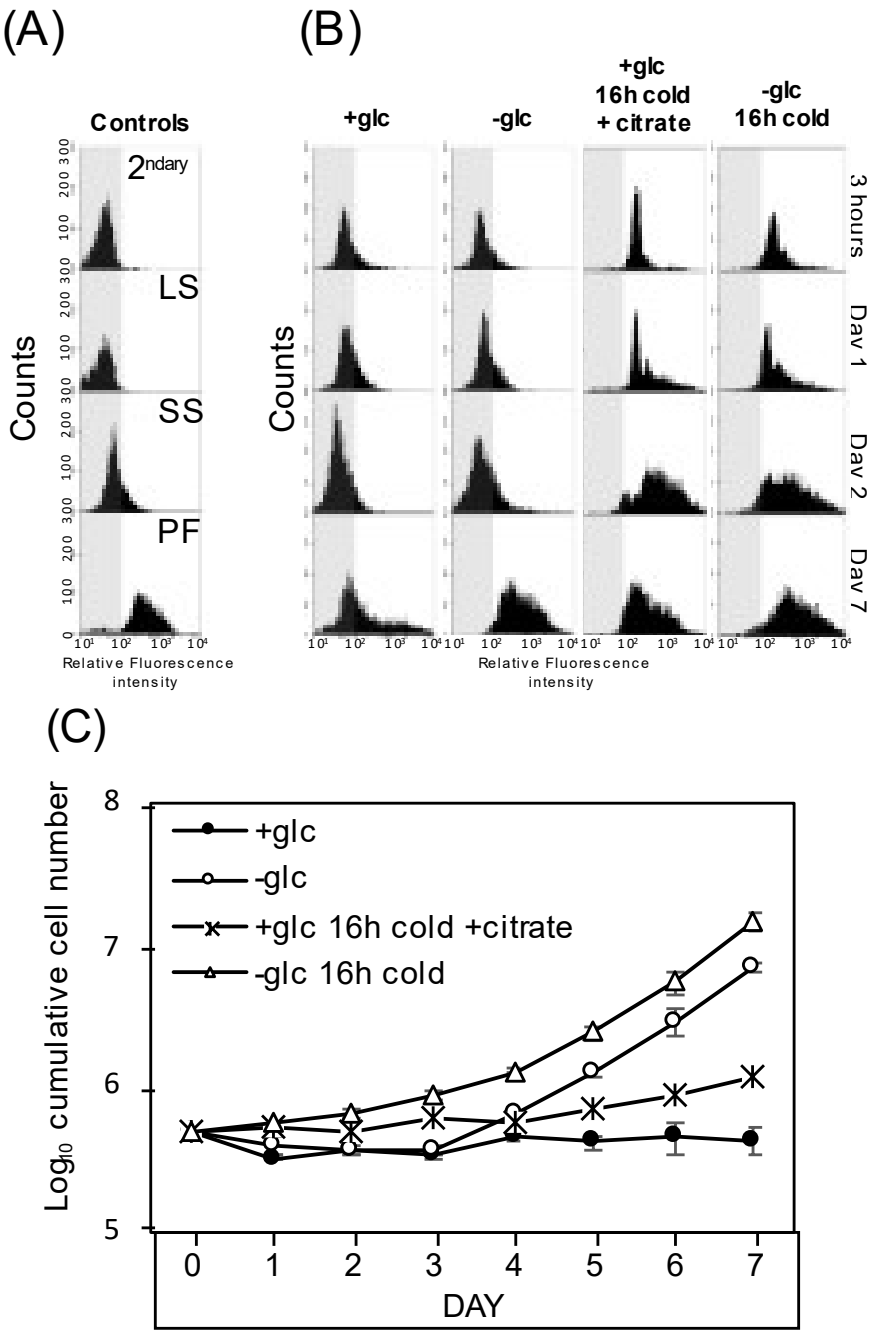

Fig 2.3: The near-absence of glucose is synergistic with cold treatment in triggering differentiation from SS to PF.

Fig 2.3: The near-absence of glucose is synergistic with cold treatment in triggering differentiation from SS to PF. Flow cytometry of (A) control experiments (secondary alone (2^{ndary}); LS, SS, and PF stained with antiserum to EP procyclin) and (B) SS parasites after culture at 37ºC or exposure to 20ºC for 16 hours in HMI9 prior to washing and resuspension in SDM79θ supplemented with 5 mM glucose (+glc) or with physiological levels of citrate (15.9 μM). Cells were fixed at the indicated times, stained with antiserum to EP procyclin, and scored by cytometry (5,000 cells/assay) (C) Growth of parasites exposed to cold shock (20ºC) or 37ºC for 16 hours prior to initiation of this experiment with combinations of other environmentally-relevant cues (at 27ºC). Bars indicate standard deviation in triplicate assays.

Mitochondrial metabolism is required during GRS differentiation

SS parasites can metabolize the abundant glucose in the blood of the mammalian host much like LS parasites. However, SS parasites also express genes that prepare them for life in the glucose-poor environment of the fly gut by upregulating genes required for mitochondrial metabolic functions, including cytochrome C oxidase subunits (20) and respiratory chain complex I genes (21). To test the potential contribution of mitochondrial amino acid metabolism to differentiation, parasite growth was scored after manipulating the available amino acids in the very low glucose (~ 5 μM) bloodstream form medium RPMIθ. When SS parasites were cultured in medium that included proline and threonine for two days prior to being transferred into glucose-free PF medium that had abundant

amino acids (SDM79θ), most cells remained viable and differentiation occurred (**Fig 2.4A**, open circles). Inclusion of threonine alone did not support parasite differentiation (open triangles) while culture in proline alone (open squares) led to a slightly delayed entry into growth when compared to medium with both proline and threonine. RPMIθ medium lacking glucose and both amino acids did not support parasite viability (x symbol), with a greater than 80% loss of SS parasite viability on day one (**Fig 2.4B**). Inhibition of oxidative phosphorylation with oligomycin, an ATP synthase inhibitor, prevented differentiation and was toxic to SS parasites cultured in very low glucose (**Fig 2.4C**, open squares and **Fig 2.4D**). These observations indicated that amino acid metabolism is likely important for satisfying the metabolic needs of the trypanosomes in a minimal glucose environment during GRS differentiation. The ability to adapt to the new carbon source in the absence of glucose is limited to SS parasites, as LS forms are not viable under the same conditions.

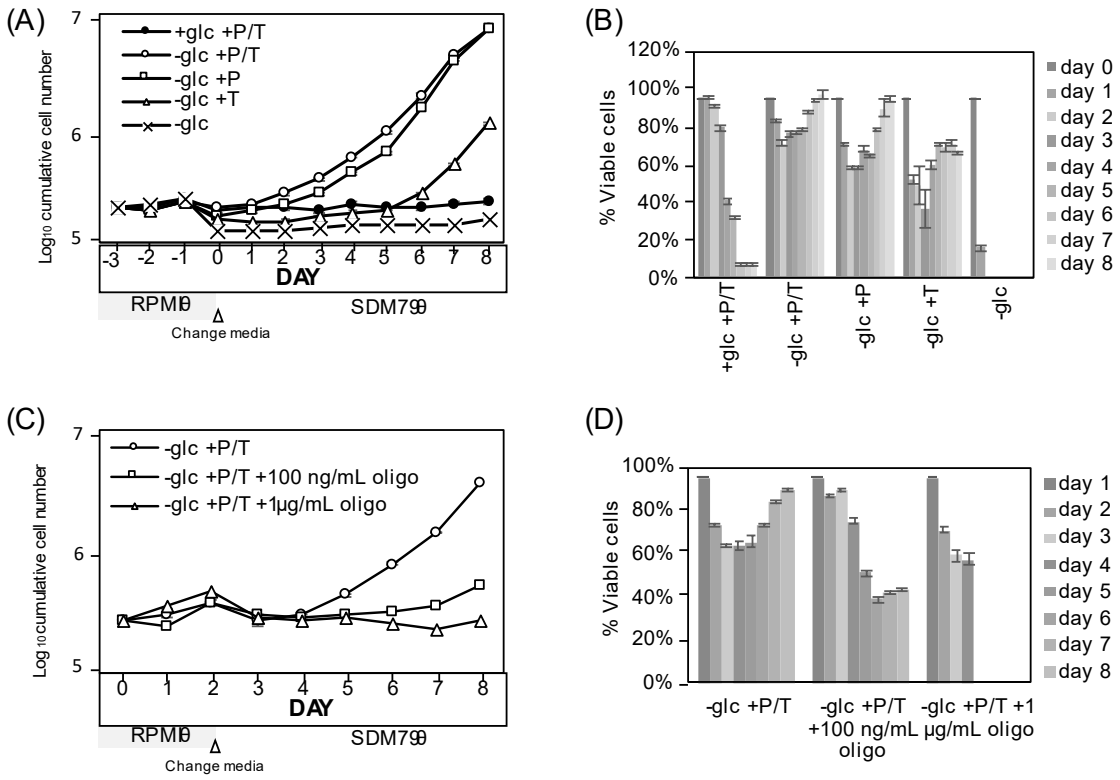

Fig 2.4: Amino acids are required for completion of SS differentiation and cell viability in very low glucose medium. SS parasites cultured in bloodstream form very low glucose medium, RPMIθ (which allowed manipulation of amino acid content) supplemented with or without glucose, proline (P, 4.6 mM), threonine (T, 3.4 mM), or proline and threonine for two days followed by transfer to amino acid-replete SDM79θ were scored for (A) outgrowth and (B) viability by flow cytometry and propidium iodide (PI) staining. (C) Assessment of parasite outgrowth and (D) viability after oxidative phosphorylation inhibition by treatment with oligomycin (either 100 ng/mL or 1 µg/mL) for two days in RPMIθ with proline and threonine (AA) followed by transfer to SDM79θ to provide amino acids for PF parasites. Bars indicate standard deviation in triplicate assays.

GRS differentiation is not enhanced by glycolysis inhibitors

In *Saccharomyces cerevisiae*, nutrient adaptation responses to glucose availability are mediated through non-metabolic pathways that transduce extracellular or intracellular glucose levels into recognizable signals (22). However, the importance of glucose to BF parasite metabolism raises the possibility that culture in very low concentrations of the carbon source could initiate a stress response related to either insufficient ATP production by glycolysis or a failure to synthesize required glycolytic intermediates.

To elucidate the role of glycolysis on the GRS differentiation response in *T. brucei*, parasites were cultured with a variety of sugars at different concentrations and their impact on differentiation was scored. First, conditions were tested to determine if they met the metabolic needs of the glycolysis-dependent LS parasites. As anticipated, 2-DOG, which is phosphorylated by hexokinase and can then inhibit downstream glycolysis, was toxic to LS parasites. While 2-DOG metabolism may cause a disruption in cellular ATP homeostasis (as ATP is consumed during phosphorylation of 2-DOG), 6-deoxy-glucose (6-DOG), an analog of glucose that cannot be phosphorylated by hexokinase, and the five-carbon sugar xylose did not support LS viability (S2 Fig A).

SS parasite outgrowth paralleled the depletion of glucose from the medium, although the minimum concentration of glucose required to trigger this response is unclear. When SS parasites were seeded into RPMIθ supplemented with increasing concentrations of glucose (0, 5, and 50 μM), outgrowth was noted at about the same time regardless of the concentration of glucose (S2 Fig B). Confounding the interpretation of this experiment,

however, SS parasites rapidly metabolize glucose to low levels in culture (**Fig 2.1**), making the assessment of the critical glucose concentration needed to initiate outgrowth difficult.

Non-metabolizable glucose analogs were considered next, in part because SS parasites were anticipated to be less sensitive than LS to these compounds given their ability to persist in the near-absence of glucose (**Fig 2.1**). Incubation with 2-DOG, much like glucose, prevented SS GRS differentiation (**Fig 2.5A**), but this compound was acutely toxic to the SS parasites with >70% lethality after two days of exposure (**Fig 2.5B**). The compound 6-DOG is not a substrate for cellular hexokinases and thus cannot be phosphorylated to enter glycolysis. Similar to 2-DOG and glucose, culturing SS parasites with 5 mM 6-DOG prevented differentiation (**Fig 2.5A**). While incubation in 50 μM 6-DOG prevented outgrowth, 5 μM compound had no impact on cells (**Fig 2.5C**). High concentrations of both glucose and 6-DOG were gradually toxic to SS parasites, with near-complete loss of viability after four days in 5 mM of either compound (**Fig 2.5D**). Lastly, xylose had no inhibitory impact on SS parasite GRS differentiation (**Fig 2.5A**) and, like culturing in very low glucose, was minimally toxic to the SS parasites (**Fig 2.5B**).

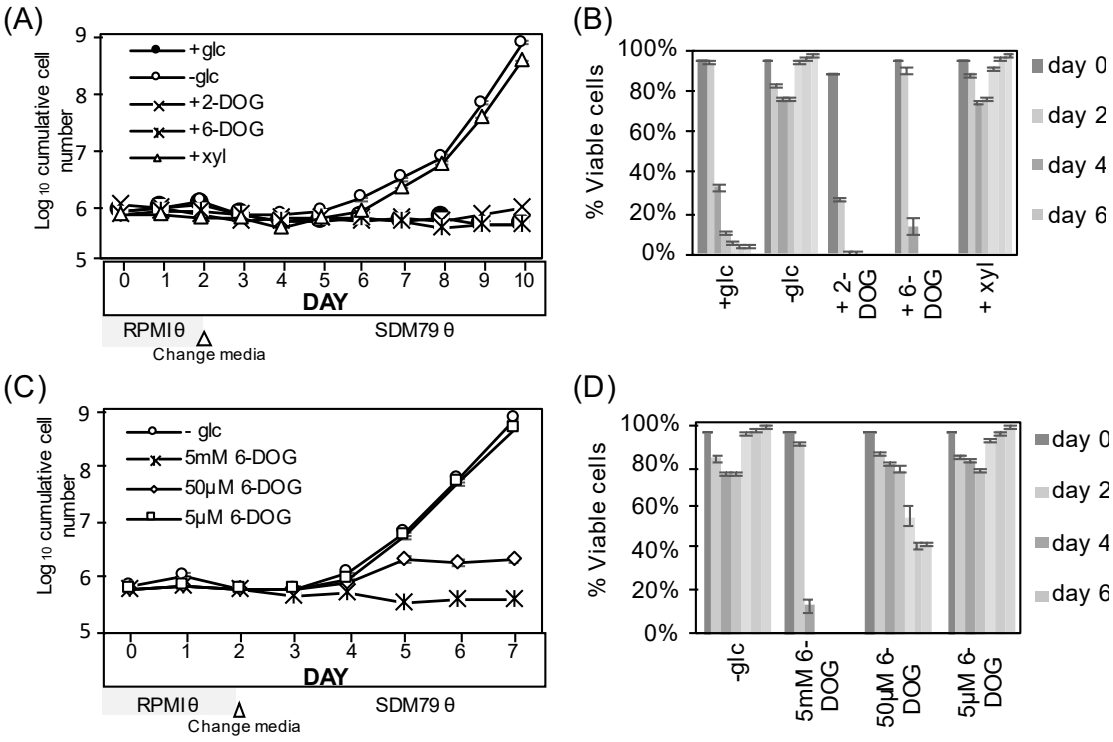

Fig 2.5: Glucose inhibition of differentiation is independent of glycolysis. (A) Outgrowth and (B) cellular viability of SS cultures after treatment with 5 mM of the indicated compound s (xyl, xylose; 2-DOG, 2-deoxyglucose; 6-DOG, 6-deoxyglucose). SS parasites were washed and resuspended (5 x 10^5/mL) in RPMIθ with proline and threonine for the first two days and then transferred to the very low glucose PF medium SDM79θ supplemented with 5 mM of the indicated compound and growth monitored. (The transfer was necessary to provide amino acids required for PF viability.) (C) Impact of varied levels of 6-DOG on SS outgrowth and (D) viability by flow cytometry and propidium iodide (PI) staining. Concentrations of 6-DOG were maintained throughout the experiment. Bars indicate standard deviation in triplicate assays.

Pre-adaption of SS cells at the transcriptome level

SS parasites occupy two extremely different niches (the glucose-rich mammalian blood and the glucose-poor fly midgut) and they express metabolic characters that would allow survival in both hosts (2,23,24). SS parasites isolated from mammalian blood have undergone a dramatic change in gene expression as they developed from LS forms (S1 Table). These SS parasites, and those generated *in vitro* from cultured LS pleomorphic cells through a density-dependent mechanism (25), share similar profiles of statistically significant differentially downregulated genes in a comparison of of Log_2FC with an FDR adjusted $p < 0.05$ in at least one of the two studies (S3 Fig A, S2 Table). The trends for upregulated differentially expressed genes were different but the total number of total upregulated genes in the transition from LS to SS was also smaller.

SS cells were more resistant to culture in very low glucose media, a characteristic of the tsetse fly midgut environment (**Fig 2.1B**). To explore the role that glucose depletion has on gene expression, the transcriptomes of LS parasites, SS parasites cultured in high glucose media, SS parasites cultured in very low glucose media, and PF parasites differentiated from very low glucose media were used to generate a principle response curve (PRC) (26) (S3 FigB). Overall, differentiation from LS to PF parasites yielded changes in expression of many life-stage specific genes (S1 Table). During the transition from LS to SS in the presence of glucose, there was a dramatic change in expression profiles. However, the removal of glucose in the SS life cycle stage only led to a minor alteration in gene expression (S3 Fig B) with a total of 14 upregulated and 21 downregulated genes detected when SS parasites cultured in very low glucose were

compared to those maintained in high glucose through differential gene expression analysis (S3 Table). Interestingly, one of the upregulated genes, DRBD5 (Tb927.6.3480), is required to suppress ESAG9 expression (27,28). ESAG9 is a known stumpy-elevated transcript, so its suppression is anticipated to occur as part of the developmental program to the PF lifecycle stage. Three of the significantly regulated transcripts were also found to be among the top genes associated with progression from LS to PF (**Table 2.1**).

Table 2.1: The fold-change and adjusted p-values from the SS (+glc +AA) vs. SS (-glc +AA) DGE comparison.

Top genes changing towards progression					
Gene ID	**Gene product[1]**	**LogFC (LS vs PF)[2]**	**Adj. p-Value[3]**	**LogFC (SS+glc vs SS-glc)[4]**	**Adj. p-Value[3]**
Tb927.6.510	GPEET	6.22	0.00E+00	0.94	4.70E-14
Tb927.10.15410	gMDH	5.23	0.00E+00	0.57	3.00E-27
Tb927.10.10260	EP1	6.41	8.53E-318	0.86	1.20E-47
Tb927.11.6280	PPDK	4.25	0.00E+00	0.3	1.30E-06
Tb927.10.2560	mMDH	3.51	0.00E+00	0.3	1.70E-07
Tb927.6.520	EP3-2	5.76	0.00E+00	0.46	1.40E-19
Tb927.7.5940	PAD2	2.14	9.7596E-103	1.2	1.50E-76
Tb927.3.4500	FHc	3.70	2.89E-310	0.28	2.80E-05
Tb927.7.210	PRODH	2.65	5.36E-316	0.57	9.70E-24
Tb927.9.5900	GDH	2.86	5.3834E-138	1.2	1.30E-82
Top genes changing against progression					
Gene ID	**Gene product[1]**	**LogFC (LS vs PF)[2]**	**Adj. p-Value[3]**	**LogFC (SS+glc vs SS-glc)[4]**	**Adj. p-Value[3]**
Tb11.1690	VSG	-22.12	0.00E+00	0.01	9.20E-01
Tb927.10.5620	ALD	-1.51	1.69E-184	-0.41	3.40E-17
Tb927.3.3270	PFK	-2.09	6.80E-129	-0.18	2.10E-02
Tb927.10.14140	PYK1	-2.76	0.00E+00	-0.5	3.40E-18
Tb927.10.8230	PDI2	-2.00	2.3277E-174	-1.1	2.20E-97
Tb927.10.2890	ENO	0.06	3.42E-01	-0.24	2.10E-05
Tb927.1.3830	PGI	-1.49	8.29E-93	-0.29	2.50E-06
Tb927.1.700	PGKC	-3.21	6.71E-310	-0.43	2.50E-08
Tb927.10.3990	DHH1	-0.55	8.16E-08	-0.33	3.60E-07
Tb927.10.6880	GAP	-0.65	1.01E-25	-0.75	6.50E-47

[1]GPEET, GPEET procyclin; gMDH, glycosomal malate dehydrogenase; EP1, EP1 procyclin; PPDK, pyruvate phosphate dikinase; mMDH, mitochondrial malate dehydrogenase; EP3-2, EP3-2 procyclin; PAD2, protein associated with differentiation 2; FHc, cytosolic fumarate hydratase; PRODH, proline dehydrogenase; GDH, glutamate

dehydrogenase; VSG, variant surface glycoprotein; ALD, fructose-bisphosphate aldolase; PFK, ATP-dependent 6-phosphofructokinase; PYK1, pyruvate kinase 1; PDI2, protein disulfide isomerase 2; ENO, enolase; PGI, glucose-6-phosphate isomerase; PGKC, phosphoglycerate kinase C; DHH1, DExD/H-box ATP-dependent RNA helicase.

[2]LogFC (LS vs PF), the $\log_2$-fold change value of transcripts from LS incubated in in glucose rich media compared to that from PF very low glucose media.

[3]Adjusted p-value was calculated using the Benjamini-Hochberg method on p-values generated by likelihood ratio.

[4]LogFC (SS+glc vs SS-glc), the $\log_2$-fold change value of transcripts from SS incubated in very low glucose media compared to that from SS in glucose rich media.

Pleomorphic PF cell growth is inhibited by glucose

Differentiation of PF parasites from SS parasites by either citrate treatment (6 mM) or incubation in the near-absence of glucose yielded parasites with a growth deficiency upon culture in glucose-rich medium (**Fig 2.6A**). These pleomorphic PF cells had average doubling times (between days 4 and 7) that were 4.3-fold and 2.9-fold greater, respectively, than the doubling time of parasites maintained in medium without glucose generated by the same differentiation means (**Fig 2.6A**, compare filled symbols to open circles and asterisks). The growth defect in the presence of glucose persisted for several weeks, with cell division becoming nearly undetectable on day 12. However, cells continuously cultured in glucose-replete medium eventually (3-4 weeks) resumed growth (S1 Fig B).

The addition of 5 mM glucose to the environment slowed the growth of PF parasites previously differentiated by glucose deprivation when compared to similar cells maintained in very low glucose (**Fig 2.6B**, open squares compared to open circles, day 3-7). This growth retardation was relieved within one day of glucose removal from the medium (open squares, day 8-14). While citrate-treated cells differentiated in the presence of glucose within one day (filled triangles), these PF parasites had a reduced growth rate when compared to cells differentiated by glucose depletion (open circles, day 3-7). This growth retardation was partially relieved after ~3 days of culture in very low glucose (filled triangles, day 8-14) but the ~30 hour doubling time still lagged behind the ~18 hours doubling time of cells differentiated by glucose depletion (open squares, based on rates on days 11-14). Glucose was not alone in its ability to temper pleomorphic PF growth, as 5 mM 6-DOG, but not lower concentrations (**Fig 2.6D**), was able to inhibit parasite growth even though it is not a metabolizable sugar (**Fig 2.6C**, x symbol). Similarly, 2-DOG inhibited growth of pleomorphic PF parasites differentiated in the absence of glucose (not shown). Xylose had no impact on PF cell growth (**Fig 2.6C**, open triangles).

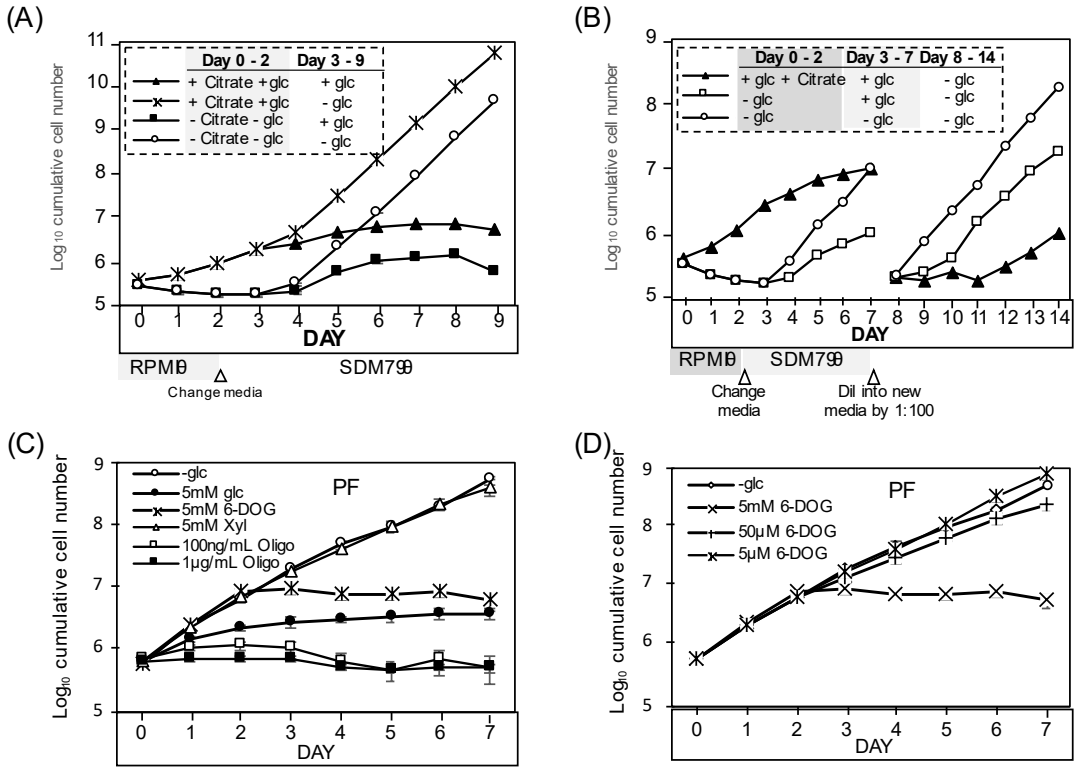

Fig 2.6: Pleomorphic PF cell growth is suppressed in the presence of glucose. (A) Comparison of growth of PF parasites differentiated from SS parasites by treatment with 6 mM citrate in the presence of glucose (5 mM) to those differentiated by glucose depletion. (B) Growth suppression was reversible by removal of glucose. SS parasites were cultured for two days in the presence of citrate (6 mM) or near-absence of glucose and then cultures were resuspended in glucose-replete or deficient SDM79θ for five days, prior to dilution in fresh medium on the eighth day of growth. (C) Growth of pleomorphic PF cells (differentiated for 7 days from SS) in SDM79θ with assorted sugars (6-DOG, 6-deoxy-glucose; xyl, xylose) or (D) in different concentrations of 6-DOG. Panel A and B are representative of at least duplicate assays, while in panel C the bars indicate standard deviation in triplicate assays.

PF parasites differentiated in glucose depleted medium upregulate amino acids metabolism

Comparison of transcriptome profiles of LS parasites to PF parasites differentiated by culture of SS parasites in very low glucose (5 μM) by differential gene expression analyses revealed that a total of 1,310 transcripts were differentially-regulated in the PF cells, with 694 upregulated and 616 downregulated genes (false discovery rate (FDR) < 0.05, $|\log FC| \geq 1.0$, and counts per million (CPM) > 10; S1 Table for a complete list and verification of a subset by qRT-PCR). This result agrees with previous transcriptome studies which found that a similar number of total genes were differentially expressed between the LS and PF life stages (23,29).

To determine if the different cues used to trigger differentiation yielded distinct transcript profiles, the data sets for PF parasites differentiated by culture in very low glucose or by culture with CCA in the presence of glucose were compared to the transcriptome of LS parasites (23,29). Transcripts encoding proteins known to be enriched in BF parasites, like ESAG2, ESAG11, THT1-, and phosphoglycerate kinase C (PGKC) were significantly downregulated in both PF transcriptomes, whereas those known to be enriched in PF parasites, including EP1, EP2, EP3, GPEET, trypanosome hexose transporter 2A (THT2A), purine nucleoside transporter NT10, and several proteins involved in electron transport chain and mitochondrial translation were significantly upregulated (**Fig 2.7A**).

While these life-stage-specific marker genes were similarly regulated, differences in the regulation of genes involved in major metabolic pathways were observed. Genes

required for glycolysis, the primary catabolic pathway used for ATP production in BF parasites, were largely downregulated (60% of the known or predicted genes in the pathway) in PF parasites differentiated by culture in glucose depleted medium, while PF parasites differentiated by the presence of cis-aconitate had 20% of the known or predicted genes in the pathway downregulated (**Fig 2.7B**, S4 Table). The percentage of upregulated genes involved in gluconeogenesis was higher in PF parasites differentiated by glucose depletion (50%) than those differentiated by cis-aconitate, where the expression of genes in the pathway remained largely unchanged (**Fig 2.7B**, S4 Table). Similarly, the percentage of upregulated genes known to be required for succinate and acetate/acetyl-CoA metabolism were higher in PF parasites generated by glucose depletion (56% of known genes involved) than in cis-aconitate differentiated PF parasites (11%).

A larger difference was noted for changes in expression of genes in pathways associated with amino acid metabolism. While the cis-aconitate differentiated PF parasites showed upregulation in several transcripts involved in proline catabolism and electron transport chain (such as succinyl-CoA synthetase alpha subunit (Tb927.3.2230), succinate dehydrogenase assembly factor 2 (SDHAF2, Tb927.6.2510), and the mitochondrial precursor of Rieske iron-sulfur protein (RISP, Tb927.9.14160), to name a few, the majority of transcripts in the pathways were unchanged (**Fig 2.7B**, S4 Table). By comparison, expression of most of the known genes involved in proline, threonine, and electron transporter chain (~78%, ~100%, and ~93%, respectively) were upregulated in PF parasites generated by GRS differentiation.

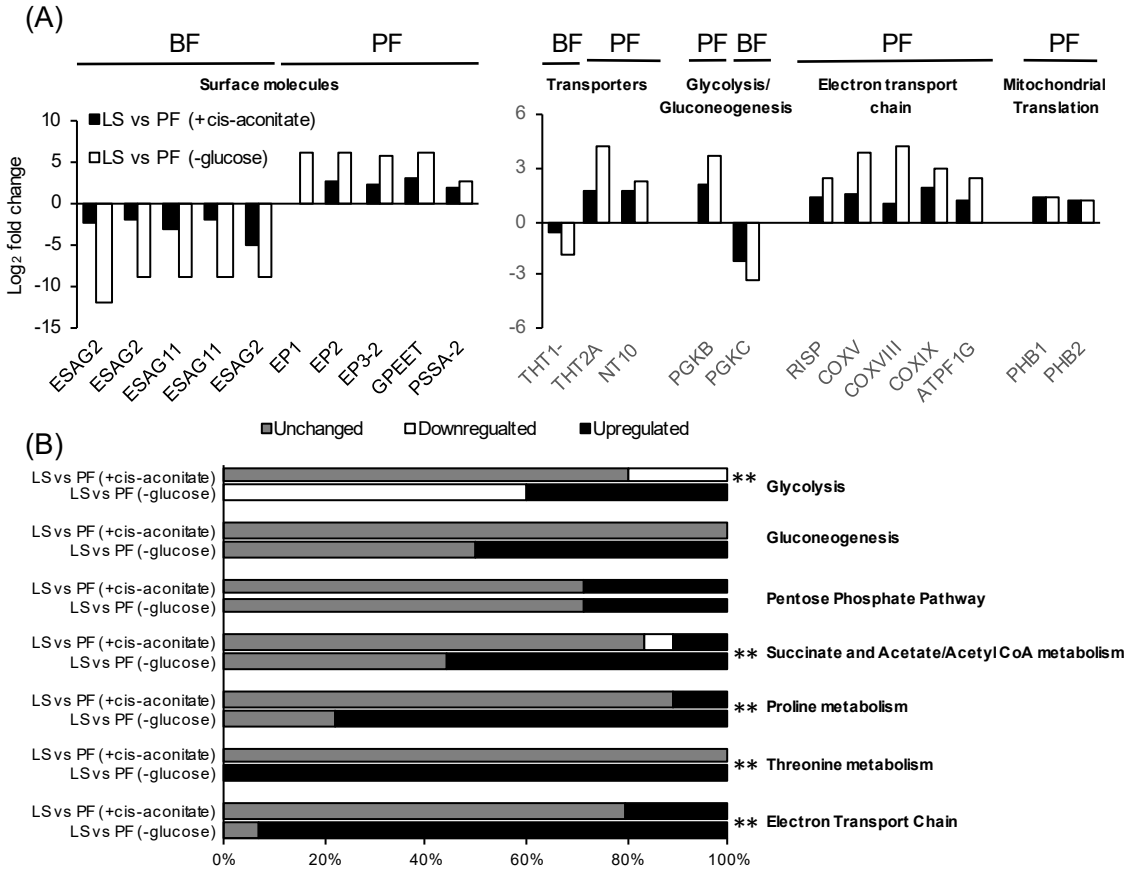

Fig 2.7: Evaluation of pleomorphic PF differentiated by different cues at the transcriptome level. (A) A comparison of the relative transcript abundance of PF parasites to LS parasites for a subsect of life stage-enriched genes. PF were generated by differentiation of SS parasites using either glucose depleted medium (-glc) or cis-aconitate treatment (+cis-aconitate). All transcripts included had >2-fold change and adjusted p-values < 0.05 except for THT1- in PF (+cis-aconitate), which was downregulated less than twofold with an adjusted p-value > 0.05. N/A, data not available. ESAG2, expression site-associated gene 2; ESAG11, expression site-associated gene 11; EP1, EP1 procyclin; EP2, EP2 procyclin; EP3-2, EP3-2 procyclin; GPEET, GPEET procyclin; PSSA-2, procyclic form surface phosphoprotein;

Fig 2.7: Evaluation of pleomorphic PF differentiated by different cues at the transcriptome level. THT1-, glucose transporter 1B; THT2A, glucose transporter 2A; NT10, purine nucleoside transporter 10; PGKB, phosphoglycerate kinase B; PGKC, phosphoglycerate kinase C; RISP, rieske iron-sulfur protein; COXV, cytochrome oxidase subunit V; COXVIII, cytochrome oxidase subunit VIII; COXIX, cytochrome oxidase subunit IX; ATPF1G, ATP synthase F1 subunit gamma protein; PHB1, prohibitin 1, PHB2, prohibitin 2 (B) The percentage of transcripts in major metabolic pathways (as identified by GO term definition and confirmed in TrypanoCyc (60)) that are regulated in PF differentiated by cis-aconitate or glucose depletion compared to LS. For glycolysis and gluconeogenesis, only enzymes that participate in one of the reactions were included. Upregulated transcripts are those that increased > 2-fold and had adjusted p-values < 0.05 in PF compared to LS, while downregulated transcripts were decreased > 2-fold with adjusted p-values < 0.05. Chi-squared goodness of fit tests were performed for genes in each pathway to determine whether the proportions of regulated genes between PF differentiated by cis-aconitate and glucose depletion were different. ** indicates p-value < 0.01, suggesting transcripts involved in the pathway are differentially regulated in PFs differentiated by the two cues.

Discussion

Cellular mechanisms for adaptation to environmental nutrient availability are found in organisms as divergent as microbes and humans. These mechanisms typically initiate upregulation of alternative metabolic pathways, reduction of macromolecule synthesis in response to limited nutrients, and enhancement of the expression of genes that may improve organism dispersal to ultimately lead to colonization of new, nutrient-rich environments. Additional responses include those that trigger development into quiescent or environmental-resistant forms that can tolerate exposure to hostile environments.

The rapid depletion of glucose from a tsetse fly blood meal, as described by Vickerman (11), suggests that glucose abundance could serve as a cue for developmental programming. However, the rate of GRS differentiation is, by itself, likely too slow to be biologically relevant. It is interesting, however, that combination with other treatments known to influence differentiation (but that are by themselves insufficient to trigger differentiation) potentiated the rate of differentiation to levels similar to those observed with described cues. A temporary cold shock treatment (9) combined with culture in very low glucose led to detectable EP procyclin protein expression after three hours and outgrowth within one day. This was a notable reduction from the three-day period required when parasites were grown in minimal glucose alone (**Fig 2.3**). Cold shock treatment also upregulates the carboxylate transporter PAD2 and is therefore important for sensitizing SS parasites to physiologically-relevant levels of CCA (3,4). Interestingly, glucose depletion also upregulated PAD2 expression. Given that glucose is precipitously depleted from the blood meal (11), the upregulation of PAD2 in response to glucose depletion may serve as

an additional or alternative means of increasing SS parasite sensitivity to CCA. It is also interesting that many expression site associated genes (ESAGs) are significantly regulated both during the transition from LS to PF and when glucose is removed from SS (S1, S3 Table). Expression changes of these genes, which are proximal to telomeres, suggests a potential variation in active expression sites. Others have postulated that environmental stimuli can influence gene expression and ultimately developmental fate by modification of chromatin at the epigenetic level (30).

The differentiation of SS parasites in response to reduced glucose availability required inclusion of amino acids in the medium at the initiation of, and throughout, differentiation and yielded PF parasites with transcriptome-wide alteration of the expression of major metabolic pathway genes, a pattern not found in PF parasites differentiated through cis-aconitate treatment. This difference suggests that glucose availability may influence activation of metabolic pathways required for different developmental stages. To assess if the gene expression pattern was uniquely associated with glucose depletion, the transcriptome changes in response to glucose depletion were compared to transcriptional data generated from analysis of nine other transcriptomes (S4 Table) (17,25,29,31-36). The analyses include transcriptomes from pleomorphic EATRO1125 LS and PF and pleomorphic TREU927 LS and PF generated from mouse-derived SS parasites with 6 mM of cis-aconitate, monomorphic Lister 427 BF and lab-adapted PF parasites, and monomorphic BF (Lister 427) parasites with RBP10 knocked down. These datasets provide insight at a genome-wide scale of the regulation of transcripts during transition of trypanosomes from blood to insect stages. Because these

were generated using different sample preparation methods, library construction approaches, and bioinformatic methodologies, comparing the transcriptomes is challenging and may potentially reduce the value of the data found in samples scored by more sensitive approaches. Therefore, for this comparison, genes with a fold-change ≥ 2 and a p-value <0.05 in a given study were considered as significantly regulated and the regulation (noted as up- or downregulated) were then compared to those identified in this work. Five of the transcriptomes with accessible statistical analysis were chosen as representatives and differences and similarities to the transcriptome generated in this study were compared (S4 Fig). The cells used in the five treatments were maintained in media that contained at least 5 mM glucose (17,23,31,33,36).

While PF cells generated in these studies generally downregulated glycolytic genes and upregulated amino acid metabolism genes, the proportion of the genes differentially regulated in these categories was significantly different from the regulation generated by glucose depletion (S4 Fig). Interestingly, the upregulation of the two hexokinase genes was only observed when PF were maintained in media with very low glucose levels or when the cells were supplemented with glycerol (S4 Table, Qiu, Queiroz, and Naguleswaran columns). While the trend was not statistically significant, the overall regulation of the glycolytic and amino acid metabolic pathways in these three PF lines was highly similar. This similarity may not be a coincidence but may reflect the influence of glucose and glycerol on a regulatory pathway. Consistent with this, inclusion of glucose or glycerol in growth medium have been shown to have the opposite impact on GPEET transcript levels, a marker of early PF parasites (19).

In *T. brucei*, the transcriptional regulation largely occurs at the post-transcriptional level, a process that frequently involves the action of RNA binding proteins (37). One such RNA binding protein, RBP10, has been shown to play a major role during the transition of parasites from blood to insect stages (17,38). As an RNA binding protein that is exclusively expressed in BF parasites, RBP10 influences gene expression at both transcript and protein levels. Knocking down RBP10 in BF parasites has been found to trigger a series of developmental changes that eventually give rise to PF parasites (38). Consistent with a role in regulating development, RBP10 transcript levels were found to be downregulated in most of the PF transcriptomes compared here, including the one derived from glucose depletion in this study (S4 Table). Comparison of the genes that were statistically significantly differentially expressed in the work presented here and in the Mugo and Clayton study (38) revealed that transcriptional changes during transition from the LS to PF tended to be similar in direction (either up or downregulated) but were of greater magnitude than those found when RBP10 was silenced in BF parasites (S3 Fig C,D, S1 Data). This suggests potential differences in the differentiation induced by the two approaches (S3 Fig C) and may explain why the dramatic alteration of transcript abundance for genes involved in energy metabolism observed in our study was also not observed in RBP10 knockdown BF cells (S4 Fig; S4 Table). A similar trend was visible when comparing the transition from LS to SS to BF with RBP10 RNAi but the number of statistically significantly differentially expressed genes shared between these comparisons were significantly lower (S3 Fig D, S1 File).

GRS differentiation includes a nutrient adaptation mechanism that responds to glucose, either as a result of the perception of a signal through glucose metabolism or by signaling through a glucose-specific receptor-mediated pathway. The observation that GRS differentiation in SS parasites was inhibited by low concentrations of 6-DOG, a glucose analog that is not a substrate for glycolysis, suggests that *T. brucei* perceives the presence of the hexose through a glycolysis-independent pathway. In other eukaryotes, glucose receptor-mediated signaling is known to influence cellular responses to extracellular glucose (39,40). The identity of potential glucose receptors that would participate in this sort of response in *T. brucei* is unknown, but it is possible that one or more of the trypanosome hexose transporter family members, or one of the hexokinases, could serve this role, given that they have similar K_M values (52 μM for the trypanosome hexose transporter 2 and 90 μM for the trypanosome hexokinase 1) to the concentration of glucose required to inhibit GRS differentiation (50 μM) (41,42). However, the involvement of glucose metabolism in cellular development and nutrient adaptation cannot be completely ruled out. Treatment of monomorphic BF with phloretin, a glucose uptake inhibitor, has been shown to trigger a differentiation-like transcriptome change in the parasites (16).

The pleomorphic PF parasites generated by the GRS differentiation offer additional evidence for two pathways to sense glucose. First, 6-DOG inhibited growth of these PF cells, suggesting metabolism was connected to the observed growth repression. However, the onset of growth inhibition by addition of glucose to the medium was more rapid than that observed using 6-DOG (**Fig 2.6C**), possibly because it activated both the glycolysis-

dependent and the glucose receptor-mediated pathways simultaneously, while 6-DOG could only initiate the receptor-mediated pathway. Alternatively, glucose uptake may have been more efficient which could impact the activity of an intracellular glucose binding protein-based response.

While LS parasites are dependent on host glucose for ATP production, PF parasites have a more dynamic metabolism and are capable of utilizing either amino acids or sugars as carbon sources. Laboratory-adapted PF parasites grown in glucose-rich culture media preferentially metabolize glucose with coincident downregulation of proline consumption (43,44). PF parasites generated by culture of SS forms in reduced glucose media responded to the sugar differently, by displaying growth inhibition (**Fig 2.6**). This was similar to glucose-induced growth inhibition noted in PF parasites isolated from tsetse fly midguts (45), which presumably occurred because these parasites had been adapted to the amino acid-rich fly gut environment (46). Additionally, the negative impact of glucose on parasite growth may explain why trypanosome infections are more readily established in blood-starved tsetse flies than in fed insects (47,48).

In conclusion, the glucose signaling pathway in the African trypanosome may not be directly connected to glycolysis, but the pathway does play an important role in the metabolic adaptation of the parasite (**Fig 2.7**, S3 Fig A, S4 Table), which may in turn influence other aspects of developmental differentiation through known pathways.

Materials & Methods

Ethics Statement

All procedures were carried out in accordance with the PHS Policy on the Care and Use of Laboratory Animals and in accord with the CU PHS Assurance Number A3737-01 under the approval of the Clemson University Institutional Animal Care and Use Committee (IACUC). Clemson University animal research and teaching facilities and programs are registered by USDA, Animal Care (AC) [Registration Number 56-R-0002] and animal research programs and facilities have full accreditation from the Association for Assessment and Accreditation of Laboratory Animal Care, International (AAALAC). Euthanasia by heavy anesthetization followed by bilateral pneumothorax was used based on recommendations from the AVAM Guidelines for the Euthanasia of Animals.

Trypanosomes and cell culture conditions

Trypanosoma brucei brucei 427 BF parasites, a representative monomorphic strain, were cultured as described in HMI-9 medium (49). LS and SS *T. brucei* EATRO1125 were isolated from infected Swiss Webster mice 3-4 or 6-7 days after infection, respectively, by preparation of buffy coats and purification through DEAE chromatography. Cells were maintained in HMI-9 medium (with LS density kept under 5×10^5 cells/mL) for one day before use.

To assess trypanosome responses to environmental manipulations, a BF medium with very low glucose, RPMIθ, was made by modifying HMI-9 (49) with additional features adapted from (50) including replacement of IMDM with glucose-free RPMI that

has been buffered with HEPES to pH 7.4, elimination of SerumPlus and use of dialyzed FBS (10% f.c.). A PF medium with very low glucose, SDM79θ, was generated by eliminating glucose from SDM79 (51) using dialyzed FBS (10% f.c.) in lieu of standard serum. Both media have a final glucose concentration of ~5 μM. To score the impact of culturing under extremely low glucose conditions, parasites were washed three times in warmed PBS to eliminate residual glucose before resuspension at ~5 × 10^5 cells/mL in prewarmed (at 27°C) SDM79θ with or without additional carbon sources or glucose analogs added. Cultures were incubated at 27°C in 5% CO_2 with their medium changed every two days. Cell numbers were scored daily during the first week and every-other-day in the second week and cell viability determined by propidium iodide (PI) staining (0.5 μg/ml final concentration) followed by flow cytometry on an Accuri BD flow cytometer (BD Biosciences, San Jose, CA).

Glucose measurements

To assay the glucose concentration in the parasite growth medium, an Amplex™ Red Glucose/Glucose Oxidase Assay Kit (Invitrogen, Carlsbad CA) was used. All time points were tested in triplicate, with parasites removed by centrifugation (16,000 x g, 2 min) and supernatant tested according to the protocol provided by the manufacturer.

RNA analysis

To assess the consequence of glucose availability on steady-state transcript abundance, RNAseq was performed on LS cells isolated from rodents and cultured in

HMI9 for one day, SS cells incubated for one day in RPMIθ with or without added glucose (5 mM) supplemented with or without proline and threonine, and PF cells differentiated from SS in very low glucose. Three biological replicates of each treatment were conducted and RNA was isolated using an Aurum Total RNA Mini Kit (Bio-Rad). Libraries were constructed using the TruSeq Stranded mRNA Library Prep Kit (Illumina, San Diego, CA USA). The total RNA fraction was enriched for mRNA using poly(A) capture and libraries were constructed using the TruSeq Stranded mRNA kit. Quality metrics were analyzed for all samples using FastQC (http://www.bioinformatics.babraham.ac.uk/projects/fastqc). Trimming of low quality bases and adapter sequences was performed using trimmomatic (52). Trimmed reads were aligned using gsnap to the TriTrypDB-28_TbruceiTREU927 genome, minus the 11 bin scaffold/chromosome. The maximum number of mismatches allowed was determined by the formula ((readlength+index_interval-1)/kmer - 2)), where readlength = 150 and index_interval=3. Subread's featureCounts counted by transcript including only uniquely mapped, concordantly aligned, reversely stranded paired-end reads (53). Raw read counts (S5 Table) were then used as input to edgeR for differential gene expression (DGE) analysis using generalized linear models (GLM) (54,55). The BioProject accession number is PRJNA438967, which contains all raw data in this study. Genes with low coverage across all samples were filtered out, and library sizes were normalized using the trimmed mean of M-values method. Sample comparisons were set up as likelihood ratio tests, and genes having a FDR of < 0.05, $|\log FC| \geq 1.0$, and CPM >10 were considered to have significant expression abundance changes.

To verify the quality of RNAseq, qRT-PCR was performed using a Verso 1-step RT-qPCR Kit (ThermoFisher) in a CFX96 Touch™ Real-Time PCR Detection System (Bio-Rad) for selected transcripts. Ct values of transcripts were used to solve relative expression by the comparative Ct ($2^{-\Delta\Delta CT}$) method using the expression of the telomerase reverse transcriptase (TERT) gene or 60S ribosomal protein L10a (RPL10A) as reference as described (16,56,57). Primers for transcripts were designed through Genscript Real-time PCR (TaqMan) Primer Design (https://www.genscript.com/tools/real-time-pcr-tagman-primer-design-tool) and confirmed by blasting against the *Trypanosoma brucei brucei* TREU927 transcriptome database on TritrypDB (http://tritrypdb.org/tritrypdb/). A list of primers used in qRT-PCR can be found in S5 Table.

Flow cytometry and epifluorescence microscopy

For analysis of surface molecule expression of parasites by flow cytometry, antibody staining was performed using protocols modified from (58). Briefly, $0.5\text{-}2 \times 10^6$ cells were washed in PBS and fixed in 4% formaldehyde/0.05% glutaraldehyde for 1 hour at 4°C. Cells then incubated in blocking solution (2% BSA in PBS) for 1 hour before application of FITC-conjugated EP procyclin antibody (monoclonal antibody TBRP1/247, Cedarlane Laboratories, 1:1000) or PAD1 antibody (a generous gift of Dr. Keith Matthews, University of Edinburgh, 1:1000). Cells were washed three times in PBS before addition of Alexa Fluor 488-conjugated goat anti-mouse (1:1000) or goat anti-rabbit secondary antibody (ThermoFisher Scientific, 1:1000) prior to analysis by flow cytometry.

Immunofluorescence assays were performed using a protocol modified from (59). Parasites (1×10^6 cells) were harvested (800 x *g*, 8 min), washed with PBS, and then fixed in 4% formaldehyde in PBS for 30 minutes at 4°C. Cells were washed with PBS, allowed to settle on poly-lysine coated slides, and permeabilized with 0.1% Triton X-100 in PBS for 30 min. After being washed in PBS, cells were incubated in blocking solution (10% normal goat serum and 0.1% Triton X-100 in PBS) for 1 hour at room temperature, followed by addition of the FITC conjugated EP procyclin antibody diluted at 1:100 or PAD1 antibody diluted at 1:100 in blocking solution. Primary antibodies were detected with Alexa Fluor 488-conjugated antiserum diluted at 1:1000. Vectashield mounting medium with DAPI was applied for the detection of nucleus and kinetoplast DNA. Cells were visualized on a Zeiss Axiovert 200M using Axiovision software version 4.6.3 for image analysis.

Metadata analyses

SRA data was downloaded from BioProjects PRJEB13058 (38) and PRJEB19907 (25). Due to differences in library preparation and sequencing, the Qiu *et al.* dataset had to exclude all R2 reads, Qiu *et al.* and Naguleswaran *et al.* datasets had to be truncated to 50 bps, and Mugo and Clayton and Naguleswaran *et al.* datasets had to be downsampled to 10 million reads per sample. Seqtk was used for truncating and downsampling. The downsampling was done post-trimming, with trimmomatic, for low quality bases and adapter sequences. The resulting fastq files were aligned by gsnap to the TriTrypDB-28_TbruceiTREU927 genome, minus the 11 bin chromosome. Subread's featureCounts

was used to identify reads uniquely aligned to known genes. All reads were considered unstranded for alignment and feature calling. A table of all samples' counts was used as input to edgeR for differential gene expression analyses. Following the pipeline used in this study, DGE analysis was used to compare total RNA fractions of BF to BF RBP10 RNAi from Mugo and Clayton, LS to SS from Naguleswaran *et al*., and, LS to SS and LS to PF from *Qui et al.* The normalization, modeling and comparison for the dataset from Mugo and Clayton. had to be analyzed separately post-filtering due to considerable technical variations in the gene counts. DGE tables are presented in supplementary table 5 (S5 Table) and supplementary data 1 (S1 Data). Comparison by comparison $\log_2$FC scatterplot are presented in S3 Fig C and D.

Acknowledgements

The authors would like to thank Sarah Grace McAlpine for her technical assistance and Drs. Kimberly Paul and Meredith Morris for their comments on the manuscript. We also thank Dr. Keith Matthews for generously supplying the PAD1 antisera.

Abbreviations: BF, bloodstream form *T. brucei*; GDP, glucose-dependent pathway; GIP, glucose-independent pathway; IF, immunofluorescence; LS, long slender bloodstream form *T. brucei*; PF, procyclic form *T. brucei*; RPMIθ, a BF medium with minimal glucose; SDM79θ, a PF medium with minimal glucose; SS, short stumpy bloodstream form *T. brucei*.

Supporting Information

doi: : 10.1128/mSphere.00366-18

References

1. Reuner, B., Vassella, E., Yutzy, B., and Boshart, M. (1997) Cell density triggers slender to stumpy differentiation of *Trypanosoma brucei* bloodstream forms in culture. *Mol Biochem Parasitol* **90**, 269-280
2. Rico, E., Rojas, F., Mony, B. M., Szoor, B., Macgregor, P., and Matthews, K. R. (2013) Bloodstream form pre-adaptation to the tsetse fly in *Trypanosoma brucei*. *Front Cell Infect Microbiol* **3**, 78
3. Engstler, M., and Boshart, M. (2004) Cold shock and regulation of surface protein trafficking convey sensitization to inducers of stage differentiation in *Trypanosoma brucei*. *Genes Dev* **18**, 2798-2811
4. Dean, S., Marchetti, R., Kirk, K., and Matthews, K. R. (2009) A surface transporter family conveys the trypanosome differentiation signal. *Nature* **459**, 213-217
5. Hunt, M., Brun, R., and Kohler, P. (1994) Studies on compounds promoting the in vitro transformation of *Trypanosoma brucei* from bloodstream to procyclic forms. *Parasitol Res* **80**, 600-606
6. Rolin, S., Hancocq-Quertier, J., Paturiaux-Hanocq, F., Nolan, D. P., and Pays, E. (1998) Mild acid stress as a differentiation trigger in *Trypanosoma brucei*. *Mol Biochem Parasitol* **93**, 251-262
7. Yabu, Y., and Takayanagi, T. (1988) Trypsin-stimulated transformation of *Trypanosoma brucei* gambiense bloodstream forms to procyclic forms in vitro. *Parasitol Res* **74**, 501-506

8. Sbicego, S., Vassella, E., Kurath, U., Blum, B., and Roditi, I. (1999) The use of transgenic *Trypanosoma brucei* to identify compounds inducing the differentiation of bloodstream forms to procyclic forms. *Mol Biochem Parasitol* **104**, 311-322

9. Szoor, B., Dyer, N. A., Ruberto, I., Acosta-Serrano, A., and Matthews, K. R. (2013) Independent pathways can transduce the life-cycle differentiation signal in *Trypanosoma brucei*. *PLoS Pathog* **9**, e1003689

10. Szoor, B., Ruberto, I., Burchmore, R., and Matthews, K. R. (2010) A novel phosphatase cascade regulates differentiation in *Trypanosoma brucei* via a glycosomal signaling pathway. *Genes Dev* **24**, 1306-1316

11. Vickerman, K. (1985) Developmental cycles and biology of pathogenic trypanosomes. *Br Med Bull* **41**, 105-114.

12. Mantilla, B. S., Marchese, L., Casas-Sanchez, A., Dyer, N. A., Ejeh, N., Biran, M., Bringaud, F., Lehane, M. J., Acosta-Serrano, A., and Silber, A. M. (2017) Proline metabolism is essential for *Trypanosoma brucei brucei* survival in the tsetse vector. *PLoS Pathog* **13**, e1006158

13. Millerioux, Y., Ebikeme, C., Biran, M., Morand, P., Bouyssou, G., Vincent, I. M., Mazet, M., Riviere, L., Franconi, J. M., Burchmore, R. J., Moreau, P., Barrett, M. P., and Bringaud, F. (2013) The threonine degradation pathway of the *Trypanosoma brucei* procyclic form: the main carbon source for lipid biosynthesis is under metabolic control. *Mol Microbiol* **90**, 114-129

14. Smith, T. K., Bringaud, F., Nolan, D. P., and Figueiredo, L. M. (2017) Metabolic reprogramming during the *Trypanosoma brucei* life cycle. *F1000Res* **6**

15. Milne, K. G., Prescott, A. R., and Ferguson, M. A. (1998) Transformation of monomorphic *Trypanosoma brucei* bloodstream form trypomastigotes into procyclic forms at 37 degrees C by removing glucose from the culture medium. *Mol Biochem Parasitol* **94**, 99-112.

16. Haanstra, J. R., Kerkhoven, E. J., van Tuijl, A., Blits, M., Wurst, M., van Nuland, R., Albert, M. A., Michels, P. A., Bouwman, J., Clayton, C., Westerhoff, H. V., and Bakker, B. M. (2011) A domino effect in drug action: from metabolic assault towards parasite differentiation. *Mol Microbiol* **79**, 94-108

17. Wurst, M., Seliger, B., Jha, B. A., Klein, C., Queiroz, R., and Clayton, C. (2012) Expression of the RNA recognition motif protein RBP10 promotes a bloodstream-form transcript pattern in *Trypanosoma brucei*. *Mol Microbiol* **83**, 1048-1063

18. Morris, J. C., Wang, Z., Drew, M. E., and Englund, P. T. (2002) Glycolysis modulates trypanosome glycoprotein expression as revealed by an RNAi library. *EMBO J.* **21**, 4429-4438

19. Vassella, E., Probst, M., Schneider, A., Studer, E., Renggli, C. K., and Roditi, I. (2004) Expression of a major surface protein of *Trypanosoma brucei* insect forms is controlled by the activity of mitochondrial enzymes. *Mol Biol Cell* **15**, 3986-3993

20. Feagin, J. E., Jasmer, D. P., and Stuart, K. (1986) Differential mitochondrial gene expression between slender and stumpy bloodforms of *Trypanosoma brucei*. *Mol Biochem Parasitol* **20**, 207-214

21. Bienen, E. J., Saric, M., Pollakis, G., Grady, R. W., and Clarkson, A. B., Jr. (1991) Mitochondrial development in *Trypanosoma brucei brucei* transitional bloodstream forms. *Mol Biochem Parasitol* **45**, 185-192

22. Gancedo, J. M. (2008) The early steps of glucose signalling in yeast. *FEMS Microbiol Rev* **32**, 673-704

23. Kabani, S., Fenn, K., Ross, A., Ivens, A., Smith, T. K., Ghazal, P., and Matthews, K. (2009) Genome-wide expression profiling of in vivo-derived bloodstream parasite stages and dynamic analysis of mRNA alterations during synchronous differentiation in *Trypanosoma brucei*. *BMC Genomics* **10**, 427

24. MacGregor, P., Szoor, B., Savill, N. J., and Matthews, K. R. (2012) Trypanosomal immune evasion, chronicity and transmission: an elegant balancing act. *Nat Rev Microbiol* **10**, 431-438

25. Naguleswaran, A., Doiron, N., and Roditi, I. (2018) RNA-Seq analysis validates the use of culture-derived *Trypanosoma brucei* and provides new markers for mammalian and insect life-cycle stages. *BMC Genomics* **19**, 227

26. Van den Brink, P. J., and Braak, C. J. F. T. (1999) Analysis of time-dependent multivariate responses of biological community to stress. *Environ Tox Chem***18**, 10

27. Erben, E. D., Fadda, A., Lueong, S., Hoheisel, J. D., and Clayton, C. (2014) A genome-wide tethering screen reveals novel potential post-transcriptional regulators in *Trypanosoma brucei*. *PLoS Pathog* **10**, e1004178

28. Rico, E., Ivens, A., Glover, L., Horn, D., and Matthews, K. R. (2017) Genome-wide RNAi selection identifies a regulator of transmission stage-enriched gene

families and cell-type differentiation in *Trypanosoma brucei*. *PLoS Pathog* **13**, e1006279

29. Queiroz, R., Benz, C., Fellenberg, K., Hoheisel, J. D., and Clayton, C. (2009) Transcriptome analysis of differentiating trypanosomes reveals the existence of multiple post-transcriptional regulons. *BMC Genomics* **10**, 495

30. Duraisingh, M. T., and Horn, D. (2016) Epigenetic regulation of virulence gene expression in parasitic protozoa. *Cell Host Microbe* **19**, 629-640

31. Jensen, B. C., Sivam, D., Kifer, C. T., Myler, P. J., and Parsons, M. (2009) Widespread variation in transcript abundance within and across developmental stages of *Trypanosoma brucei*. *BMC Genomics* **10**, 482

32. Nilsson, D., Gunasekera, K., Mani, J., Osteras, M., Farinelli, L., Baerlocher, L., Roditi, I., and Ochsenreiter, T. (2010) Spliced leader trapping reveals widespread alternative splicing patterns in the highly dynamic transcriptome of *Trypanosoma brucei*. *PLoS Pathog* **6**, e1001037

33. Siegel, T. N., Hekstra, D. R., Wang, X., Dewell, S., and Cross, G. A. (2010) Genome-wide analysis of mRNA abundance in two life-cycle stages of *Trypanosoma brucei* and identification of splicing and polyadenylation sites. *Nucleic Acids Res* **38**, 4946-4957

34. Jensen, B. C., Ramasamy, G., Vasconcelos, E. J., Ingolia, N. T., Myler, P. J., and Parsons, M. (2014) Extensive stage-regulation of translation revealed by ribosome profiling of *Trypanosoma brucei*. *BMC Genomics* **15**, 911

35. Vasquez, J. J., Hon, C. C., Vanselow, J. T., Schlosser, A., and Siegel, T. N. (2014) Comparative ribosome profiling reveals extensive translational complexity in different *Trypanosoma brucei* life cycle stages. *Nucleic Acids Res* **42**, 3623-3637

36. Mugo, E., Egler, F., and Clayton, C. (2017) Conversion of procyclic-form Trypanosoma brucei to the bloodstream form by transient expression of RBP10. *Mol Biochem Parasitol* **216**, 49-51

37. Kolev, N. G., Ullu, E., and Tschudi, C. (2014) The emerging role of RNA-binding proteins in the life cycle of *Trypanosoma brucei*. *Cell Microbiol* **16**, 482-489

38. Mugo, E., and Clayton, C. (2017) Expression of the RNA-binding protein RBP10 promotes the bloodstream-form differentiation state in Trypanosoma brucei. *PLoS Pathog* **13**, e1006560

39. Lemaire, K., Van de Velde, S., Van Dijck, P., and Thevelein, J. M. (2004) Glucose and sucrose act as agonist and mannose as antagonist ligands of the G protein-coupled receptor Gpr1 in the yeast *Saccharomyces cerevisiae*. *Mol Cell* **16**, 293-299

40. Moriya, H., and Johnston, M. (2004) Glucose sensing and signaling in *Saccharomyces cerevisiae* through the Rgt2 glucose sensor and casein kinase I. *Proc Natl Acad Sci U S A* **101**, 1572-1577

41. Barrett, M. P., Tetaud, E., Seyfang, A., Bringaud, F., and Baltz, T. (1998) Trypanosome glucose transporters. *Mol Biochem Parasitol* **91**, 195-205.

42. Morris, M. T., DeBruin, C., Yang, Z., Chambers, J. W., Smith, K. S., and Morris, J. C. (2006) Activity of a second *Trypanosoma brucei* hexokinase is controlled by an 18-amino-acid C-terminal tail. *Eukaryot Cell* **5**, 2014-2023

43. Lamour, N., Riviere, L., Coustou, V., Coombs, G. H., Barrett, M. P., and Bringaud, F. (2005) Proline metabolism in procyclic *Trypanosoma brucei* is down-regulated in the presence of glucose. *J Biol Chem* **280**, 11902-11910

44. Coustou, V., Biran, M., Breton, M., Guegan, F., Riviere, L., Plazolles, N., Nolan, D., Barrett, M. P., Franconi, J. M., and Bringaud, F. (2008) Glucose-induced remodeling of intermediary and energy metabolism in procyclic *Trypanosoma brucei*. *J Biol Chem* **283**, 16342-16354

45. van Grinsven, K. W., Van Den Abbeele, J., Van den Bossche, P., van Hellemond, J. J., and Tielens, A. G. (2009) Adaptations in the glucose metabolism of procyclic *Trypanosoma brucei* isolates from tsetse flies and during differentiation of bloodstream forms. *Eukaryot Cell* **8**, 1307-1311

46. Bursell, E., Billing, K. J., Hargrove, J. W., McCabe, C. T., and Slack, E. (1973) The supply of substrates to the flight muscle of tsetse flies. *Trans R Soc Trop Med Hyg* **67**, 296

47. Aksoy, S., Gibson, W. C., and Lehane, M. J. (2003) Interactions between tsetse and trypanosomes with implications for the control of trypanosomiasis. *Adv Parasitol* **53**, 1-83

48. Roditi, I., and Lehane, M. J. (2008) Interactions between trypanosomes and tsetse flies. *Curr Opin Microbiol* **11**, 345-351

49. Hirumi, H., and Hirumi, K. (1989) Continuous cultivation of *Trypanosoma brucei* blood stream forms in a medium containing a low concentration of serum protein without feeder cell layers. *J Parasitol* **75**, 985-989

50. Hirumi, H., Doyle, J. J., and Hirumi, K. (1977) Cultivation of bloodstream *Trypanosoma brucei*. *Bull World Health Organ* **55**, 405-409

51. Brun, R., and Shonenberger, M. (1979) Cultivation and in vitro cloning of procyclic culture forms of *Trypanosoma brucei* in a semi-defined medium. *Acta Tropica* **36**, 289-292

52. Bolger, A. M., Lohse, M., and Usadel, B. (2014) Trimmomatic: a flexible trimmer for Illumina sequence data. *Bioinformatics* **30**, 2114-2120

53. Liao, Y., Smyth, G. K., and Shi, W. (2014) featureCounts: an efficient general purpose program for assigning sequence reads to genomic features. *Bioinformatics* **30**, 923-930

54. Robinson, M. D., McCarthy, D. J., and Smyth, G. K. (2010) edgeR: a Bioconductor package for differential expression analysis of digital gene expression data. *Bioinformatics* **26**, 139-140

55. McCarthy, D. J., Chen, Y., and Smyth, G. K. (2012) Differential expression analysis of multifactor RNA-Seq experiments with respect to biological variation. *Nucleic Acids Res* **40**, 4288-4297

56. Schmittgen, T. D., and Livak, K. J. (2008) Analyzing real-time PCR data by the comparative C(T) method. *Nat Protoc* **3**, 1101-1108

57. Brenndorfer, M., and Boshart, M. (2010) Selection of reference genes for mRNA quantification in *Trypanosoma brucei*. *Mol Biochem Parasitol* **172**, 52-55

58. Clemmens, C. S., Morris, M. T., Lyda, T. A., Acosta-Serrano, A., and Morris, J. C. (2009) *Trypanosoma brucei* AMP-activated kinase subunit homologs influence surface molecule expression. *Exp Parasitol* **123**, 250-257

59. Field, M. C., Allen, C. L., Dhir, V., Goulding, D., Hall, B. S., Morgan, G. W., Veazey, P., and Engstler, M. (2004) New approaches to the microscopic imaging of *Trypanosoma brucei*. *Microsc Microanal* **10**, 621-636

60. Shameer, S., Logan-Klumpler, F. J., Vinson, F., Cottret, L., Merlet, B., Achcar, F., Boshart, M., Berriman, M., Breitling, R., Bringaud, F., Butikofer, P., Cattanach, A. M., Bannerman-Chukualim, B., Creek, D. J., Crouch, K., de Koning, H. P., Denise, H., Ebikeme, C., Fairlamb, A. H., Ferguson, M. A., Ginger, M. L., Hertz-Fowler, C., Kerkhoven, E. J., Maser, P., Michels, P. A., Nayak, A., Nes, D. W., Nolan, D. P., Olsen, C., Silva-Franco, F., Smith, T. K., Taylor, M. C., Tielens, A. G., Urbaniak, M. D., van Hellemond, J. J., Vincent, I. M., Wilkinson, S. R., Wyllie, S., Opperdoes, F. R., Barrett, M. P., and Jourdan, F. (2015) TrypanoCyc: a community-led biochemical pathways database for Trypanosoma brucei. *Nucleic Acids Res* **43**, D637-644

CHAPTER THREE

AMPKα RESPONDS TO ENVIRONMENTAL GLUCOSE IN THE PARASITE *Trypanosoma brucei*

Jessica A. Jones[1], James C. Morris[1,2]

[1] Clemson University, Eukaryotic Pathogens Innovation Center, Department of Genetics & Biochemistry

Clemson, SC 29631

[2] Corresponding author

Abstract

Trypanosoma brucei is a unicellular protozoan parasite that causes disease in humans and cattle. Parasites are transferred from one host to another through the tsetse fly vector. The trypanosome can rapidly alter their metabolism and modify surface proteins to tolerate each environment. One stark difference between the fly digestive tract and mammalian blood is the abundance of glucose. Nutrient sensing and signaling plays a key role in development through the *T. brucei* life cycle. Here, we explore the role of the catalytic α subunit of AMPK, a eukaryotic master regulator of metabolism, in procyclic form *T. brucei*. The PF parasite expressed two AMPKα1 species and both were detected using antibodies generated against phosphorylated human AMPKα. We found that the larger species of phosphorylated AMPKα1 (p-AMPKα1), coined p-AMPKα1+, was more abundant in the presence of glucose, and other metabolizable sugars. Subcellular location of AMPKα1 was similar regardless of glucose abundance and the phosphorylated version of AMPKα1was partially associated with glycosomes and mitochondria. The glucose specific response of AMPKα1 in *T. brucei* may reflect a role of for the complex in regulating metabolism through nutrient sensing during parasite differentiation.

Introduction

Trypanosoma brucei is the eukaryotic protozoan parasite that causes the diseases African sleeping sickness and nagana, in humans and cattle, respectively. *T. brucei* is a unicellular parasite and has a strictly extracellular dixenous life cycle. In mammals, the parasite lives in the blood, lymph, fat, skin, and other tissues (1) and is transmitted between hosts by the tsetse fly (*Glossina* spp). When the parasites are ingested by the tsetse fly during a blood-meal, they are introduced into the midgut of the fly and continue through life-cycle stages required for success in the vector.

The mammalian bloodstream and the tsetse fly midgut differ dramatically in nutrient availability. When the parasites reside in the mammalian bloodstream glucose is abundant (~ 5 mM) (2) and serves as the lone carbon source for the bloodstream form parasite (BSF), which relies solely on glycolysis for generation of ATP. The long slender bloodstream form parasite (LS) grows in the blood. In a population density-dependent fashion, LS parasites differentiate to the quiescent short stumpy forms (SS) (3,4). Feeding tsetse flies take up parasites in their bloodmeal. These parasites experience a rapid change in environment when they are delivered to the fly midgut, as they are abruptly transferred from the glucose-rich blood environment to the amino acid-rich, glucose limited fly digestive tract. This change, and other cues, trigger SS parasites to differentiate into PF. The dramatic change in nutrient availability forces the parasites to reprogram their metabolism from glycolysis to oxidative phosphorylation to generate ATP (5).

Many of the environmental cues that *T. brucei* perceives function through well-defined signaling pathways (6). These signaling pathways are triggered by nutrient

availability, quorum sensing, and host extracellular signals (5, 6 , 7). Several of the triggers ultimately converge on the AMPK pathway. AMPK is a master regulator of energy metabolism that senses and responds to AMP:ATP ratios within the cell (8, 9). AMPK is a canonical regulator of eukaryotic cell metabolism (10) that consists of a heterotrimeric protein complex made up of a catalytic α domain, a β scaffold domain, and a γ regulatory domain. Activation of AMPK occurs through phosphorylation of the catalytic domain when the AMP:ATP ratio is high, which indicates an energy deficit (11), may result from carbon source deprivation or cellular stress (12). *T. brucei* have two isoforms of the catalytic subunit, α1 and α2, which have 50% identity (Chapter One, **Table 1.1**).

T. brucei undergoes rapid glucose starvation when parasites are transferred from the mammalian bloodstream to the tsetse fly midgut, with glucose depleted from the blood meal to undetectable levels within 15 minutes (13). This change in environment coincides with perception of development cues that trigger progression of SS to PF stages. Previous studies of *T. brucei* differentiation have described roles for several signaling components in development, including the eukaryotic metabolic regulator, the target of rapamycin (TOR) kinase, which plays a role in parasite metabolic reprogramming (14). TbTOR4 has been shown to play a role in differentiation of long slender parasites into short stumpy parasites in a cAMP-dependent mechanism (14, 15). Additionally, signal transduction studies in *T. brucei* have highlighted the importance of cAMP signaling through cAMP effector kinases and phosphatases in the parasite (16). cAMP signaling in *T. brucei* is distinct from that found in mammalian cells, as the parasites lack G-protein-coupled receptors, and instead, likely use receptor-type adenylate cyclases in the pathway (reviewed

in (17)). Interestingly, the trypanosome flagellum has been found to be an important site of cAMP signaling and environmental sensing. This organelle interfaces with the host environment and is ideally positioned to house these key sensing pathways (18, 21).

More recently, studies have implicated a role for AMPK in *T. brucei* differentiation (3, 20, 21). Changes in PF surface molecule expression, a part of the normal developmental progression of the parasite, are modulated by glucose abundance, an observation that manipulation of AMPK subunit abundance by RNAi can phenocopy (22). This suggests a connection between the protein complex and nutrient perception. Additionally, TbAMPKα is a positive regulator of parasite development from LS to SS, tying together nutrient abundance and metabolism in differentiation (23). It remains unclear how AMPK receives and transduces the ATP deficit signal within the parasite. We hypothesize that TbAMPKα phosphorylation occurs in response to glucose abundance and is key to successful parasite differentiation. In this study we explore the role of AMPKα in the PF response to glucose abundance to better understand activation of AMPK and to elucidate potential signaling partners.

Materials and Methods

Cells Lines and Culturing

WMI 471 Antat 1.1 pleomorphic procyclic form *Trypanosoma brucei brucei* were cultured in SDM-79 medium (Gibco, Thermofisher Scientific, Waltham, MA) supplemented with 10% FBS or SDM-79θ medium (Gibco, Thermofisher Scientific, Waltham, MA) supplemented with 10% dialyzed FBS. SDM79 has a final glucose concentration of 9 mM, while SDM79θ has a final concentration of ~4μM. For some experiments, pleomorphic procyclic form cells harboring pXS2:aldoPTSeYFP were used, as they constituently express a glycosomally targeted eYFP. Cell cultures were maintained in the log phase of growth at 27°C in 5% CO_2.

Western Blots

Whole cell lysate or subcellular fractions were resuspended in 2X cracking buffer (40 mM tris pH 6.8, 0.4% (w/v) SDS, 4% β-mercaptoethanol (v/v), 0.4% (v/v) bromophenol blue, 5% (w/v) glycerol) and electrophoresed on 8% SDS-PAGE until the dye front ran off the gel. Samples were transferred at 16V for 40 min in transfer buffer (0.58% (w/v) tris base, 2.9% (w/v) glycine, 5% (v/v) methanol, 0.0375% (v/v) 10% SDS) and transferred to 0.45 μm nitrocellulose membranes (Amershan Protran GE Healthcare Life Science). Membranes were blocked in 3% milk (w/v) (Nestle Carnation instant dry non-fat milk) in 1X TNT (10 mM Tris pH 8, 150 mM NaCl, 0.0005% (v/v) Tween-20) for 1 h shaking at RT. Membranes were incubated with primary antibodies for 1 h shaking at RT. Rabbit anti-aldolase, rabbit anti-Hsp70 (StressMarq Bioscience), mouse anti-PPDK (generous gift

from Dr. Frederic Bringaud), and rabbit anti-TbHK1 (hexokinase 1) were diluted in 3% (w/v) milk in 1X TNT at dilutions of 1:100,000 1:5,000, 1:10,000, and 1:100,000 respectively. Rabbit anti-AMPKα and rabbit anti-phosphoAMPKα antibodies (Cell Signaling Technologies 2532 and 2535, respectively) were diluted in 5% BSA (w/v) (Fisher Bioreagents) in 1X TNT at dilutions of 1:1,000 and 1:10,000 respectively. Membranes were washed 3 times for 5 min in 1X TNT. Secondary Horseradish Peroxidase (HRP) antibodies (Rockland) to each respective primary host were diluted 1:10,000 in 3% (w/v) milk in 1X TNT and incubated for 1 h shaking at RT. Membranes were developed using Enhanced Chemiluminescence (ECL) substrates (SuperSignal west pico Plus Chemiluminescent substrate ThermoScientific) and imaged using x-ray film (MTC bio). In order to reprobe transfers, membranes were washed in 1X TNT after developing and stripped using 0.1M glycine pH 2.5 for 30 min, washed 3 times for 5 min in 1X TNT, and blocked in 3%(w/v) milk in 1X TNT for 1 h shaking at RT. Densitometry analysis, through relative darkness, was scored using Image J version 64-bit.

Immunofluorescence Assays

Cells ($2x10^6$) were harvested at 800 x g for 15 min, washed once in 1X phosphate-buffered saline (PBS) and resuspend to a density of $2x10^7$ cells/mL in 1X PBS and fixed in 4% paraformaldehyde in 1X PBS. Fixed cells settled for 30 min on a glass slide, inside a pap-pen wax box, and washed 3 times in wash solution (0.1% normal goat serum (NGS) in 1X PBS). Cells were then permeabilized (0.5% (v/v) triton X-100 in 1X PBS) for 20 min then washed. Cells were blocked (10% NGS, 0.1% triton X-100 in 1X PBS) for 1 h at RT then

washed. Primary antibodies, rabbit-AMPKα or rabbit-phosphoAMPKα, were diluted 1:250 in block solution and incubated for 1 h on the slide at RT, then washed 3 times. Secondary antibody, either anti-rabbit Alexa fluor 488 or anti-rabbit Alexa fluor 568 (Abcam), were diluted 1:1,000 in block solution and incubated for 1 h on the slide at RT and kept dark. After secondary was washed three times cells were mounted in Prolonged Glass Antifade Mountant with NucBlue (Invitrogen) and a coverslip was added. The slide was allowed to cure for 48 h at RT in the dark. Slides were then sealed and imaged on a Leica DiM8 (Leica Microsystems Inc, Buffalo Grove, IL). Cells ($2x10^6$) stained with MitoTracker Red™ cmxROS (Invitrogen) were harvested at 800 x g for 15 min, washed once in 1X PBS and resuspend in 10 µM MitoTracker Red™ cmxROS (Invitrogen) in 1X PBS and incubated at 27°C and 5% CO_2 in the dark for 30 min, then proceeded to fix for immunofluorescence assays.

Differential Centrifugation

Cells ($5x10^8$) were harvested at 800 x g for 15 min and washed once in 1X PBS. Cells were resuspended in a 50% (w/v) slurry of silica carbide in 1X STE (250 mM sucrose, 25 mM Tris-HCl pH 7.4, 1 mM EDTA) supplemented with 1 mM phenylmethylsulphonyl fluoride (PMSF) in dimethyl sulfoxide (DMSO). Mechanical lysis was performed by pestle for 5 min in a microcentrifuge tube. The silica carbide slurry was removed by centrifugation at 100 x g for 30 seconds and cell lysate supernatant was transferred to a fresh microcentrifuge tube. Samples were then centrifuged (2,000 x g, 10 min, 4°C) to yield the nuclear pellet. The post-nuclear lysate was transferred to a fresh tube and the

mitochondria-rich fraction was pelleted (5,000 x g, 10 min, 4°C). Subsequent centrifugation steps (all 10 min at 4°C) at 17,000 x g and 100,000 x g yielded glycosomes and endosome-rich fractions, respectively. Post-endosomal supernatant was acetone precipitated and cytosolic proteins were pelleted (17,000 x g, 10 min, 4°C). Sub-cellular faction pellets were resuspended in 20 µL 2X cracking buffer and proteins resolved by 10% SDS-PAGE.

Sucrose Density Gradient Fractionation

Otiprep (Accurate Chemical) was diluted in dilution buffer (0.25 M sucrose, 1 mM EDTA, 5 mM MOPS, 0.1% v/v ethanol, pH 7.2) to a final concentration of 50% (v/v) Iodixanol. Fifty percent Iodixanol working solution was diluted in homogenization buffer (0.25 M sucrose, 6 mM EDTA, 30 mM MOPS, 0.6% v/v ethanol) to final concentrations of 20%, 24%, 30%, 34%, 40%, and 50% Iodixanol. Fractions were added to 14 x 95 mm thin wall polypropylene centrifuge tubes. A cushion of 300 µL of 50% Iodixanol was loaded at the base of the gradient. Discontinuous fractions of 2.4 mL of decreasing Iodixanol concentrations were gently added on top of previous layer to total 13 mL gradient from 50% Iodixanol at the bottom to 20% Iodixanol at the top. Sucrose gradients were prepared the day before sample isolation and allowed to equilibrate at 4°C overnight. Cells ($1x10^9$) were harvested at 800 x g for 15 min and washed once in 1X PBS. Cells were resuspended in a slurry silica carbide in 1X STE + 1mM PMSF. Mechanical lysis was performed by pestle for 5 min in a microcentrifuge tube. The silica carbide slurry was removed by pelleting at 100 x g, 30 seconds and cell lysate supernatant was transferred to the top of a

pre-prepared sucrose gradient. Loaded gradients were placed into a swinging bucket SW-40Ti rotor and centrifuged at 30,000 x g, 17 h, 4°C. Fractions were carefully collected in 500 µL aliquots beginning at the top of the gradient. Each fractions protein abundance was assessed through BCA assay (Thermofisher). Protein from every fraction (10 µg) was acetone precipitated at 4°C and resuspended in 20 µL 2X cracking buffer and proteins resolved by 8% SDS-PAGE for western blot analysis.

Results

AMPK is a master regulator of metabolic responses to energy homeostasis in eukaryotes. Previous studies have shown that AMPK plays a role in differentiation of *T. brucei* with AMPKα playing a role in the quorum sensing pathway as a potential signal transducer, acting upstream of TbTOR4 (24,25). AMPKα1, the catalytic subunit, has been shown to act as a central signaling molecule in the differentiation of *T.brucei* (3,20). Here, we explored the phosphorylation of AMPKα in PF parasites cultured in the presence or absence of glucose, as well as subcellular location of AMPKα. Interestingly, we have found that further phosphorylation (with putative activation) of AMPKa1 does not coincide with changes in glucose abundance. Rather, the phosphorylated (putatively active) protein is further post-translationally modified in response to glucose.

In other systems, AMPK is phosphorylated in response to high AMP levels by an autocatalytic phosphorylation of threonine 172 on the AMPKα subunit (11,26). To determine if glucose availability impacted phosphorylation of the active loop threonine in the trypanosome enzyme (TbAMPKα1 and TbAMPKα2 at Thr165 and Thr167 respectively), we performed western blotting using an antibody specific for phosphorylated human AMPKα (p-AMPKα) that has been used by others to score activation of AMPK in trypanosomes (20). This phosphorylated threonine in the active loop of the catalytic domain and serves as a marker for activation of AMPKα.

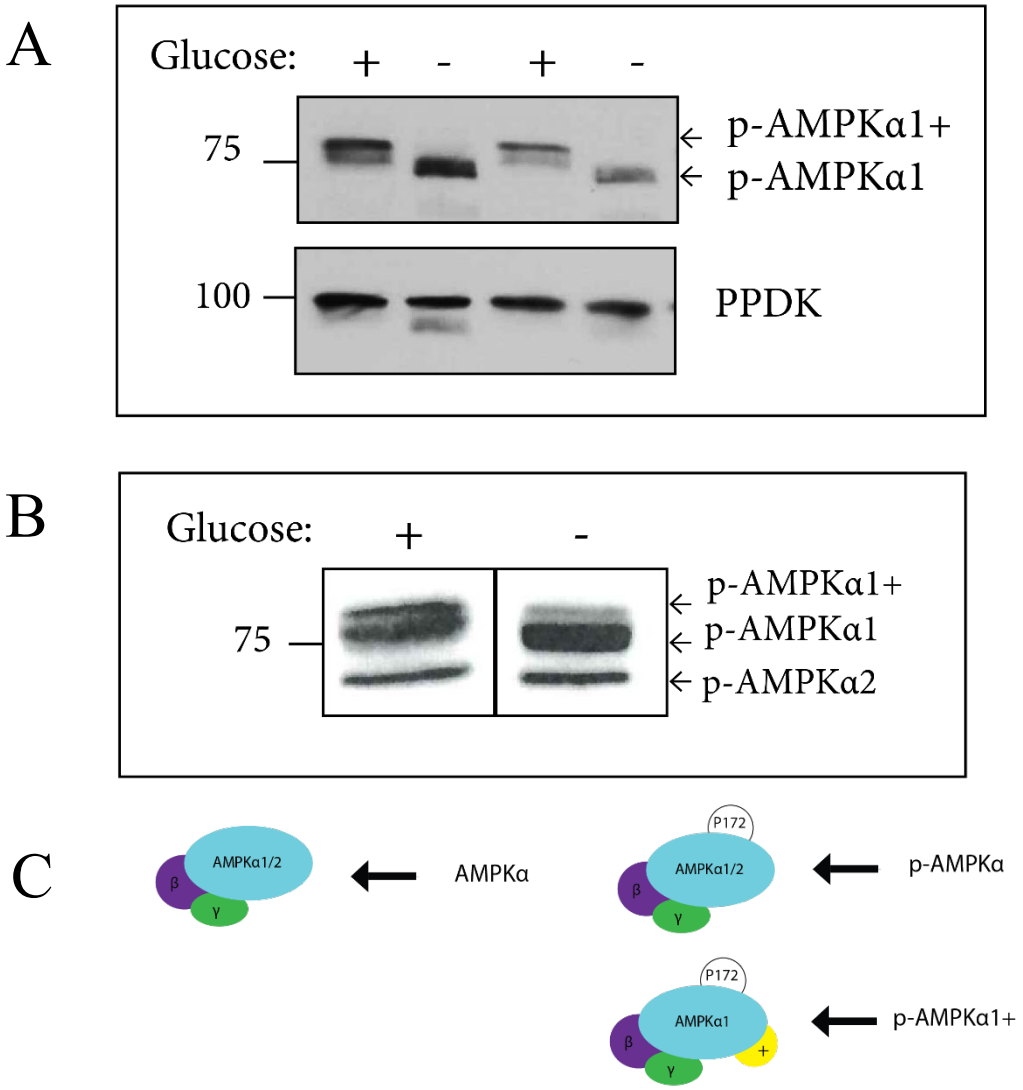

Figure 3.1: The phosphorylated AMPKα1 subunit is modified in the presence of glucose. (A) Western blot of PF whole cell lysate from cells cultured in the presence or absence of glucose using an antibody that detects phosphorylated AMPKα. (B) Both AMPK α1 and α2 are delectable with the anti-phosphoAMPK antibody in trypanosomes. (C) Schematic showing two species of p-AMPKα1, with the larger species observed in the presence of glucose (p-AMPKα1+) and the smaller species prevalent in the absence of glucose (p-AMPKα1).

There are two α subunits (α1 and α2) in trypanosomes, which share 50% identity, **Figure 3.1A** shows that phosphorylated AMPKα1 (p-AMPKα1) was detectable in parasites independent of the presence of glucose in culture medium. Similarly, AMPKα2 was phosphorylated. in cells cultured in the presence and absence of glucose (**Figure 3.1B**, lower band, approx. 70 kDa). However, we detected two subspecies of p-AMPKα1, each around 80 kDa. The modest difference in mobility of the two p-AMPKα1 on the western blot suggested the presence of an additional post-translational modification (PTM) on p-AMPKα1, which we hypothesize is an additional phosphorylation (**Figure 3.1C**). Notably, culture of parasites in the presence of glucose resulted in the predominance of the larger species of p-AMPKα1, which we coined p-AMPKα1+, hypothesized to be hyperphosphorylated AMPKα1. PF cultured in the absence of glucose yielded predominately smaller of p-AMPKα1 species (**Figure 3.1A**).

To determine if there was a difference in the abundance of p-AMPKα protein levels between PF in the presence and absence of glucose we performed densitometry analysis on western blots probed with the anti-phosphoAMPKα antibody. Comparing activated p-AMPKα signal to a loading control of tubulin (which does not change in response to glucose) we calculated the relative protein abundance of both p-AMPKα1 and p-AMPKα2 (**Figure 3.2A)**. Both isoforms were significantly more abundant in PF parasites cultured in the absence of glucose (**Figure 3.2B**). There was no change in overall AMPKα protein level in response to glucose (**Figure 3.2C**).

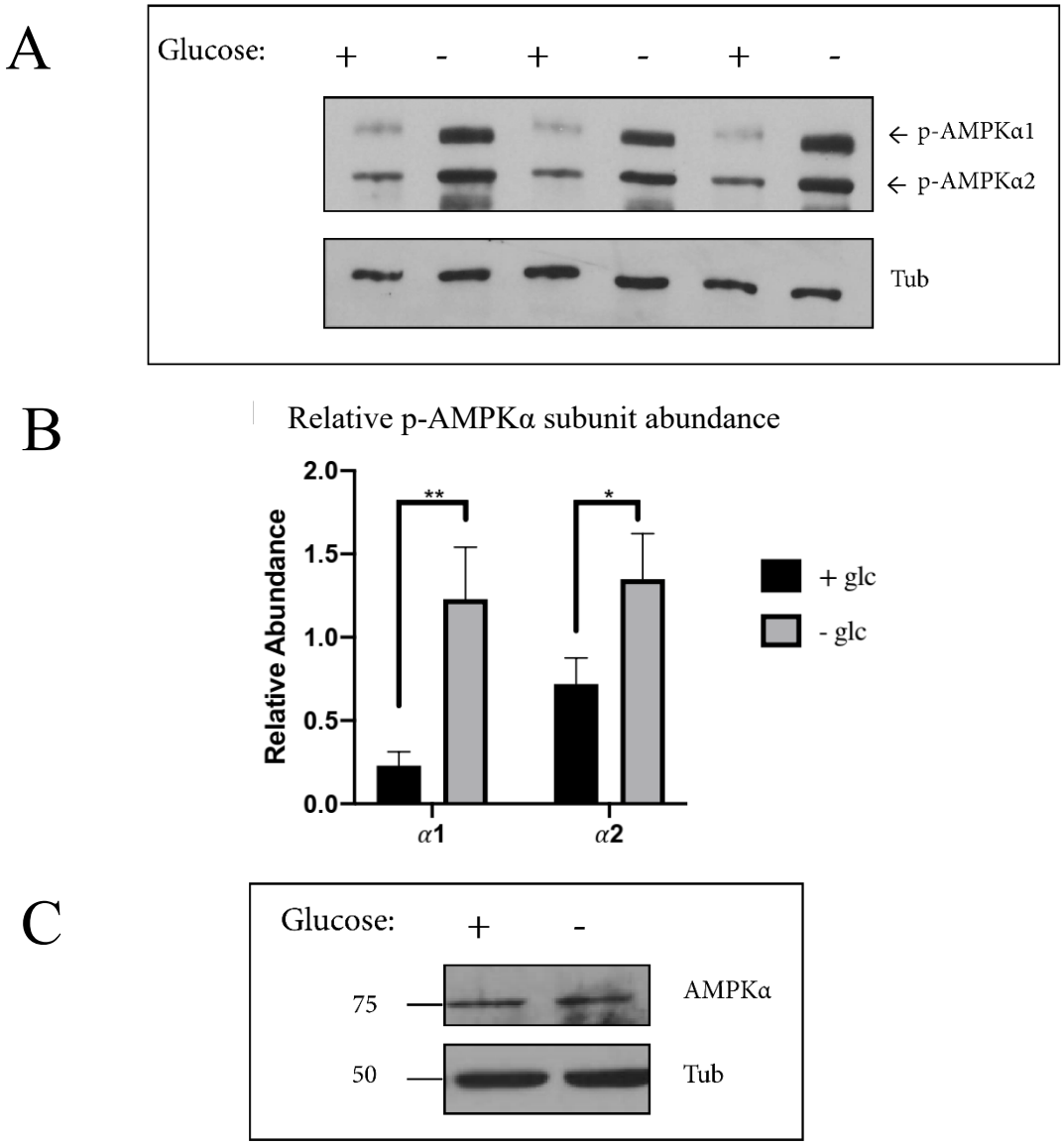

Figure 3.2: p-AMPKα is more abudant in the absence of glucose. (A) Western blot on PF whole cell lysate of cells cultured in the presence or absence of glucose. TUB is tubulin loading control (B) Densitometry analysis of three biological replicates p-AMPKα1 and p-AMPKα2 subunits in the presence and absence of glucose. * = $p < 0.05$ ** = $p < 0.01$ (C) representative western blot of AMPKα abundance of cells cultured in the presence or absence of glucose polyclonal anti-AMPKα antibody TUB is tubulin loading control

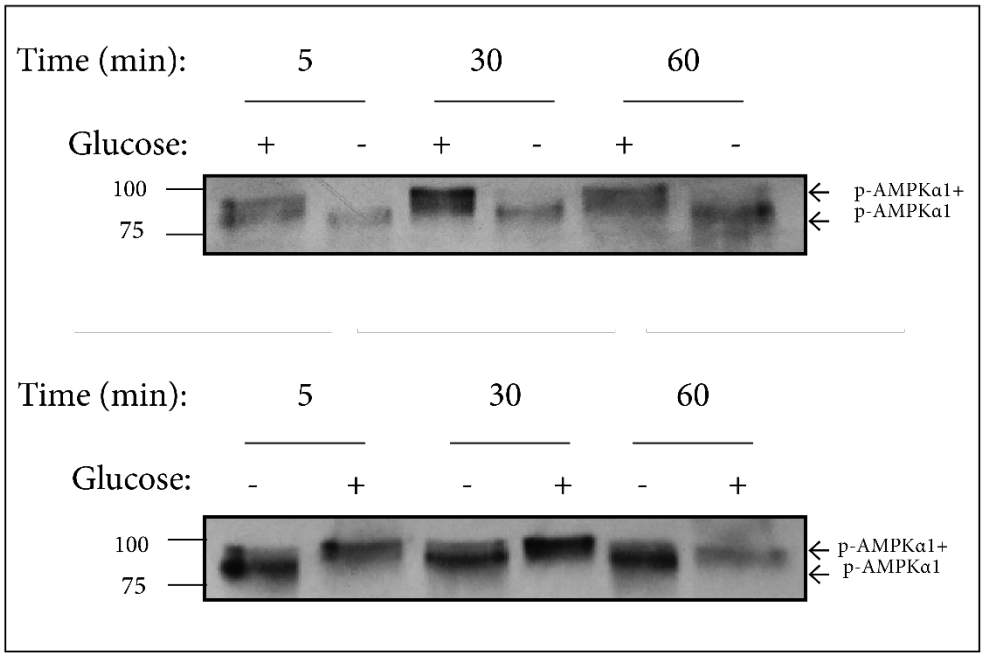

Figure 3.3: p-AMPKα1 is modified within 5 min of glucose treatment. Western blot of PF parasites continuously cultured in the presence (top panel), or absence (bottom panel), were treated in either the presence or absence of glucose and incubated for 5, or 30, or 60 min. p-AMPKα2 did not respond to glucose abundance.

PF parasites continuously cultured in either the presence (**Figure 3.3**, top panel), or absence (**Figure 3.3**, bottom panel), of glucose were centrifuged, washed to remove residual culture media, and resuspended in media supplemented with or without glucose for various amounts of time. The p-AMPKα1+ levels of PF cultured in presence of glucose rapidly falls when glucose is removed from the environment (**Figure 3.3**, top panel). When

PF cultured in the absence of glucose were resuspended in glucose-bearing media, p-AMPKα1 was rapidly (~ 5 minutes) modified to p-AMPKα1+ (**Figure 3.3**, bottom panel).

To decipher if this response was occurring through either glucose sensing or glucose metabolism, we exposed PF cultured in the absence of glucose to various sugars. p-AMPKα1 was modified into p-AMPKα1+ in the presence of glucose, mannose, and fructose, but not galactose (**Figure 3.4A**). It has been established that trypanosomes transport glucose, mannose, and fructose into the cell, while galactose is not a substrate for the cellular transport machinery (27), suggesting that a hexose must enter the cell before triggering a response. To better understand the role of glucose metabolism in p-AMPKα1 response we treated PF parasites cultured in the absence of glucose with either glucose or the glucose analogs 2-deoxyglucose (2DOG), or 6-dexoyglucose (6DOG) (**Figure 3.4B**). These analogs have different fates in the cell. Both are transported into the parasite, but only 2DOG is phosphorylated by the trypanosome hexokinase (TbHK). In the presence of glucose p-AMPKα1 is modified into p-AMPKα1+. Interestingly, this modification also occurs when the cells were cultured with the glucose analog 2DOG. Both glucose and 2DOG are substrates for TbHK. Notably, 6DOG, which is not a substrate of TbHK, was unable to trigger the change in AMPKα1. **Figure 3.4C** is a schematic of TbHK activity in the presence of glucose, 2DOG, or 6DOG.

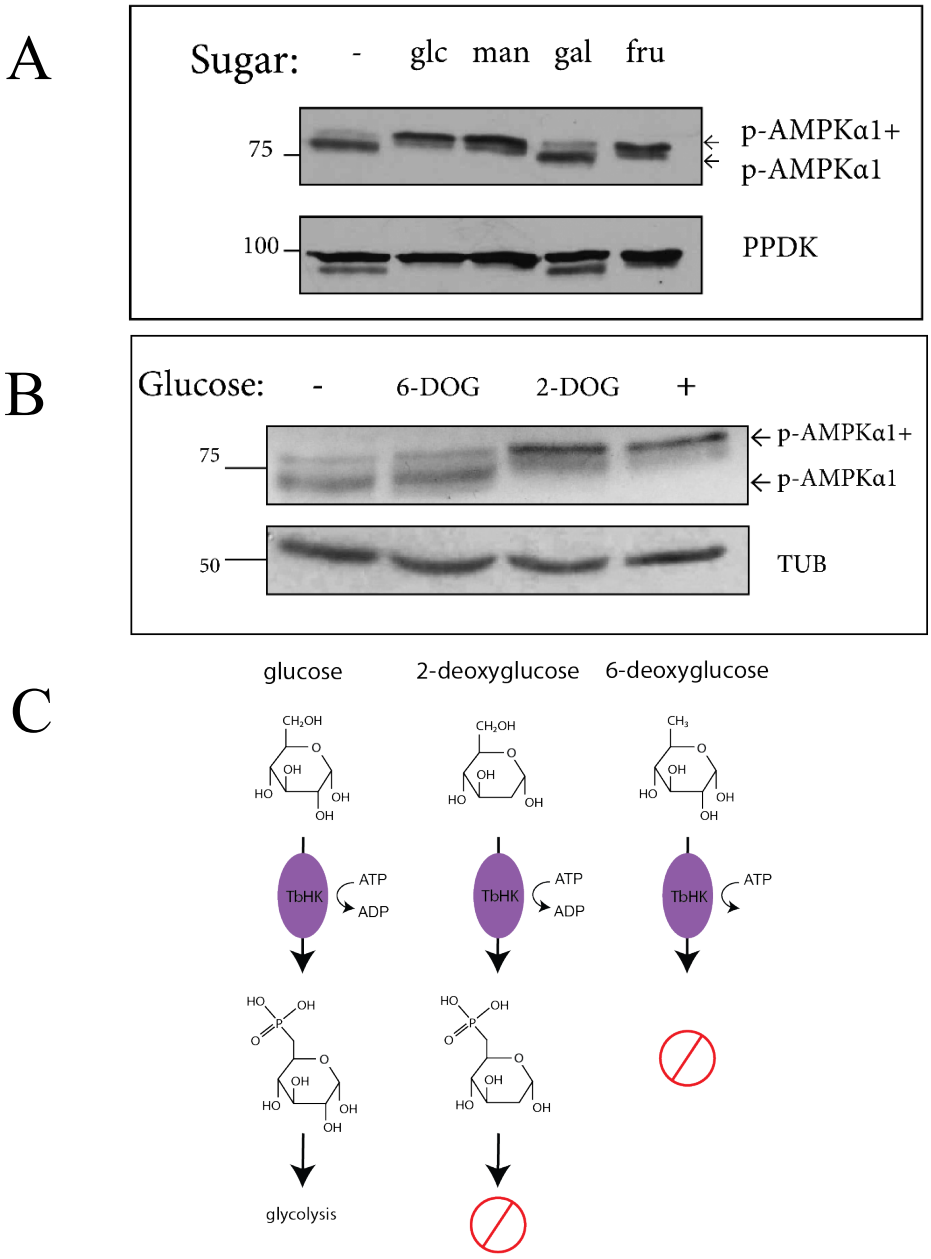

Figure 3.4: p-**AMPKα1 is only modified in the presence of metabolizable sugars**. (A) Western blot of PF treated with 10mM various sugars, pyruvate phosphate dikinase (PPDK) as a loading control (B) western blot of PF treated with 500μM glucose analogs, tubulin (TUB) as a loading control (C) Schematic showing glucose analog metabolism through TbHK

To further explore the role of glucose metabolism in the modification of AMPKα1, we assessed the impact of a known AMPK activator, the AMP analog AICAR, on the modification of AMPKα1. Western blot analysis of PF parasites treated with 2DOG or AICAR resulted in the modification of p-AMPKα1 into p-AMPKα1+ (**Figure 3.5A**). However, treatment with 6DOG did not elicit the p-AMPKα1+ modification. This suggests that p-AMPKα1+ is generated as a consequence of AMPK activity and that hexokinase substrates can trigger the same response through glucose metabolism.

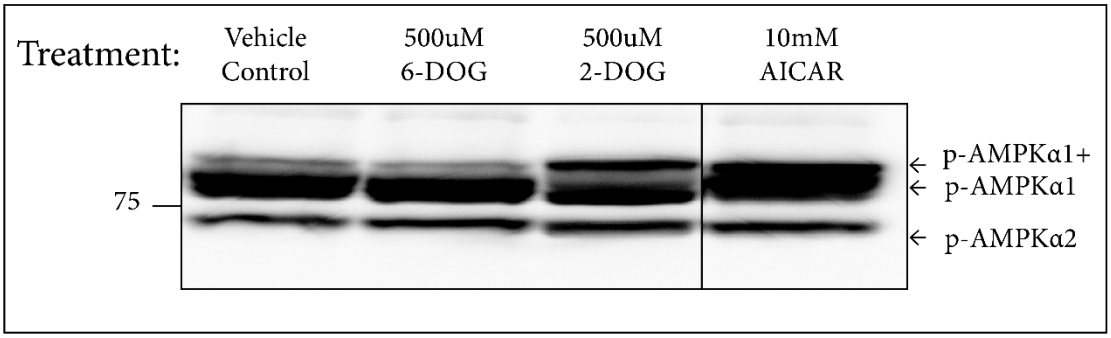

Figure 3.5: p-AMPKα1 is modified by known AMPK activators. (A) western blot of PF cultured in the absence of glucose treated with the 500μM glucose analogs, 6DOG or 2DOG, or 10mM AICAR.

Knowing that glucose abundance influences p-AMPKα1 modification, we explored subcellular distribution of AMPKα and p-AMPKα in PF parasites in response to glucose availability. We performed differential centrifugation of lysates of PF parasites cultured in the presence or absence of glucose, collecting nuclear, mitochondrial, glycosomal, endosomal, and cytosolic enriched fractions (**Figure 3.6A**). By western blotting we did not observe a difference in the distribution of p-AMPKα1 in response to the presence or absence of glucose (**Figure 3.6B**). We observed that p-AMPKα1 primarily fractionated in the nuclear fraction, suggesting association with the nucleus or fragments of the plasma membrane. We also performed crude fractionations on PF parasites after they were introduced in the opposing glucose abundance of culture media. We saw no difference in fraction location of p- AMPKα1 in response to glucose abundance.

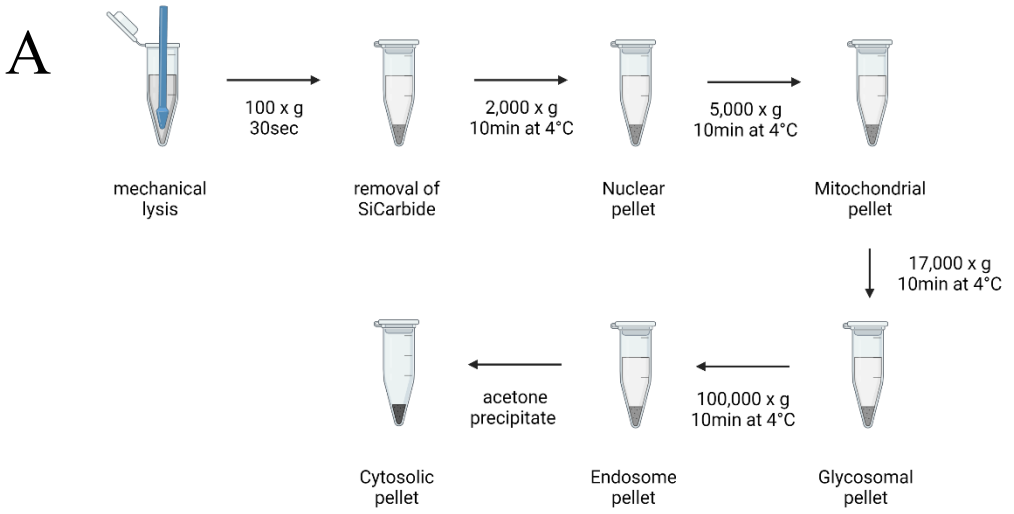

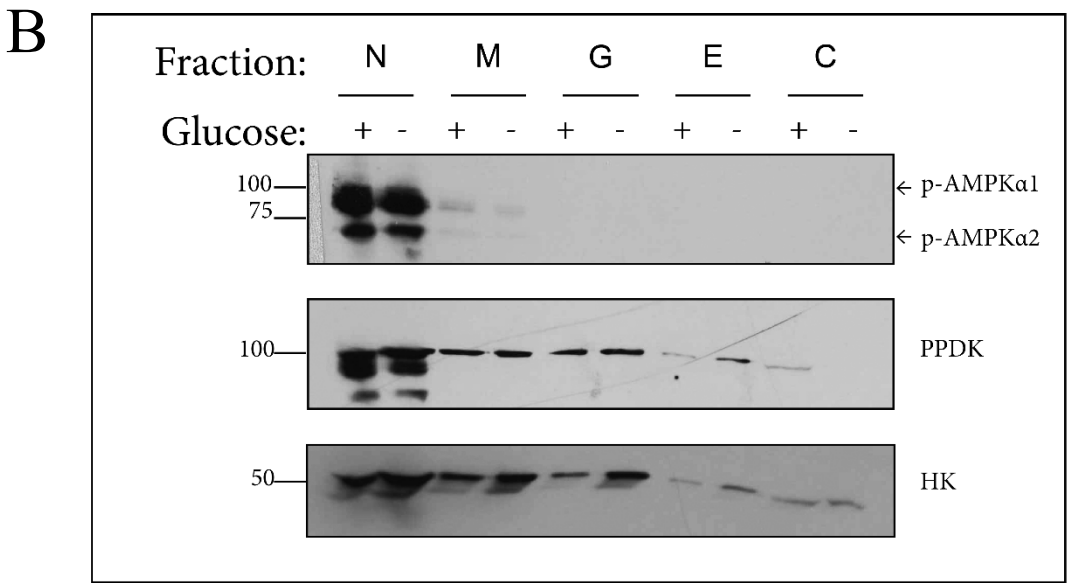

Figure 3.6: p-AMPKα does not change subcellular location in the presence of glucose. (A) cartoon method of differential centrifugation created with BioRender. N-nuclear enriched, M- mitochondria enriched, G- glycosome enriched, E- endosome enriched, C- cytosol enriched. (B) western blot of differential centrifugation fractions of PF in the presence or absence of glucose. PPDK as a glycosomal marker, HK as a glycosomal and cytosolic marker.

To further resolve the subcellular location of p-AMPKα we performed sucrose density gradient fractionation of PF parasites cultured in the presence and absence of glucose (**Figure 3.7A**). We observed a similar fractionation pattern of p-AMPKα using lysates of parasites cultured in the presence (**Figure 3.7B**) or the absence (**Figure 3.7C**) of glucose. Here, Hsp70 serves as a mitochondrial marker and aldolase as a glycosomal marker. We also observed a similar fractionation of AMPKα with the AMPKα antibody, regardless of glucose abundance. Observing p-AMPKα only in the 'top' of our gradient, we decided to precipitate protein from the first nine fractions, representing the top third of the sucrose gradient and the smallest molecules, to increase our subcellular resolution. Upon western blotting analysis of the top third of the gradients we did not observe a change in the density association of p-AMPKα in response to glucose abundance (**Figure 3.8A & B**).

Densitometry analysis of protein abundance in individual fractions showed partial overlap in distribution of AMPKα and mitochondria and glycosomes in the presence and absence of glucose (**Figure 3.8 C & D**). Glycosomes and mitochondria markers had similar fractionation patterns regardless of glucose abundance. It should be noted that this analysis cannot provide information about protein abundance, but rather presence of proteins in a fraction (above the limit of detection). The fractionation of AMPKα was similar in PF lysates in the presence and absence of glucose (**Figure 3.8E**), as was also true of p-AMPKα1 (**Figure 3.8F**). Similarity, when we compared the density fractionation of AMPKα to p-AMPKα in the first nine fractions, we observed a similar distribution of the two proteins, in both the presence and absence of glucose (**Figure 3.9 A & B**). Rather than

glucose abundance altering the protein abundance of AMPKα, it seemed that phosphorylation of AMPKα1 plays a larger role in subcellular location, in a glucose independent mechanism.

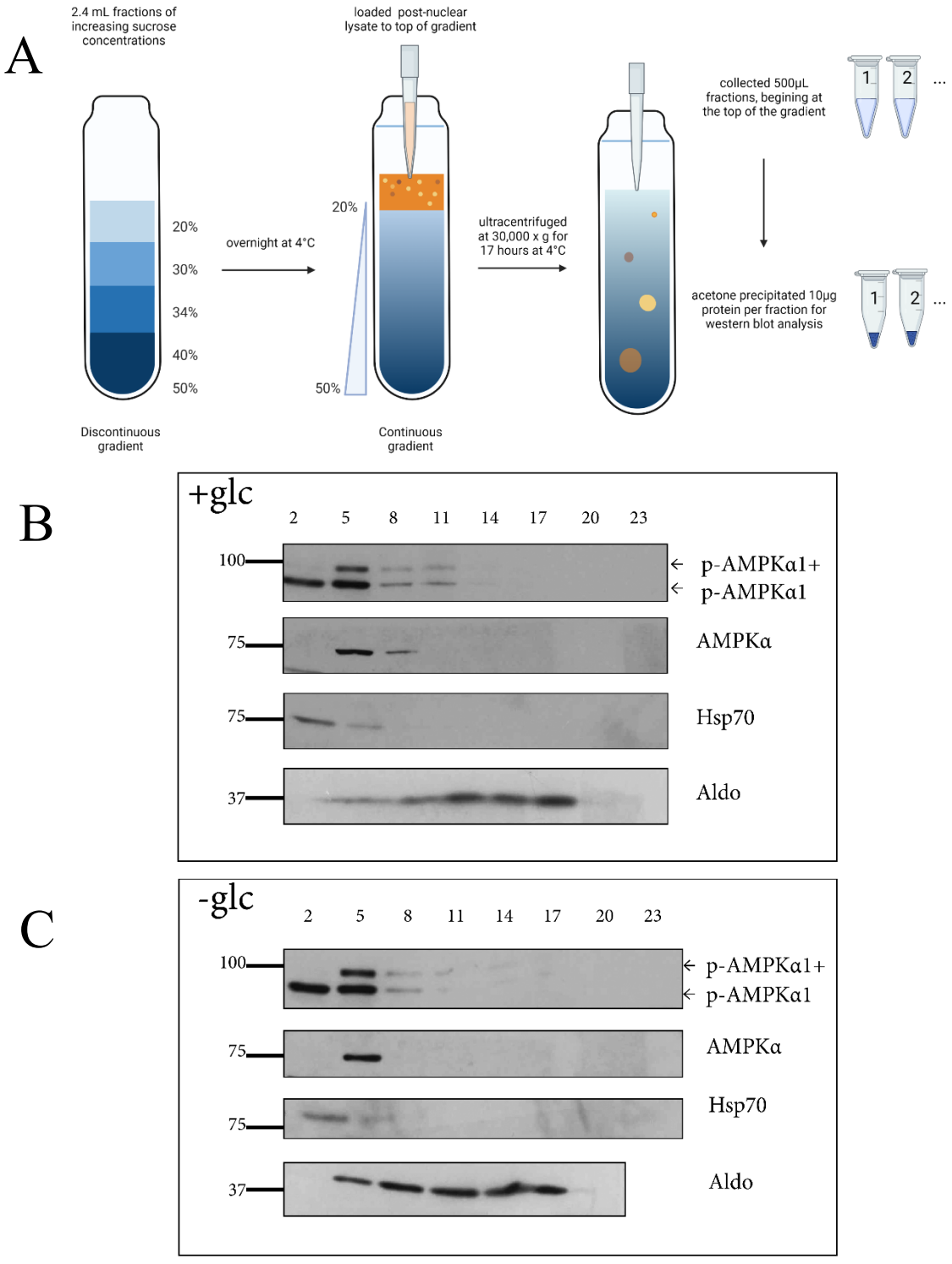

Figure 3.7: p-AMPKα has similar subcellular distribution regardless of glucose abundance.

Figure 3.7: p-AMPKα has similar subcellular distribution regardless of glucose abundance (A) Cartoon rendition of sucrose gradient fractionation method created with BioRender (B) western blot analysis of every third fraction collected from PF parasites cultured in the presence of glucose. Hsp70 as a mitochondrial marker and aldolase as a glycosomal marker (C) western blot analysis of every third fraction collected from PF parasites cultured in the absence of glucose. Hsp70 as a mitochondrial marker and aldolase as a glycosomal marker

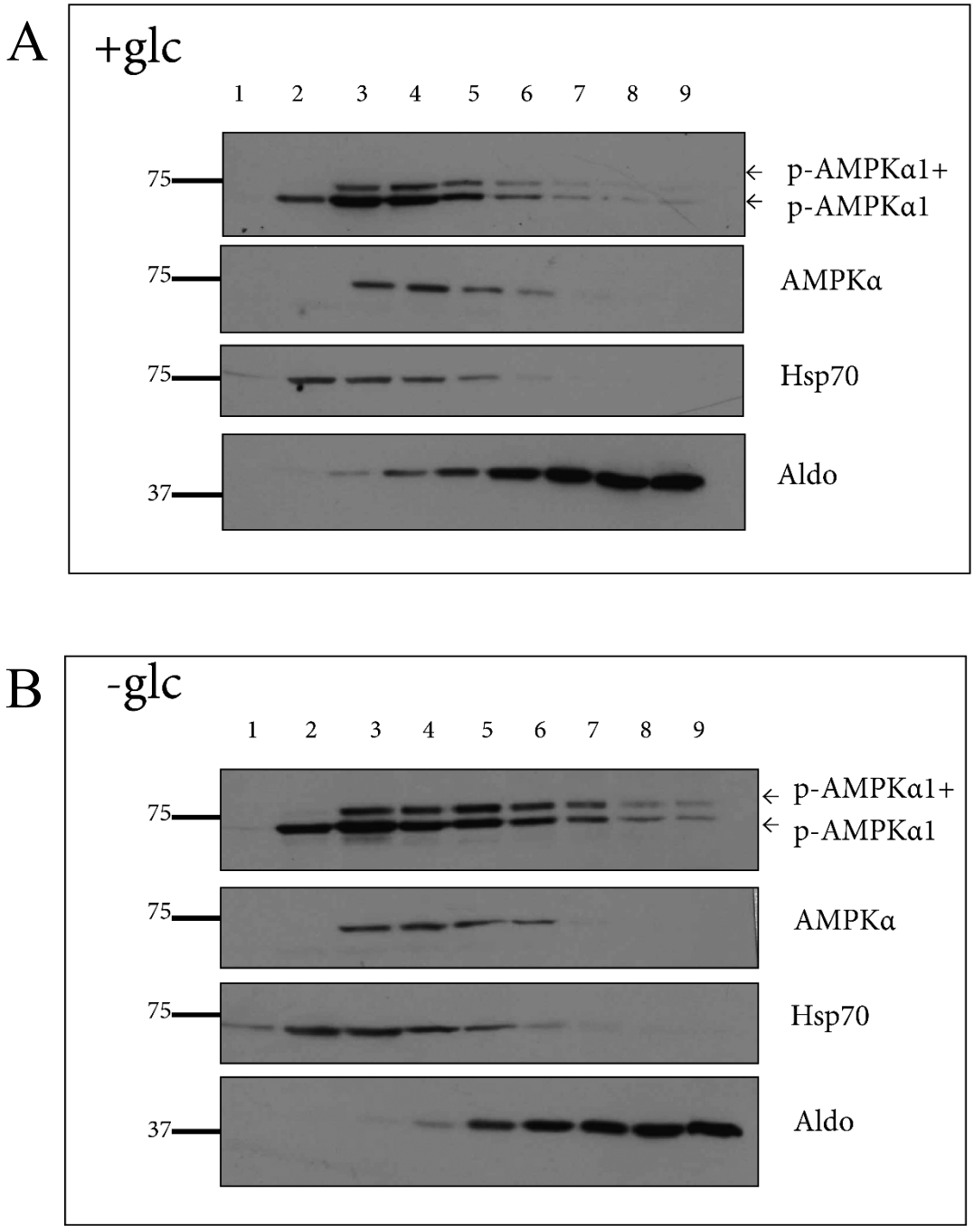

Figure 3.8: AMPKα has similar subcellular distribution to other organelle markers

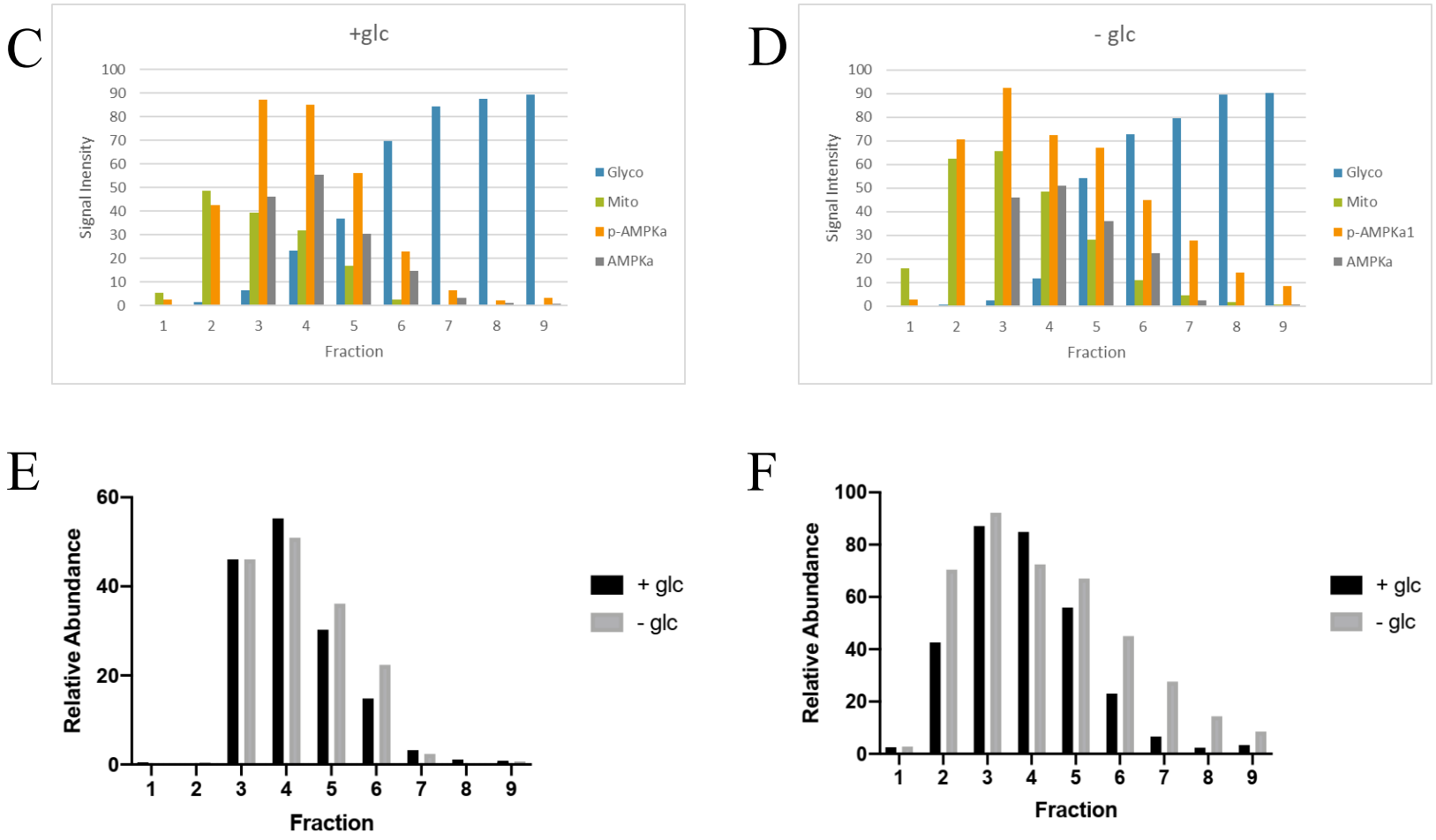

Figure 3.8: AMPKα has similar subcellular distribution to other organelle markers.

Figure 3.8: AMPKα has similar subcellular distribution to other organelle markers. (A) western blot analysis of first nine fractions of sucrose gradient fractionation collected from PF parasites cultured in the presence of glucose, Hsp70 as a mitochondrial marker and aldolase as a glycosomal marker (B) western blot analysis of first nine fractions of sucrose gradient fractionation collected from PF parasites cultured in the absence of glucose, Hsp70 as a mitochondrial marker and aldolase as a glycosomal marker (C) densitometry analysis of protein abundance of specific subcellular markers per first nine fractions in the presence of glucose. Glyco- aldolase signal, mito- Hsp70 signal (D) densitometry analysis of protein abundance of specific subcellular markers per first nine fractions in the absence of glucose. Glyco- aldolase signal, mito- Hsp70 signal (E) densitometry analysis of AMPKα in the first nine fractions the presence or absence of glucose (F) densitometry analysis of p-AMPKα in the first nine fractions the presence or absence of glucose

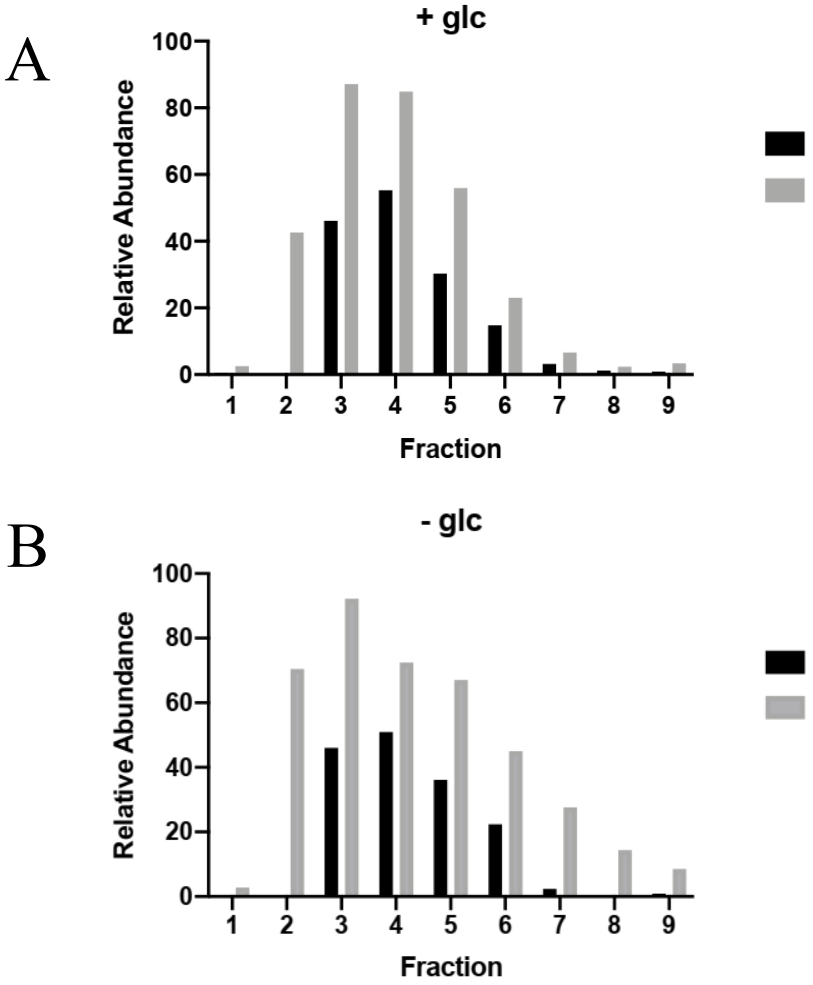

Figure 3.9: p-AMPKα has a distinct subcellular distribution when compared to AMPKα, regardless of glucose abundance. (A) densitometry analysis of AMPKα vs p-AMPKα in the first nine fractions the presence of glucose (B) densitometry analysis of AMPKα vs p-AMPKα in the first nine fractions the absence of glucose.

In addition to sucrose gradient fractionation, we performed immunofluorescence assays on PF parasites cultured in the presence or absence of glucose. Here, we aimed to complement our previous data showing partial organellar cofractionation of parasite lysate through localization studies on PF parasites. We observed partial overlap in fluorescence, visualized by yellow color, of the glycosomal marker, in red, with AMPKα, in green (**Figure 3.10A**). We also observe partial overlap in fluorescence of the glycosomal marker with p-AMPKα (**Figure 3.10B**). This corroborates our previous data of cofractionation of p-AMPKα1 with glycosomes. Further, Clemmens et al previously demonstrated that AMPKβ, in red, was partially associated with glycosomes, in green (**Figure 3.10C**) (22). AMPK is widely distributed in the cell, with protein localization shown to overlap with mitochondria, visualized by the yellow color (**Figure 3.11A**). This localization did not change after activation of the enzyme (**Figure 3.11B**). This supports our previous sucrose gradient fractionation data of partial association of AMPKα with mitochondria.

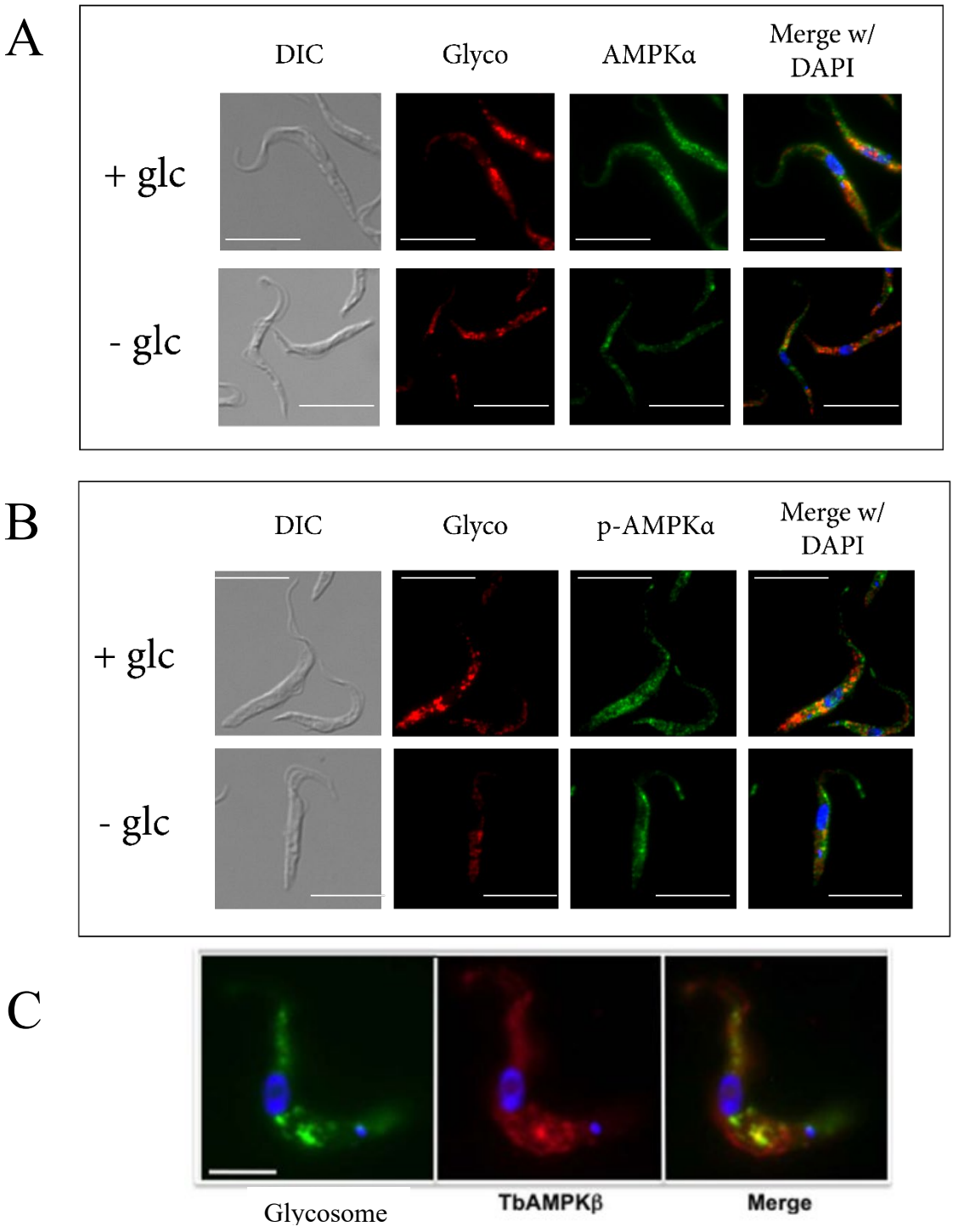

Figure 3.10: AMPKα may be associated with glycosomes.

Figure 3.10: AMPKα may be associated with glycosomes. (A) Immunofluorescence on PF parasites expressing glycosomally directed fluorophore cultured in the presence of glucose, top row, or absence of glucose, bottom row. Stained with native AMPKα, green. Scale bar = 10μm (B) Immunofluorescence on PF parasites expressing glycosomally directed fluorophore cultured in the presence of glucose, top row, or absence of glucose, bottom row. Stained with p-AMPKα, green. Scale bar = 10μm (C) Immunofluorescence on PF parasites expressing glycosomally directed fluorophore, green, stained with AMPKβ, red. Scale bar = 5μm. Reprinted with permission from Elsevier Science & Technology Journals, Experimental Parasitology. Copyright: Elsevier Science & Technology Journals, 2009 (22).

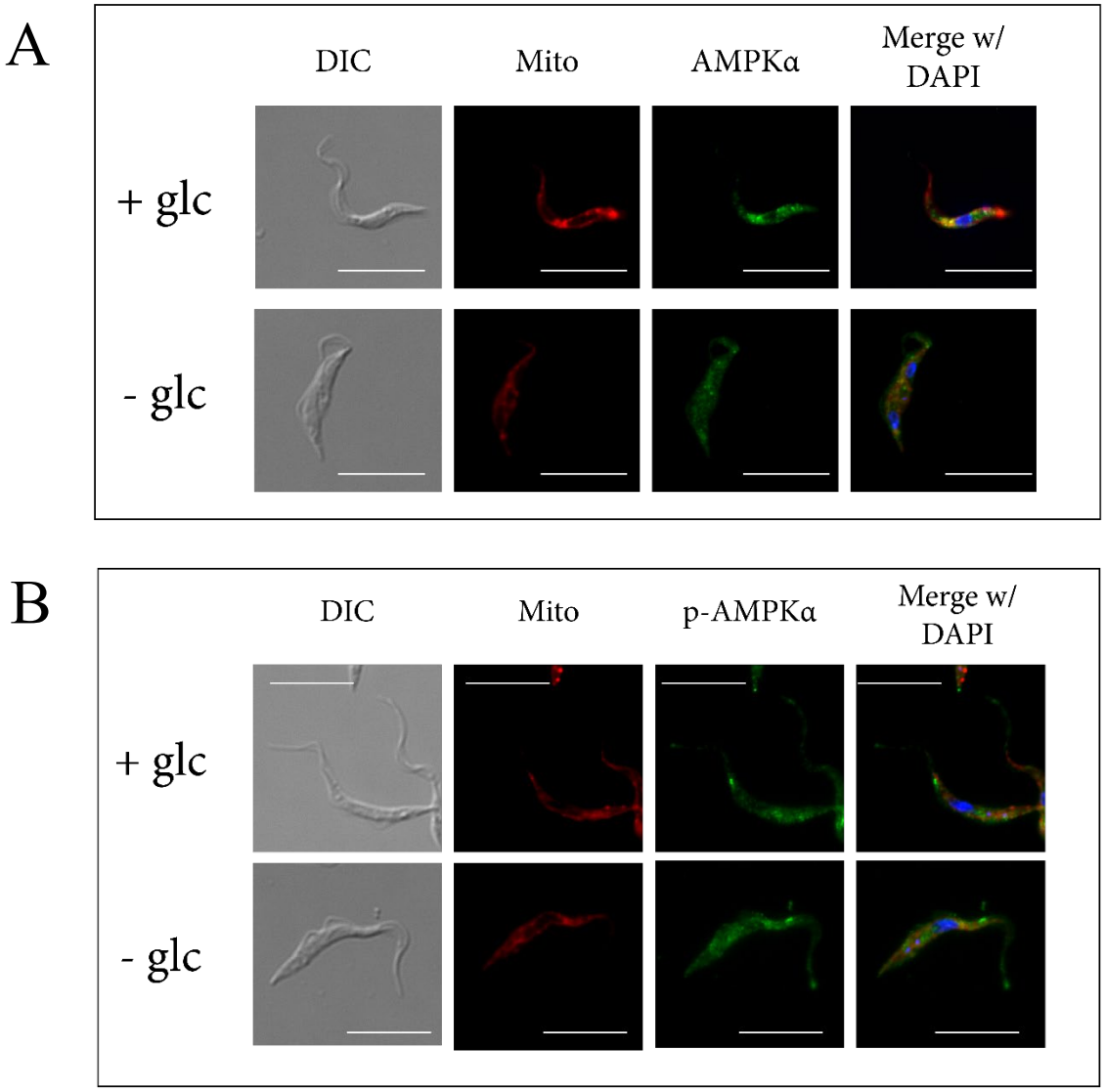

Figure 3.11: AMPKα is partially associated with mitochondria. (A) Immunofluorescence on PF parasites cultured in the presence of glucose, top row, or absence of glucose, bottom row. Live PF parasites stained with 10μM MitoTracker Red, then fixed and stained with AMPKα, green. Scale bar = 10μm (B) Immunofluorescence on PF parasites cultured in the presence of glucose, top row, or absence of glucose, bottom row. Live PF parasites stained with 10μM MitoTracker Red, then fixed and stained with p-AMPKα, green. Scale bar = 10μm

Discussion

In this study, we have found that phosphorylated AMPKα1 can be present in two subspecies in a glucose dependent fashion, suggesting additional dynamic post-translational modifications (PTM) of the catalytic domain. The additional modification of p-AMPKα1, which we coined p-AMPKα1+, was repeatedly detected in parasites cultured in the presence of glucose (**Figure 3.1**). Phosphorylated AMPKα (α1 & α2) were more abundant in parasites cultured in the absence of glucose, (**Figure 3.2**). This was likely due to an increase in AMPKα phosphorylation in the absence of glucose, rather than an increase in total protein abundance.

The activation of AMPK may be related to its role in down-regulation of anabolism and induction of catabolic programs similar to the function of the complex in other eukaryotic systems. Introduction of environmental glucose led to rapid (within five minutes) modification of p-AMPKα1 (**Figure 3.3**). We hypothesize that glucose-dependent modification may be the activity of increased cellular AMP responsive pathways. However, the *T. brucei* genome does not contain a predicted homolog of the LKB1 gene, which is responsible for direct activation of AMPK in other eukaryotic systems. This may be similar to the path triggered by canonical AMPK activators in other systems that cause autophosphorylation of AMPKα1 in response to cAMP analogs (**Figure 3.5**).

Figure 3.12 shows our current working model for AMPKα modification in relationship to glucose metabolism. In the presence of extracellular glucose (**Figure 3.12A**), glucose enters the parasite cytoplasm through a THT and is shuttled to the

glycosome in a mechanism that is not fully understood. Once in the glycosome, glucose is metabolized into glucose-6-phosphate (G6P) by TbHK. This substrate-level phosphorylation alters the ADP:ATP ratio inside the parasite. Also occurring in the cytoplasm AMPKα is phosphorylated, activating the AMPK complex, as a result of natural cellular processes that increase cytosolic AMP levels. We hypothesize that this activated AMPK complex nears the glycosome, senses the energy imbalance caused by TbHK metabolism and the AMPK complex becomes hyper-phosphorylated (p-AMPKα1+). This modification of the AMPK complex may play a role in decreasing activity of the complex through reversible PTMs rather than protein degradation. The hyper-phosphorylated AMPK complex is also hypothesized to play a role in surface molecule composition by favoring EP procyclins.

In the absence of extracellular glucose (**Figure 3.12B**) TbHK is not active. Here, in the cytoplasm AMPKα is phosphorylated, activating the AMPK complex, as a result of natural cellular processes that increase cytosolic AMP levels. The activated AMPK complex is hypothesized to signal mitochondrial metabolism, increasing catabolic activities. Surface molecule composition is altered, with GPEET procyclins being detected on the PF parasite cell surface in the absence of glucose. This proposed model of AMPKα PTM and AMPK signaling ties together glucose metabolism, mitochondrial metabolism, and surface molecule composition.

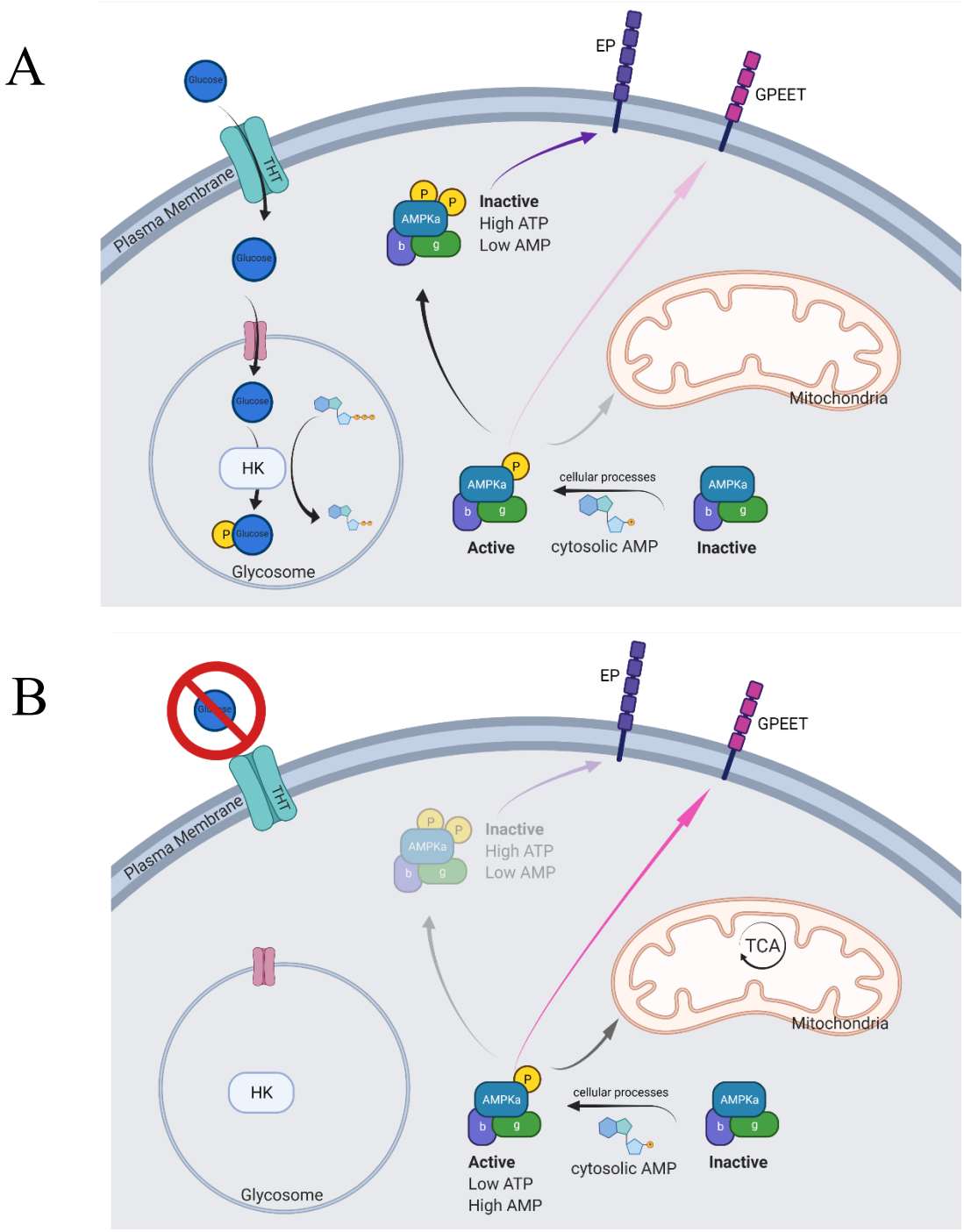

Figure 3.12: Working model of AMPKα modification in response to glucose metabolism. (A) AMPK signaling in the presence of glucose. Created with BioRender. (B) AMPK signaling in the absence of glucose. Created with BioRender.

Having found partial overlap of AMPKα with both glycosomes and mitochondria, in both our fractionation and immunofluorescence experiments, it is possible that AMPKα may be reversibly associated with membranes. The N-terminus of the TbAMPKβ subunit contains a putative myristoylation site that has been shown to direct cytoplasmic to membrane translocation of the AMPK complex in other systems (28). We did not investigate the β-subunit in this study. However, it would be interesting to see the β-subunit is causing the change in AMPK subcellular localization in response to glucose depletion.

Parasite surface molecule expression is tightly associated with differentiation, as particular life cycle stages require expression of surface proteins for success in their host niche (29). LS and SS parasites express a dense surface coat of variant surface glycoprotein (VSG) which enable antigenic variation and host immune evasion in mammals (30) while PF parasites express procyclins on their surface, which are important for tissue tropism in the fly. In Chapter Two we explored the role that glucose depletion plays in parasite differentiation. In this chapter, I suggest a role of AMPKα signaling in a glucose metabolism-dependent manner.

RNAi screens found AMPKα2 to play a role in differential gene expression of parasite differentiation (25). RNAi knockdown of AMPKβ, the scaffold subunit of the heterotrimeric complex, caused a change in parasite surface molecule composition, a result that phenocopied how PF cells respond to glucose deprivation (Chapter 1, **Figure 1.10**) (22). This suggests that AMPK signaling is potentially involved in regulation of surface molecule expression in response to environmental cues.

Two phosphatases, TbPTP1 and TbPIP39, have been found to play a role in *T. brucei* differentiation from SS to PF (31). TbPTP1, a tyrosine phosphatase, dephosphorylates TbPIP39, a serine/threonine phosphatase, a cascade that is necessary for parasite development. Recent studies have tied phosphorylation of AMPKα with TbPIP39 expression (32) suggesting that AMPK is upstream of TbPTP1. Other phosphatases and kinases have been shown to potentially play a role in *T. brucei* differentiation, including TbTOR4, a known negative regulator of LS to SS development (23,33). AMPKα1 has been found to be upstream of TOR4 in *T. brucei*, these pathways are inversely connected in other eukaryotic systems (34). Taken together, these results suggest that TbAMPKα is playing a role in nutrient sensing and signaling in PF parasites, and this signaling may be communicating with other known pathways. Metabolism reprogramming and environmental sensing are essential to the completion of the parasite life cycle, and TbAMPKα phosphorylation, and hypothesized hyper-phosphorylation, appears to respond to glucose metabolism in PF parasites.

References

1. Walsh B, Hill KL. Right place, right time: Environmental sensing and signal transduction directs cellular differentiation and motility in Trypanosoma brucei. Mol Microbiol. 2021;115(5):930–41.
2. VISSER N, OPPERDOES FR. Glycolysis in Trypanosoma brucei. Eur J Biochem. 1980;103(3):623–32.
3. Mony BM, Matthews KR. Assembling the components of the quorum sensing pathway in African trypanosomes. Mol Microbiol. 2015;96(2):220–32.
4. Silvester E, McWilliam K, Matthews K. The Cytological Events and Molecular Control of Life Cycle Development of Trypanosoma brucei in the Mammalian Bloodstream. Pathogens [Internet]. 2017;6(3):29. Available from: http://www.mdpi.com/2076-0817/6/3/29
5. Matthews KR. The developmental cell biology of Trypanosoma brucei. J Cell Sci [Internet]. 2005;118(2):283–90. Available from: http://jcs.biologists.org/cgi/doi/10.1242/jcs.01649
6. Szöőr B, Silvester E, Matthews KR. A Leap Into the Unknown – Early Events in African Trypanosome Transmission. Trends Parasitol. 2020;36(3):266–78.
7. Walsh B, Hill KL. Right place, right time: Environmental sensing and signal transduction directs cellular differentiation and motility in Trypanosoma brucei . Mol Microbiol. 2021;0–1.
8. Kim JH, Roy A, Jouandot D, Cho KH. The glucose signaling network in yeast. Biochim Biophys Acta - Gen Subj [Internet]. 2013;1830(11):5204–10. Available

from: http://dx.doi.org/10.1016/j.bbagen.2013.07.025

9. Hardie DG. Sensing of energy and nutrients by AMP-activated protein kinase. Am J Clin Nutr. 2011;93(4).

10. Crozet P, Margalha L, Confraria A, Rodrigues A, Martinho C, Adamo M, et al. Mechanisms of regulation of SNF1/AMPK/SnRK1 protein kinases. Front Plant Sci. 2014;5(MAY):1–17.

11. Hardie DG. AMPK—Sensing Energy while Talking to Other Signaling Pathways. Cell Metab [Internet]. 2014 Dec;20(6):939–52. Available from: https://linkinghub.elsevier.com/retrieve/pii/S1550413114004100

12. Hardie DG, Lin SC. AMP-activated protein kinase - not just an energy sensor. F1000Research. 2017;6(0):1–11.

13. Vickerman K. DEVELOPMENTAL CYCLES AND BIOLOGY OF PATHOGENIC TRYPANOSOMES. Br Med Bull. 1985;41(2):105–14.

14. Barquilla A, Saldivia M, Diaz R, Bart JM, Vidal I, Calvo E, et al. Third target of rapamycin complex negatively regulates development of quiescence in Trypanosoma brucei. Proc Natl Acad Sci U S A. 2012;109(36):14399–404.

15. Barquilla A, Saldivia M, Diaz R, Bart J-M, Vidal I, Calvo E, et al. Third target of rapamycin complex negatively regulates development of quiescence in Trypanosoma brucei. Proc Natl Acad Sci [Internet]. 2012;109(36):14399–404. Available from: http://www.pnas.org/cgi/doi/10.1073/pnas.1210465109

16. Tagoe DNA, Kalejaiye TD, de Koning HP. The ever unfolding story of cAMP signaling in trypanosomatids: Vive la difference! Front Pharmacol. 2015;6(SEP):1–

13.

17. Salmon D. Adenylate cyclases of Trypanosoma brucei, environmental sensors and controllers of host innate immune response. Pathogens. 2018;7(2).

18. Shaw S, DeMarco SF, Rehmann R, Wenzler T, Florini F, Roditi I, et al. Flagellar cAMP signaling controls trypanosome progression through host tissues. Nat Commun [Internet]. 2019;10(1):1–13. Available from: http://dx.doi.org/10.1038/s41467-019-08696-y

19. Shaw S, Knüsel S, Abbühl D, Naguleswaran A, Roditi I. Cyclic AMP signalling and glucose metabolism mediate pH taxis by African trypanosomes. bioRxiv [Internet]. 2021;2021.01.01.424252. Available from: http://biorxiv.org/content/early/2021/01/01/2021.01.01.424252.abstract

20. Saldivia M, Ceballos-Pérez G, Bart J, Navarro M. The AMPKα1 Pathway Positively Regulates the Developmental Transition from Proliferation to Quiescence in Trypanosoma brucei. Cell Rep [Internet]. 2016 Oct;17(3):660–70. Available from: https://linkinghub.elsevier.com/retrieve/pii/S2211124716312803

21. Quintana JF, Zoltner M, Field MC. Evolving Differentiation in African Trypanosomes. Trends Parasitol [Internet]. 2020;xx(xx):1–8. Available from: https://doi.org/10.1016/j.pt.2020.11.003

22. Clemmens CS, Morris MT, Lyda TA, Acosta-serrano A, Morris JC. Trypanosoma brucei AMP-Activated Kinase Subunit Homologs Influence Surface Molecule Expression. 2010;123(3):250–7.

23. Saldivia M, Ceballos-Pérez G, Bart JM, Navarro M. The AMPKα1 Pathway

Positively Regulates the Developmental Transition from Proliferation to Quiescence in Trypanosoma brucei. Cell Rep. 2016;17(3):660–70.

24. Mony BM, Macgregor P, Ivens A, Rojas F, Cowton A, Young J, et al. Europe PMC Funders Group Genome wide dissection of the quorum sensing signaling pathway in Trypanosoma brucei. Nature. 2014;505(7485):681–5.

25. Toh JY, Nkouawa A, Sánchez SR, Shi H, Kolev NG, Tschudi C. Identification of positive and negative regulators in the stepwise developmental progression towards infectivity in Trypanosoma brucei. Sci Rep [Internet]. 2021;11(1):1–14. Available from: https://doi.org/10.1038/s41598-021-85225-2

26. Ruiz A, Liu Y, Xu X, Carlson M. Heterotrimer-independent regulation of activation-loop phosphorylation of Snf1 protein kinase involves two protein phosphatases. Proc Natl Acad Sci U S A. 2012;109(22):8652–7.

27. Eisenthal R, Game S, Holman GD. Specificity and kinetics of hexose transport in Trypanosoma brucei. BBA - Biomembr. 1989;985(1):81–9.

28. Oakhill JS, Chen ZP, Scott JW, Steel R, Castelli LA, Linga N, et al. β-Subunit myristoylation is the gatekeeper for initiating metabolic stress sensing by AMP-activated protein kinase (AMPK). Proc Natl Acad Sci U S A. 2010;107(45):19237–41.

29. Landfear SM, Zilberstein D. Sensing What's Out There – Kinetoplastid Parasites. Trends Parasitol [Internet]. 2019;35(4):274–7. Available from: http://dx.doi.org/10.1016/j.pt.2018.12.004

30. Zimmermann H, Subota I, Batram C, Kramer S, Janzen CJ, Jones NG, et al. A

quorum sensing-independent path to stumpy development in Trypanosoma brucei. Vol. 13, PLoS Pathogens. 2017. 1–33 p.

31. Szöor B, Ruberto I, Burchmore R, Matthews KR. A novel phosphatase cascade regulates differentiation in Trypanosoma brucei via a glycosomal signaling pathway. Genes Dev. 2010;24(12):1306–16.

32. Tripathi A, Singha UK, Paromov V, Hill S, Pratap S, Rose K, et al. Erratum for Tripathi et al., "The Cross Talk between TbTim50 and PIP39, Two Aspartate-Based Protein Phosphatases, Maintains Cellular Homeostasis in Trypanosoma brucei " . mSphere. 2019;4(5):1–20.

33. McDonald L, Cayla M, Ivens A, Mony B, MacGregor P, Silvester E, et al. Non-linear hierarchy of the quorum sensing signalling pathway in bloodstream form African trypanosomes. Vol. 14, PLoS Pathogens. 2018. 1–31 p.

34. González A, Hall MN, Lin SC, Hardie DG. AMPK and TOR: The Yin and Yang of Cellular Nutrient Sensing and Growth Control. Cell Metab. 2020;31(3):472–92.

CHAPTER FOUR

CONCLUSIONS AND FUTURE DIRECTIONS

African trypanosomes are unicellular protozoan parasites with a dixenous life cycle. As the parasites are transferred between mammalian hosts through the tsetse fly their metabolic requirements drastically change. While parasites live extracellularly in the mammalian bloodstream, they metabolize glucose to generate ATP. Conversely, the procyclic form parasites, living in the tsetse fly, have limited access to glucose and rather metabolize amino acids to generate ATP (1). The stark difference in nutrient availability is one of many cues required to drive completion of their lifecycle (2). Here, we hypothesize that glucose metabolism plays a role in parasite differentiation through a mechanism that shares some similarities but has differences from other eukaryotes.

Yeast utilize Snf1, a heterotrimeric protein complex consisting of a catalytic α subunit, β scaffold subunit, and regulatory γ subunit, and this serves as a master regulator in nutrient abundance perception (3). Snf1 is activated by high AMP:ATP ratios, signifying cellular starvation, and transduces signals to induce catabolic activities while suppressing anabolic activities (4). Activation of Snf1 occurs through phosphorylation of Thr210 of the catalytic α subunit (5), an event that can occur in response to glucose uptake and metabolism in *Saccharomyces cerevisiae* (6).

Mammalian cells contain the protein complex AMPK, a homologue of Snf1, which consists of the homologs of the three Snf1 subunits. Similarly, AMPK is activated through high AMP:ATP ratios, sensing low intracellular energy and signaling catabolic pathways (7). The catalytic α subunit can be activated by phosphorylation of Thr172, which may

only occur after allosteric interaction of adenine nucleotides with the regulatory γ subunit (8). The canonical activation of AMPK, phosphorylation of catalytic α subunit Thr172, has been tied to the depletion of environmental glucose. Other studies have shown AMPK acting as a sensor of glucose abundance, partially through association with subcellular membranes (9). The scaffold β subunit can be myristoylated to alter the subcellular location of the AMPK complex as part of a cellular nutrient response (10).

Trypanosoma brucei has a complex lifecycle. The proliferative mammalian bloodstream long slender (LS) form transitions into the quiescent short stumpy (SS) form in a density-dependent fashion (11). SS parasites are preadapted to life in the tsetse fly with proteins associated with differentiation (PAD) surface proteins, upregulated mitochondrial transcripts, and resistance to mild acid. Upon a tsetse fly bloodmeal LS and SS parasites are ingested and LS parasites are degraded. SS parasites receive several environmental cues, including depletion of glucose and introduction of citrate/cis-aconitate, and further differentiation into procyclic (PCF) form parasites (12). The transition from SS to PCF is controlled through a protein phosphatase cascade which has found to be associated with glycosomes. Glycosomes are parasite specific specialized peroxisomes that compartmentalize most of glycolysis, along with components of other metabolic pathways (13,14). Our lab previous showed that glucose abundance played a key role in SS to PCF differentiation (15). Another eukaryotic master regulator, TbTOR4, was found to negatively regulate parasite development from LS to SS (16). We hypothesized that AMPK to be at the center of coordination of parasite differentiation, influencing metabolic changes

in the mitochondria and glycosome (17). This work aims to tie together glucose abundance and metabolism to AMPK signaling in *T. brucei*.

In Chapter two I found that TbAMPKα1 is modified in response to glucose in PCF parasites. We observed a species of TbAMPKα1 with slightly larger mobility on SDS-PAGE, coined TbAMPKα1+, in the presence of glucose and other metabolizable sugars. This response occurred rapidly, and with a similar phenotype to known AMPK activators. The modification of TbAMPKα1 did not alter subcellular location. The modification of TbAMPKα1+ remains unresolved. We have made several attempts to epitope tag the catalytic α subunit to aid in the precipitation of the protein for further analysis without success. Additionally, immunoprecipitation (IP) using native AMPKα antibodies have also been unsuccessful. IP purification (and resulting very low concentration of what is anticipated to be a signaling molecule) followed by mass spectrometry analysis could be key unlocking TbAMPK interacting partners and piecing together the signaling cascade that controls parasite differentiation.

In Chapter three I contributed to work that described how the depletion of glucose is crucial, but not the only trigger, for SS to PCF differentiation. Pleomorphic SS parasites isolated from infected rodents were subject to several experimental conditions, along with published differentiation cues that included cold shock and citrate/cis-aconitate treatment. Successful differentiation to PCF parasites was scored through outgrowth of the population, metabolic transcript profile, and surface protein coat. I performed the flow cytometry experiments of monitoring expression of the PCF surface molecule EP procyclin on SS parasites subjected to experimental cues (experimental and published). I also

prepared RNA samples from various stage of parasites for RNAseq and qRT-PCR analysis. These RNA studies revealed that depletion of glucose induced a transcript profile in PCF more similar to that found in PCFs from infected flies and distinct from those from PCFs derived from SS that had been subjected to other differentiation cues. This work established the foundation of thinking that glucose sensing and metabolism may be playing separate roles in parasite differentiation.

Taken together, glucose metabolism and perception have been found to be key regulators of parasite developmental programs. In a step toward better understanding of the glucose-responsive signaling mechanisms in the parasite we have found that glucose availability impacts the master metabolic regulator AMPK. Glucose and glucose metabolism play roles in the activation of TbAMPKα1 and parasite differentiation, but connections between the two have not been resolved and will require future efforts to identify interacting partners in order to fully elucidate the pathway.

References

1. Landfear SM, Zilberstein D. Sensing What's Out There – Kinetoplastid Parasites. Trends Parasitol [Internet]. 2019;35(4):274–7. Available from: http://dx.doi.org/10.1016/j.pt.2018.12.004
2. Rojas F, Matthews KR. Quorum sensing in African trypanosomes. Curr Opin Microbiol [Internet]. 2019;52:124–9. Available from: https://doi.org/10.1016/j.mib.2019.07.001
3. Hedbacker K, Carlson M. SNF1/AMPK pathways in yeast. Front Biosci. 2008;13(7):2408–20.
4. Hardie DG. AMP-activated/SNF1 protein kinases: Conserved guardians of cellular energy. Nat Rev Mol Cell Biol. 2007;8(10):774–85.
5. Ruiz A, Liu Y, Xu X, Carlson M. Heterotrimer-independent regulation of activation-loop phosphorylation of Snf1 protein kinase involves two protein phosphatases. Proc Natl Acad Sci U S A. 2012;109(22):8652–7.
6. Kim JH, Roy A, Jouandot D, Cho KH. The glucose signaling network in yeast. Biochim Biophys Acta - Gen Subj [Internet]. 2013;1830(11):5204–10. Available from: http://dx.doi.org/10.1016/j.bbagen.2013.07.025
7. Mulukutla BC, Yongky A, Le T, Mashek DG, Hu WS. Regulation of Glucose Metabolism – A Perspective From Cell Bioprocessing. Trends Biotechnol [Internet]. 2016;34(8):638–51. Available from: http://dx.doi.org/10.1016/j.tibtech.2016.04.012

8. Ross FA, MacKintosh C, Hardie DG. AMP-activated protein kinase: a cellular energy sensor that comes in 12 flavours. FEBS J. 2016;283:2987–3001.

9. Hardie DG, Lin S-C. AMP-activated protein kinase – not just an energy sensor. F1000Research [Internet]. 2017 Sep 22;6(0):1724. Available from: https://f1000research.com/articles/6-1724/v1

10. Oakhill JS, Chen ZP, Scott JW, Steel R, Castelli LA, Linga N, et al. β-Subunit myristoylation is the gatekeeper for initiating metabolic stress sensing by AMP-activated protein kinase (AMPK). Proc Natl Acad Sci U S A. 2010;107(45):19237–41.

11. Mony BM, Matthews KR. Assembling the components of the quorum sensing pathway in African trypanosomes. Mol Microbiol. 2015;96(2):220–32.

12. Silvester E, McWilliam K, Matthews K. The Cytological Events and Molecular Control of Life Cycle Development of Trypanosoma brucei in the Mammalian Bloodstream. Pathogens [Internet]. 2017;6(3):29. Available from: http://www.mdpi.com/2076-0817/6/3/29

13. VISSER N, OPPERDOES FR. Glycolysis in Trypanosoma brucei. Eur J Biochem. 1980;103(3):623–32.

14. Kessler PS, Parsons M. Probing the role of compartmentation of glycolysis in procyclic form Trypanosoma brucei: RNA interference studies of PEX14, hexokinase, and phosphofructokinase. J Biol Chem. 2005;280(10):9030–6.

15. Qiu Y, Milanes JE, Jones JA, Noorai RE, Shankar V, Morris JC. Glucose signaling is important for nutrient adaptation during differentiation of pleomorphic African trypanosomes. bioRxiv. 2018;3(5):1–18.

16. Barquilla A, Saldivia M, Diaz R, Bart J-M, Vidal I, Calvo E, et al. Third target of rapamycin complex negatively regulates development of quiescence in Trypanosoma brucei. Proc Natl Acad Sci [Internet]. 2012;109(36):14399–404. Available from: http://www.pnas.org/cgi/doi/10.1073/pnas.1210465109

17. Tripathi A, Singha UK, Paromov V, Hill S, Pratap S, Rose K, et al. Erratum for Tripathi et al., "The Cross Talk between TbTim50 and PIP39, Two Aspartate-Based Protein Phosphatases, Maintains Cellular Homeostasis in Trypanosoma brucei " . mSphere. 2019;4(5):1–20.

18. Saldivia M, Ceballos-Pérez G, Bart JM, Navarro M. The AMPKα1 Pathway Positively Regulates the Developmental Transition from Proliferation to Quiescence in Trypanosoma brucei. Cell Rep. 2016;17(3):660–70.